UC Santa Cruz

UC Santa Cruz Electronic Theses and Dissertations

Title

Confirmation Of The Cellular Targets Of Benomyl And Rapamycin And Studies Into The Mode Of Action Of Cationic Amphiphilic Drugs (CADs)

Permalink

https://escholarship.org/uc/item/1p44d774

Author

Wride, Dustin

Publication Date

2016

Peer reviewed|Thesis/dissertation

eScholarship.org Powered by the California Digital Library
University of California

UNIVERSITY OF CALIFORNIA
SANTA CRUZ

CONFIRMATION OF THE CELLULAR TARGETS OF BENOMYL AND RAPAMYCIN AND STUDIES INTO THE MODE OF ACTION OF CATIONIC AMPHIPHILIC DRUGS (CADS)

A dissertation submitted in partial satisfaction
of the requirements for the degree of

DOCTOR OF PHILOSOPHY

in

CHEMISTY

by

DUSTIN A. WRIDE

March 2016

The Dissertation of Dustin A. Wride
is approved:

_____
Professor Ted Holman, Chair

_____
Professor Scott Lokey, Advisor

_____
Professor Grant Hartzog

_____
Tyrus Miller
Vice Provost and Dean of Graduate Studies

Copyright © by

Dustin A. Wride

2016

TABLE OF CONTENTS

List of Figures

List of Tables

List of Schemes

ABSTRACT

THE CONFIRMATION OF THE CELLULAR TARGETS OF BENOMYL AND RAPAMYCIN AND STUDIES INTO THE MODE OF ACTION CATIONIC AMPHIPHILIC DRUGS (CADS)

By Dustin Wride

Investigating the mechanisms of action (MOAs) of bioactive compounds and the deconvolution of their cellular targets is an important and challenging undertaking. Drug resistance in model organisms such as *S. cerevisiae* has long been a means for discovering drug targets and MOAs. Strains are selected for resistance to a drug of interest, and the resistance mutations can often be mapped to the drug's molecular target using classical genetic techniques. Here we demonstrate the use of next generation sequencing (NGS) to identify mutations that confer resistance to two well-characterized drugs, benomyl and rapamycin. Applying NGS to pools of drug-resistant mutants, we develop a simple system for ranking single nucleotide polymorphisms (SNPs) based on their prevalence in the pool, and for ranking genes based on the number of SNPs that they contain. We clearly identified the known targets of benomyl (*TUB2*) and rapamycin (*FPR1*) as the highest-ranking genes under this system. The highest-ranking SNPs corresponded to specific amino acid changes that are known to confer resistance to these drugs. We also found that by screening in a *pdr1D* null background strain that lacks a transcription factor regulating the expression of drug efflux pumps, and by pre-screening mutants in a panel of unrelated anti-fungal agents, we were able to mitigate against the selection of multi-drug

resistance (MDR) mutants. We call our approach "Mutagenesis to Uncover Targets by deep Sequencing, or "MUTseq", and show through this proof-of-concept study its potential utility in characterizing MOAs and targets of novel compounds.

Cationic amphiphilic drugs (CADs) are a broad class of chemicals that can cause adverse effects in humans, and particularly liver toxicity; the origin of this toxicity is not well understood. The CAD haloperidol, for example, is known to cause drug induced liver cholestasis and phospholipidosis (DIPL), severe side effects similar to those seen in familial intrahepatic cholestasis (FIC). In a high throughput screen in yeast, we discovered that several known CADs, as well as a number of novel related compounds, exhibit synthetic lethality with *RCY1*, a gene encoding an F-box protein involved in endocytic recycling of membrane proteins. To investigate the origin of this synthetic lethality, we isolated *S. cerevisiae* mutants resistant to the CADs haloperidol and a novel CAD identified in this study, 3346-2086. Whole genome sequencing revealed that resistance is often associated with mutations in the yeast phospholipid transporters, *DRS2*, *DNF1* and *DNF2*. Further investigations showed that in the absence of these mutations, Rcy1- cells treated with 3346-2086 rapidly lose the ability to transport fluorescent analogues of phosphatidylcholine (PC) and phosphatidylethanolamine (PE), an effect that is largely blocked in the mutants. Our findings provide insight into the functional relationship between Rcy1p and phospholipid transporters and the conditions under which administration of CADs can give rise to drug-induced liver cholestasis and phospholipidosis.

Dedicated to my loving wife. You are an inspirational model of perseverance and hard work. And to my parents who have supported me through thick and thin and always encouraged me to pursue higher education.

Acknowledgments

I would like to acknowledge the following for their contributions to this work. Walter Bray for assisting and advising with all things biological, especially in the chemical screening center. Grant Hartzog for being a patient and effective mentor in the realm of yeast genetics and a contributor to my publications. Nader Pourmand for his collaboration with regard to next generation sequencing. Undergraduate researchers; Jake Kosarchuk, Sean Nisam and Ray Berkeley for their hard work and dedication in the lab. Jake and Sean both contributed to the isolation of resistant mutants. Ray contributed to isolating resistant mutants, organic synthesis and miscellaneous molecular biology tasks. The Lokey lab graduate student researchers; Rushia Turner, Andy Bockus, Cameron Pye, Josh Schwochert, Jessica Ochoa (the elasto-belt) and Chad Townsend (Mr. T) for making our lab an amazing place to work and for the intellectual scientific (and other) conversations and advice. The Bogomolni lab for the use of their fluorometer. The Partch and Rubin labs for the use of various reagents and instruments. Scott Lokey for giving me the opportunity to research in his lab and for his mentorship and guidance. Scott, the perpetual optimist that he is, always had faith in my projects and always saw them through. My wife and I got married and had two children during my graduate studies at UCSC and Scott has been incredibly understanding about my wanting and needing to take time for my family. For this I am extremely grateful. Thank you Scott and to all the others that have helped me achieve this degree.

1. PHENOTYPIC SCREENING AND THE TARGET IDENTIFICATION PROBLEM

1.1. Introduction

The discovery new drugs and drug targets are of the utmost importance due to the incessant nature of disease and the ever-increasing incidence of drug resistance. With the completion of the Human Genome Project, a decade and a half-ago, came a sense of optimism among pharmaceutical researchers that this enormous amount of data would generate a boom in therapeutic treatments of disease. This has not been the case however. In fact, the approval rate for drugs targeting human gene products has remained steady from 1982 to 2010 producing on average 18 approvals per year[1], a majority of which target previously established entities (Figure 1A, shows from 1987). The approval rate of drugs with novel targets, during the same time span, has also remained quite steady despite the influx of new genetic data and investments made towards this end (Figure 1B, shows from 1987). Two reasons to explain this trend is that either we have exhausted the "drugable target space" or new methods for discovering them need to be developed. There are three major approaches by which pharmaceutical and academic researchers attempt to find new drugs with or without novel mechanisms of action (MOAs); target-based, phenotypic screening and natural product-based. Between 1999 and 2008 the Food and Drug Administration (FDA) approved 259 new drugs, of these, 50 were first-in-class small molecules with novel

MOAs[2]. Of the 50 first-in-class drugs, 28 came from phenotypic screens and 17 from target-based approaches, this coming during an era when target-based approaches

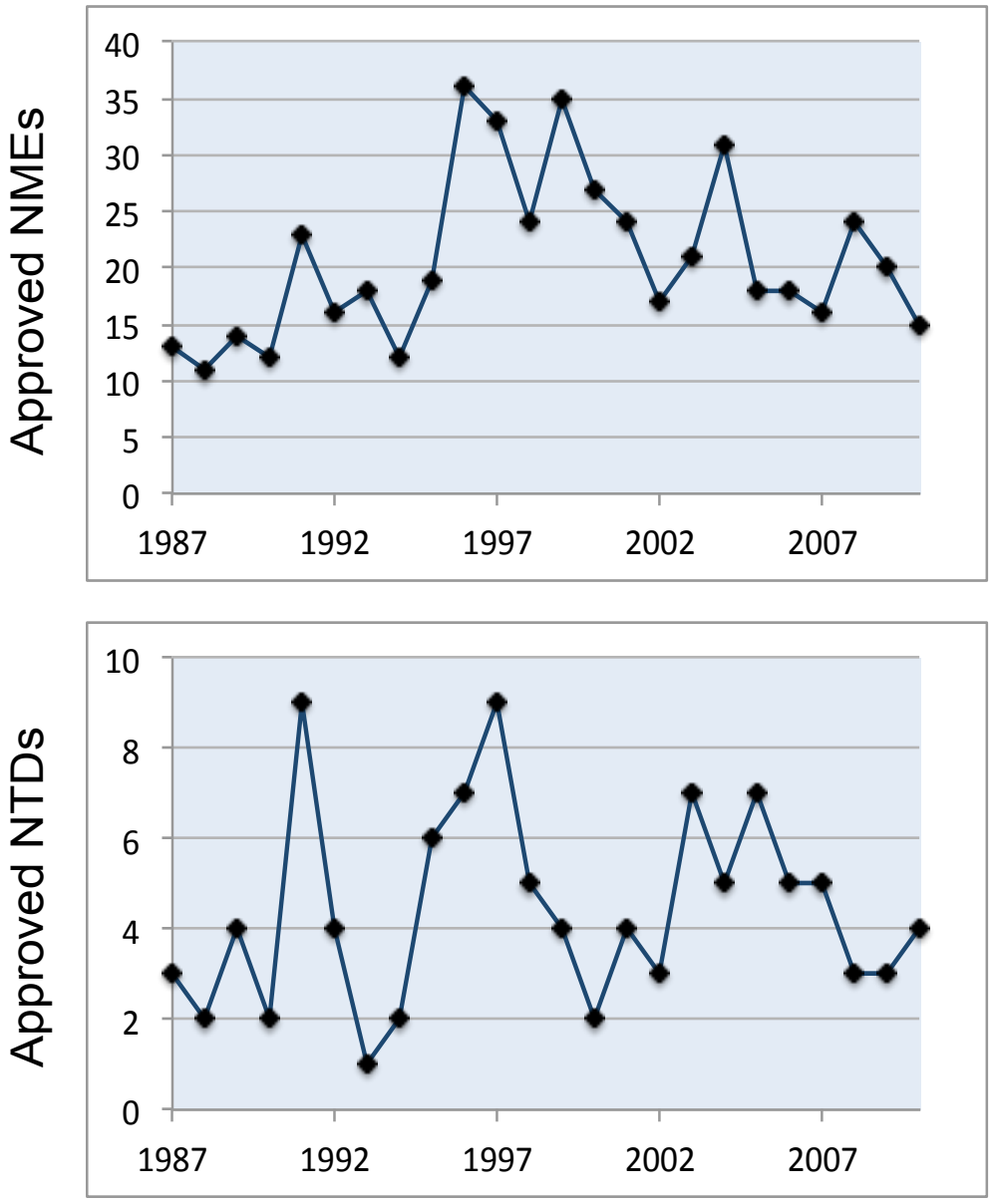

Figure 1-1. A) New small molecule drugs (NMEs) approved by the FDA between 1987 and 2010. Does not include biologics. B) New drugs with novel targets (NTDs) approved between 1987 and 2010.

were more heavily used. The inherent biasedness of target-based efforts points towards phenotypic screening as the answer for the discovery of drugs with novel targets and MOAs.

"The single biggest impediment to drug discovery is the small number of new, validated targets that we have. Phenotypic screening is one way of moving beyond well-defined targets from the literature to discover new therapeutic targets and new disease biology"- Mark Fishman, President of the Novartis Institute

Phenotypic screening however, has drawbacks as well, most importantly is the problem of identifying the targets of bioactive compounds. In this report, we will examine some of the ways that researchers attempt to determine the targets and MOAs of bioactive compounds.

1.2. Yeast as a Model Organism

In 1996 the genome of the budding yeast, *Saccharomyces cerevisiae*, was completely sequenced making it the first eukaryotic genome to be viewed in its entirety. Comprised of 12,068 kilobases coding for 5885 genes, the *S. cerevisiae* genome may well be the most highly characterized among eukaryotic organisms[3]. Researchers have had nearly 20 years to develop and apply functional genomics methodology for this organism. One effort in particular was the *Saccharomyces*

genome deletion project that created deletion mutants for nearly all open reading frames (ORFs) in the *S. cerevisiae* genome[4]. The collection is comprised of a set of ~6000 heterozygous diploid deletion strains used for heterozygous insufficiency profiling (HIP) as well the homozygous deletion set for the ~5000 non-essential genes (HOP) in *S. cerevisiae.* Additional tools that have been developed to study the yeast genome include proteome chips[5], micro-arrays[6] and genome-wide two hybrid[7] collections. There are several databases that catalog yeast genes and information about their sequence, expression, genetic and physical interactions, phenotypes, literature, etc. Two of the most notable are the Saccharomyces Genome Database[8] (SGD) and the Comprehensive Yeast Genome Database[9] (CYGD). Aside from these recent advancements, yeast have other more general attributes that make them attractive model organisms for studying the effects of chemicals on biological systems. For one, is the remarkably high genetic conservation of basic cellular functions among higher eukaryotes. An estimated 2700 yeast genes share at least a portion of their amino acid sequence with at least one human protein[10]. Of these are hundreds that are implicated in human disease[11-13]. For instance, the immunosuprressants FK506 and cyclosporine A (CsA) form toxic complexes with FKBP12 and cylcophilin A, respectively. These complexes target the Ca^{2+}-calmodulin-regulated serine/threonine-specific protein phosphatase, calcineurin in both *S. cerevisiae* and T-cells[14-16]. Another favorable aspect of yeast is the ease of which it can be genetically modified. The creation of whole gene deletions and single nucleotide polymorphisms (SNPs) using polymerase chain reaction (PCR) and/or

homologous recombination have become trivial laboratory tasks and provide an invaluable avenue for discerning the functions of gene products and/or the MOAs of drugs. Finally, the yeast genome is a compact one with one protein-coding gene every 2.3 kb of which only 4% are interrupted by introns[17] .

1.3. Forward Versus Reverse Drug Discovery

Reverse drug discovery (target-based drug discovery) begins with validating a target of interest, usually one that has been demonstrated to be relevant to a specific biological process or disease of interest. Selection and preparation of a suitable target can be time-consuming, since the protein needs be purified and well characterized. Once a validated target is selected a biochemical assay needs to be developed to enable detection of chemicals that bind and/or inhibit the targets function. Hits that are discovered in the assay represent candidate small molecule leads, which are often modified to enhance binding. Once a *bona fide* lead is established it then needs to be tested in animal models to further characterize the MOA and optimize pharmacokinetic (PK) properties (Figure 2). Beside the requirement of a well-characterized target, there are other drawbacks to the target-based approach, one being its inherent biasedness. Screening only against well-characterized protein targets leaves essentially little chance of discovering new, perhaps more effective, modes of modifying cellular processes. During a time of increasing occurrence of drug-resistance, this deficiency is a concern. Another disadvantage is that compounds

are screened *in vitro*, which does not accurately reflect the nature of a cellular environment and can lead to false positive hits that don't behave well *in vivo*.

A

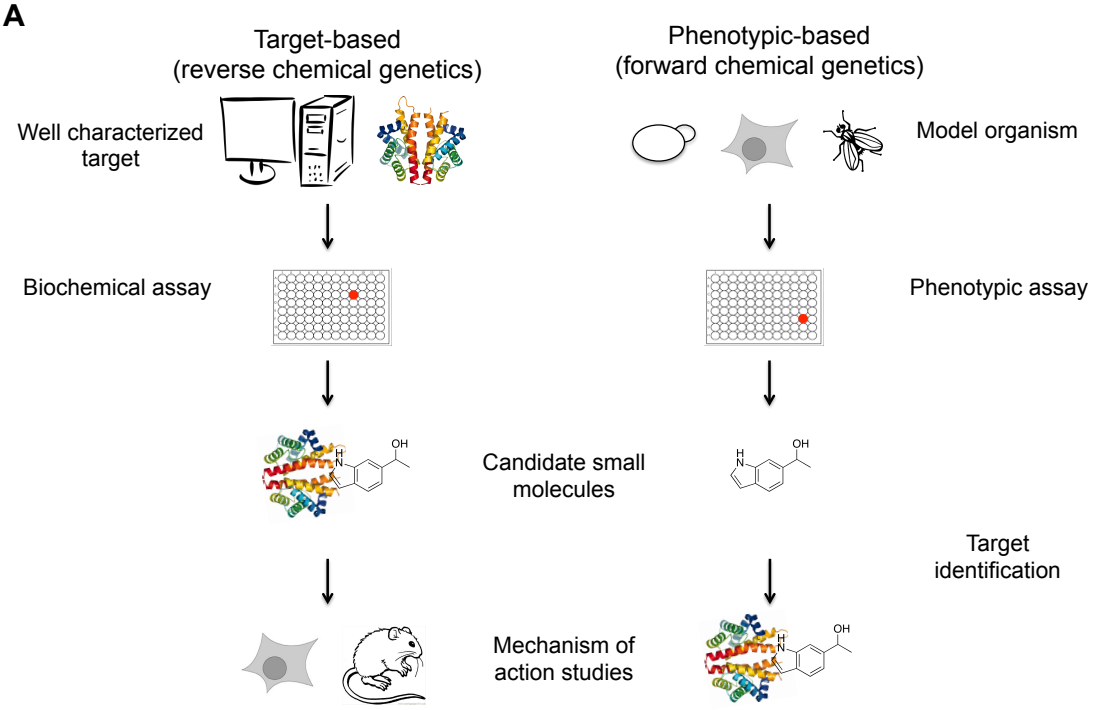

B

Aspects	Target-based	Phenotypic-based
Well-characterized target	yes	no
Biased	yes	no
Model organism	yes	yes
Requires target identification	no	yes
Screen	biochemical	phenotypic

Figure 1-2. A) Typical work-flow for target and phenotypic-based methods of drug discovery. B) Summary of requirements for target and phenotypic-based methods for drug discovery.

Forward drug discovery, in contrast, involves the screening of large libraries of compounds *in vivo* (phenotypic screening), allowing for a genome-wide sampling of possible targets of bioactive entities in an environment that preserves the cellular context of protein function. This approach requires a model organism including those that have been genetically modified to more specifically report on a biological function (i.e. knock-out, knock-down stains). Hits resulting from a phenotypic screen usually give little information about the MOA of the compound requiring follow up studies to gain more information about the causative effect(s) of the compound. There are over one hundred FDA-approved drugs on the market with unknown targets[1]. This is surprising since knowledge about the target of drug can assist medicinal chemistry efforts to improve efficacy while the lack of information can pose safety issues. It is often assumed that the phenotypic effect that a drug elicits is due to an interaction with a discrete target, but many drugs show unwanted off-target effects (side-effects) due to interactions with multiple cellular entities. This underscores the need for methods to quickly, easily and accurately determine the efficacy targets and off-targets of bioactive compounds.

1.4. Methods for Target ID

1.4.1. Classical Genetics

Historically, classical genetics has long been a means for understanding protein function. Using this approach geneticists search for phenotypic changes, often under selective conditions, followed by identification of the gene(s) responsible for the

observed phenotype. Genetics has also been used to understand MOAs of bioactive compounds in biological systems. This involves the isolation of organisms that have developed resistance to the compound of interest followed by the elucidation of the mutation(s) responsible for resistance. It is well documented that resistance-conferring mutations can often be mapped to the cellular target of bioactive compounds. For instance, the MOA and target of the immunosuppressant, rapamycin was discovered in a yeast genetic screen for mutants that confer rapamycin resistance[18]. The resistance mutations were found in the genes *FPR1, TOR1* and *TOR2* the latter of which are named after their association with rapamycin (target of rapamycin). It was observed that the effect of rapamycin resembled that of the *tor1*Δ *tor2*Δ double mutant and that strains depleted of Fkbp12 (protein product of *FPR1*) are viable and rapamycin-resistant. These observations in addition to the fact that the *fpr1, tor1* and *tor2* point mutants are non-allelic and non-complementing led to a model in which rapamycin forms a complex that physically interacts with the Tor proteins causing cell cycle arrest. This model was confirmed when Tor1p and the human homolog mTOR were found to bind the rapamycin-FKbp12 complex *in vitro* [19-23]. Additionally, the rapamycin-FKpb12 complex was shown to interact with yeast Tor2p and mTOR in the two-hybrid system[24,25].

1.4.2. Direct Biochemical Methods

As the name implies, biochemical methods can directly identify cellular proteins, *in vitro,* that physically interact with small molecules. This approach, also referred to as affinity purification, generally requires an immobilized derivative of the

compound of interest that is then exposed to cellular extracts, usually in a vertical column, in an attempt to "fish out or pull down" the target. For expample, an active biotinylated derivative of spliceostatin A was used show that it binds to components of the SF3b splicing subcomplex, which ultimately inhibits spliceosome activity[26]. Similar methods were used to determine that the cyclotetrapeptide, trapoxin, interacts with the histone deacetylase catalytic subunit, HD1, which inhibits histone deacetylation[27]. Another study used an affinity-based approach to determine the target of a small molecule that modulates the circadian clock. They found that it specifically binds cryptochrome (CRY) proteins that are known to function in the circadian clock[28].

While biochemical methods can provide an unbiased and direct route to targets of bioactive compounds, they have their drawbacks as well. For instance, time-consuming synthetic efforts are often needed to immobilize the compound of interest while retaining its cellular activity. Inactive derivatives are also needed to serve as controls, which can be just as challenging if not more in that the inactive version must be different enough that it does not bind the target but not so different that it acquires new physiochemical properties and ultimately new non-specific interactions with cellular entities. After the immobilized compound has been exposed to cell lysate, of which is abundantly required (often pre-fractioned), stringent wash conditions are used to elute out the high affinity proteins. Such conditions are appropriate in situations were a high-affinity compound binds an abundant protein which may not reflect an accurate depiction of the compounds cellular MOA.

Additionally, high stringency washes will likely preclude detecting proteins involved in complexes with the direct target.

Recent advancements have attempted to overcome some of these challenges. Photo-affinity derivatives have been used to covalently secure the target-compound complex enabling the capture of low-abundance and/or low affinity targets[29]. Coupling of covalent modification techniques with two-dimension gel electrophoresis has been used to reduce non-specific interactions[30]. Another approach is to make compound derivatives adorned with peptides to allow for immunoaffinity purification[31].

Another interesting methodology that is quite different from traditional affinity approaches is called drug affinity responsive target stability (DARTS). It is based on the fact that when a target is bound to its ligand the interaction stabilizes the target protein rendering it less susceptible to degradation by proteases[32]. The advancement of mass spectrometry has also greatly enhanced target ID methods. Quantitative proteomics has been applied to exploring protein-small molecule interactions most notably are stable-isotope labeling by amino acids in cell culture (SILAC) and chemical labeling[33]. Isotope-coded affinity tag (ICAT) technology was used to determine that malate dehydrogenase was the target of anticancer compound E707[34].

1.4.3. Genomic Approaches

As a result of the *Saccharomyces* genome project, deletion mutants for almost all annotated yeast ORFs in *S. cerevisiae* were created[4,35]. The collection contains nearly 6000 heterozygous diploid strains corresponding to each gene of the *cerevisiae*

genome, including the ~1000 essentials. A homozygous deletion set, in both mat **a** and mat **α**, was also created for the ~5000 non-essential genes. These collections allow for facile genome-wide chemical-genetic screens otherwise known as haploinsufficiency (for the heterozygous set) and homozygous profiling (for the homozygous set); HIP-HOP. The basis for these screens is that gene dosage can be used as a means of connecting a compound to its target. If more target is present in the cell then more drug is required to elicit the same effect. Conversely, if there is less of the target, as with haploinsufficiency profiling, then less compound is needed and a fitness defect will be observed in the target gene deletion strain. To assay a given compound, all 6000 deletion mutants are pooled and either mock-treated or treated with compound. These cultures are allowed to grow for a period of time followed by genomic DNA isolation and amplification of the deletion specific bar codes of all of the remaining genomes in the population. The gene-specific bar codes for the control and test samples are then quantified *via* DNA microarray or next-generation sequencing (NGS) and compared to one another. The data created by these assays can be compiled to create genome-wide fitness profiles for drugs where a given gene is either sensitive (low bar code counts compared to control), not affected (similar counts as the control) or enhanced (higher counts than the control). Profiles of compounds with unknown targets or MOAs can be clustered with those with known MOAs. Compounds that cluster together may likely have similar MOAs. These

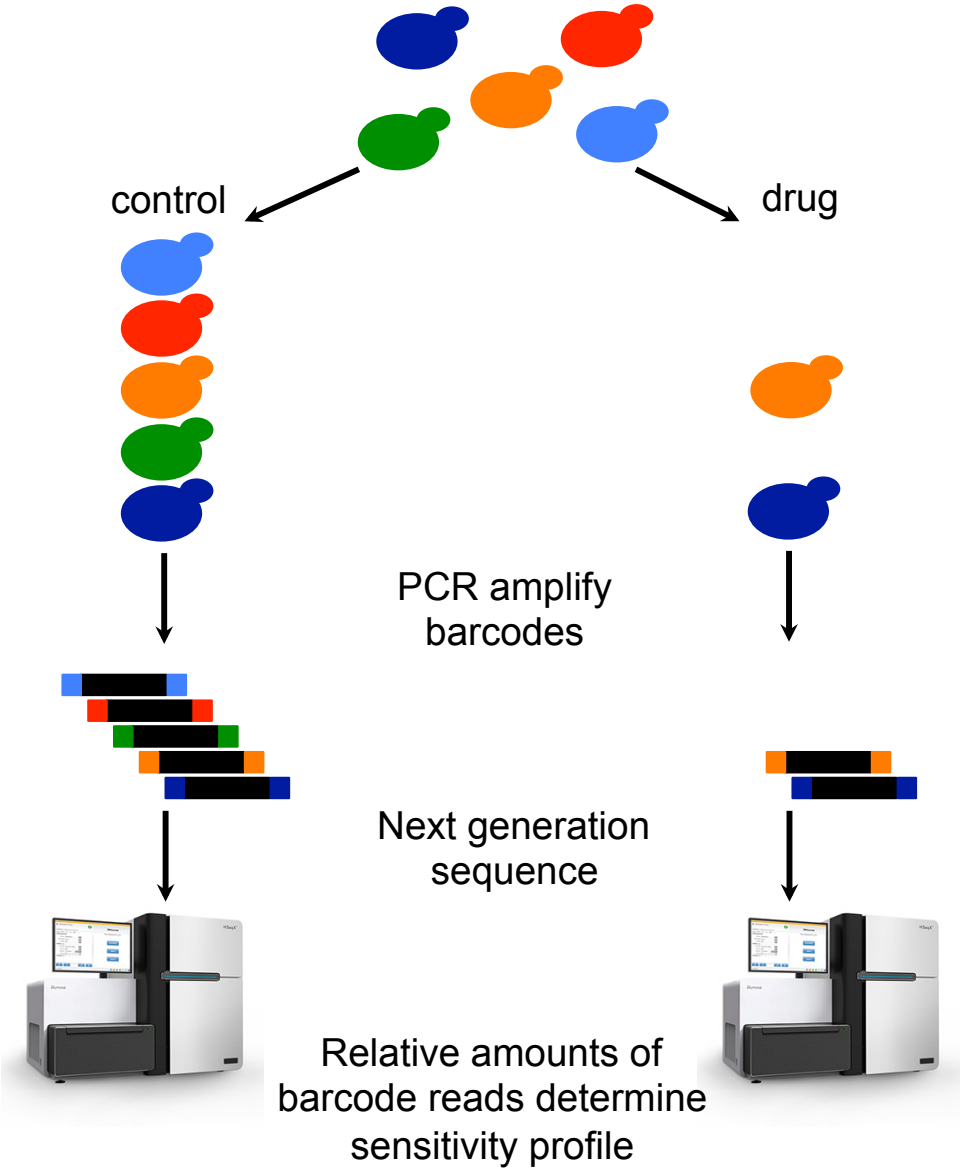

Figure 1-3. Typical work-flow of a chemical-genetic HIP-HOP assay.

methods have been used to validate previously characterized drugs as well as those with unknown MOAs[36]. For instance, the antianginal drug molsidomine was found to

target lanosterol synthase using the heterozygous library[37]. The sponge-derived inhibitor of angiogenesis and metastasis, dihydromotuporamine C[38], was shown, *via* drug-induced haploinsufficiency to target sphingolipid metabolism[39]. Additionally, the drug cincreasin was demonstrated to target the protein kinase Mps1, which is required for checkpoint function[40]. There are some drawbacks and limitations to these methods, however. First and most obviously, the compound must affect the growth rate of the cell in order to be detected. The target of the drug most also be a protein. Non-protein elements such as lipids or DNA will likely not register in the assay, although the homozygous collection may provide information on genes that are in involved in these MOAs. In a similar fashion, drugs that have non-essential targets may not give acute profiles either. The homozygous collection was created for this reason, but this assay inherently cannot report on the direct target, only genes involved in the MOA.

While reducing the amount of a drugs target gene can cause a fitness defect, increasing the amount of a target can result in resistance. This spurred the creation of an over-expression plasmid library. The plasmids can be transformed into yeast and screened against the drug of interest. Strains that confer resistance may likely harbor a plasmid encoding the drugs target. Overexpression studies were used to validate that the antifungal fluconazole targets the cytochrome P-450-dependant C-14 lanosterol α-demethylase encoded by ERG11[41]. Using similar methods, Butcher et al confirmed the target of rapamycin to be the TOR proteins and discovered several candidate targets of a small molecule suppressor of rapamycin-induced growth inhibition[42].

1.5. Target Identification using MUTseq

The aforementioned is to serve as a non-exhaustive mini-survey of target identification methods that have been developed and successfully employed. The remaining of this thesis, however, will refer to a novel method developed in-house: mutagenesis to uncover targets using next-generation sequencing[43]. MUTseq combines old and new. Using the classical genetics concept, that mutations in a drugs target can confer resistance, we isolate resistant mutants and employ next-generation sequencing to locate and quantify the mutations. Genes with high mutation counts represent possible targets. Herein we will see how MUTseq works and, as a proof of concept, how it was used to validate the targets of benomyl (tubulin) and rapamycin (TOR1, TOR2 and FPR1). Finally, a study that delves into the MOA of cationic amphiphilic drugs will be described.

1.6. References

(1) Rask-Andersen, M.; Masuram, S.; Schioth, H. B. Trends in the exploitation of novel drug targets. *Nature reviews Drug discovery* **2011**, *10*, 579-590.

(2) Swinney, D. C.; Anthony, J. How were new medicines discovered? *Nature reviews Drug discovery* **2011**, *10*, 507-519.

(3) Goffeau, A.; Barrell, B.; Bussey, H.; Davis, R.; Dujon, B.; Feldmann, H.; Galibert, F.; Hoheisel, J.; Jacq, C.; Johnston, M. Life with 6000 genes. *Science* **1996**, *274*, 546-567.

(4) Winzeler, E. A.; Shoemaker, D. D.; Astromoff, A.; Liang, H.; Anderson, K.; Andre, B.; Bangham, R.; Benito, R.; Boeke, J. D.; Bussey, H. Functional characterization of the S. cerevisiae genome by gene deletion and parallel analysis. *Science* **1999**, *285*, 901-906.

(5) Zhu, H.; Klemic, J. F.; Chang, S.; Bertone, P.; Casamayor, A.; Klemic, K. G.; Smith, D.; Gerstein, M.; Reed, M. A.; Snyder, M. Analysis of yeast protein kinases using protein chips. *Nature genetics* **2000**, *26*, 283-289.

(6) Horak, C. E.; Snyder, M. Global analysis of gene expression in yeast. *Functional & integrative genomics* **2002**, *2*, 171-180.

(7) Ito, T.; Chiba, T.; Ozawa, R.; Yoshida, M.; Hattori, M.; Sakaki, Y. A comprehensive two-hybrid analysis to explore the yeast protein interactome. *Proceedings of the National Academy of Sciences* **2001**, *98*, 4569-4574.

(8) Cherry, J. M.; Hong, E. L.; Amundsen, C.; Balakrishnan, R.; Binkley, G.; Chan, E. T.; Christie, K. R.; Costanzo, M. C.; Dwight, S. S.; Engel, S. R. Saccharomyces Genome Database: the genomics resource of budding yeast. *Nucleic acids research* **2011**, gkr1029.

(9) Guldener, U.; Munsterkutter, M.; Kastenmuller, G.; Strack, N.; van Helden, J.; Lemer, C.; Richelles, J.; Wodak, S. J.; Garcia-Martinez, J.; Perez-Ortin, J.; Enrique. CYGD: the comprehensive yeast genome database. *Nucleic acids research* **2005**, *33*, D364-D368.

(10) Hughes, T. R. Yeast and drug discovery. *Functional & integrative genomics* **2002**, *2*, 199-211.

(11) Botstein, D.; Chervitz, S. A.; Cherry, J. M. Yeast as a model organism. *Science (New York, NY)* **1997**, *277*, 1259.

(12) Reiter, L. T.; Potocki, L.; Chien, S.; Gribskov, M.; Bier, E. A systematic analysis of human disease-associated gene sequences in Drosophila melanogaster. *Genome research* **2001**, *11*, 1114-1125.

(13) Weaver, T.; Hieter, P. Genome cross-referencing and XREFdb: implications for the identification and analysis of genes mutated in human disease. *Nat Genet* **1997**, *15*, 339-344.

(14) Breuder, T.; Hemenway, C. S.; Movva, N. R.; Cardenas, M. E.; Heitman, J. Calcineurin is essential in cyclosporin A-and FK506-sensitive yeast strains. *Proceedings of the National Academy of Sciences* **1994**, *91*, 5372-5376.

(15) Liu, J.; Farmer, J. D.; Lane, W. S.; Friedman, J.; Weissman, I.; Schreiber, S. L. Calcineurin is a common target of cyclophilin-cyclosporin A and FKBP-FK506 complexes. *Cell* **1991**, *66*, 807-815.

(16) Poor, F.; Parent, S. A.; Morin, N.; Dahl, A. M.; Ramadan, N.; Chrebet, G.; Bostian, K. A.; Nielsen, J. B. Calcineurin mediates inhibition by FK506 and cyclosporin of recovery from Œ±-factor arrest in yeast. **1992**.

(17) Dujon, B. The yeast genome project: what did we learn? *Trends in Genetics* **1996**, *12*, 263-270.

(18) Heitman, J.; Movva, N. R.; Hall, M. N. Targets for cell cycle arrest by the immunosuppressant rapamycin in yeast. *Science* **1991**, *253*, 905-909.

(19) Cardenas, M. E.; Heitman, J. FKBP12-rapamycin target TOR2 is a vacuolar protein with an associated phosphatidylinositol-4 kinase activity. *The EMBO journal* **1995**, *14*, 5892.

(20) Brown, E. J.; Albers, M. W.; Shin, T. B.; Ichikawa, K.; Keith, C. T.; Lane, W. S.; Schreiber, S. L. A mammalian protein targeted by G1-arresting rapamycin-receptor complex. *Nature* **1994**, *369*, 756-758.

(21) Sabatini, D. M.; Erdjument-Bromage, H.; Lui, M.; Tempst, P.; Snyder, S. H. RAFT1: a mammalian protein that binds to FKBP12 in a rapamycin-dependent fashion and is homologous to yeast TORs. *Cell* **1994**, *78*, 35-43.

(22) Sabers, C. J.; Martin, M. M.; Brunn, G. J.; Williams, J. M.; Dumont, F. J.; Wiederrecht, G.; Abraham, R. T. Isolation of a protein target of the FKBP12-rapamycin complex in mammalian cells. *Journal of Biological Chemistry* **1995**, *270*, 815-822.

(23) Chen, J.; Zheng, X.-F.; Brown, E. J.; Schreiber, S. L. Identification of an 11-kDa FKBP12-rapamycin-binding domain within the 289-kDa FKBP12-rapamycin-associated protein and characterization of a critical serine residue. *Proceedings of the National Academy of Sciences* **1995**, *92*, 4947-4951.

(24) Stan, R.; McLaughlin, M. M.; Cafferkey, R.; Johnson, R. K.; Rosenberg, M.; Livi, G. P. Interaction between FKBP12-rapamycin and TOR involves a conserved serine residue. *Journal of Biological Chemistry* **1994**, *269*, 32027-32030.

(25) Chiu, M. I.; Katz, H.; Berlin, V. RAPT1, a mammalian homolog of yeast Tor, interacts with the FKBP12/rapamycin complex. *Proceedings of the National Academy of Sciences* **1994**, *91*, 12574-12578.

(26) Kaida, D.; Motoyoshi, H.; Tashiro, E.; Nojima, T.; Hagiwara, M.; Ishigami, K.; Watanabe, H.; Kitahara, T.; Yoshida, T.; Nakajima, H. Spliceostatin A targets SF3b and inhibits both splicing and nuclear retention of pre-mRNA. *Nature chemical biology* **2007**, *3*, 576-583.

(27) Taunton, J.; Hassig, C. A.; Schreiber, S. L. A mammalian histone deacetylase related to the yeast transcriptional regulator Rpd3p. *Science* **1996**, *272*, 408-411.

(28) Hirota, T.; Lee, J. W.; John, P. C. S.; Sawa, M.; Iwaisako, K.; Noguchi, T.; Pongsawakul, P. Y.; Sonntag, T.; Welsh, D. K.; Brenner, D. A. Identification of small molecule activators of cryptochrome. *Science* **2012**, *337*, 1094-1097.

(29) Evans, M. J.; Saghatelian, A.; Sorensen, E. J.; Cravatt, B. F. Target discovery in small-molecule cell-based screens by in situ proteome reactivity profiling. *Nature biotechnology* **2005**, *23*, 1303-1307.

(30) Park, J.; Oh, S.; Park, S. B. Discovery and Target Identification of an Antiproliferative Agent in Live Cells Using Fluorescence Difference in Two-Dimensional Gel Electrophoresis. *Angewandte Chemie International Edition* **2012**, *51*, 5447-5451.

(31) Saxena, C.; Bonacci, T. M.; Huss, K. L.; Bloem, L. J.; Higgs, R. E.; Hale, J. E. Capture of drug targets from live cells using a multipurpose immuno-chemo-proteomics tool. *Journal of proteome research* **2009**, *8*, 3951-3957.

(32) Lomenick, B.; Jung, G.; Wohlschlegel, J. A.; Huang, J. Target identification using drug affinity responsive target stability (DARTS). *Current protocols in chemical biology* **2011**, 163-180.

(33) Ong, S.-E.; Blagoev, B.; Kratchmarova, I.; Kristensen, D. B.; Steen, H.; Pandey, A.; Mann, M. Stable isotope labeling by amino acids in cell culture, SILAC, as a simple and accurate approach to expression proteomics. *Molecular & cellular proteomics* **2002**, *1*, 376-386.

(34) Oda, Y.; Owa, T.; Sato, T.; Boucher, B.; Daniels, S.; Yamanaka, H.; Shinohara, Y.; Yokoi, A.; Kuromitsu, J.; Nagasu, T. Quantitative chemical proteomics for identifying candidate drug targets. *Analytical chemistry* **2003**, *75*, 2159-2165.

(35) Giaever, G.; Chu, A. M.; Ni, L.; Connelly, C.; Riles, L.; Veronneau, S.; Dow, S.; Lucau-Danila, A.; Anderson, K.; Andre, B. Functional profiling of the Saccharomyces cerevisiae genome. *nature* **2002**, *418*, 387-391.

(36) Giaever, G.; Shoemaker, D. D.; Jones, T. W.; Liang, H.; Winzeler, E. A.; Astromoff, A.; Davis, R. W. Genomic profiling of drug sensitivities via induced haploinsufficiency. *Nature genetics* **1999**, *21*, 278-283.

(37) Lum, P. Y.; Armour, C. D.; Stepaniants, S. B.; Cavet, G.; Wolf, M. K.; Butler, J. S.; Hinshaw, J. C.; Garnier, P.; Prestwich, G. D.; Leonardson, A. Discovering modes of action for therapeutic compounds using a genome-wide screen of yeast heterozygotes. *Cell* **2004**, *116*, 121-137.

(38) Williams, D. E.; Craig, K. S.; Patrick, B.; McHardy, L. M.; van Soest, R.; Roberge, M.; Andersen, R. J. Motuporamines, Anti-Invasion and Anti-Angiogenic Alkaloids from the Marine Sponge Xestospongia e xigua (Kirkpatrick): Isolation, Structure Elucidation, Analogue Synthesis, and Conformational Analysis. *The Journal of organic chemistry* **2002**, *67*, 245-258.

(39) Baetz, K.; McHardy, L.; Gable, K.; Tarling, T.; Rebérioux, D.; Bryan, J.; Andersen, R. J.; Dunn, T.; Hieter, P.; Roberge, M. Yeast genome-wide drug-induced haploinsufficiency screen to determine drug mode of action. *Proceedings of the National Academy of Sciences of the United States of America* **2004**, *101*, 4525-4530.

(40) Dorer, R. K.; Zhong, S.; Tallarico, J. A.; Wong, W. H.; Mitchison, T. J.; Murray, A. W. A small-molecule inhibitor of Mps1 blocks the spindle-checkpoint response to a lack of tension on mitotic chromosomes. *Current biology* **2005**, *15*, 1070-1076.

(41) Kontoyiannis, D. P.; Sagar, N.; Hirschi, K. D. Overexpression of Erg11p by the RegulatableGAL1 Promoter Confers Fluconazole Resistance

inSaccharomyces cerevisiae. *Antimicrobial agents and chemotherapy* **1999**, *43*, 2798-2800.

(42) Butcher, R. A.; Bhullar, B. S.; Perlstein, E. O.; Marsischky, G.; LaBaer, J.; Schreiber, S. L. Microarray-based method for monitoring yeast overexpression strains reveals small-molecule targets in TOR pathway. *Nature chemical biology* **2006**, *2*, 103-109.

(43) Wride, D. A.; Pourmand, N.; Bray, W. M.; Kosarchuk, J. J.; Nisam, S. C.; Quan, T. K.; Berkeley, R. F.; Katzman, S.; Hartzog, G. A.; Dobkin, C. E. Confirmation of the cellular targets of benomyl and rapamycin using next-generation sequencing of resistant mutants in S. cerevisiae. *Molecular BioSystems* **2014**, *10*, 3179-3187.

2. CONFIRMATION OF THE CELLULAR TARGETS OF BENOMYL AND RAPAMYCIN USING NEXT-GENERATION SEQUENCING OF RESISTANT MUTANTS IN *S. CEREVISIAE*

2.1. Introduction

Phenotypic screening provides a powerful mechanism for identifying compounds with novel mechanisms of action (MOAs). Such compounds can become therapeutic leads themselves, or can be used to illuminate new druggable targets. According to one survey, of the 50 first-in-class small molecule drug approvals with novel molecular MOAs from 1999-2008, 28 were discovered through phenotypic screens while only 17 were discovered from target-based programs[1]. The major drawback with phenotypic approaches is that there is no general method for identifying the molecular targets of active compounds. The most common approaches to target ID have involved biochemical purification and affinity-based methods, which often require the costly and time-consuming synthesis of covalently immobilized derivatives. Notable exceptions include the recent application of deep sequencing technology to pinpoint drug resistance mutations in HCT-116 cells[2] and the use of mass spectrometry to identify targets based on their stability to proteolysis in the presence of ligand[3].

Although relatively uncommon in higher eukaryotes, genetic methods have been used for some time to facilitate target ID in simpler systems, especially fungi and bacteria. The budding yeast *S. cerevisiae,* in particular, is an excellent model system for the study of the mechanisms of action of small molecules due to the relative ease

with which it can be manipulated genetically and the high degree of conservation in basic cellular processes between yeast and higher eukaryotes (reviewed in[4]). Indeed, a variety of genome-wide tools have been developed for investigating small molecule MOAs in *S. cerevisiae*. These include the use of barcoded deletion strains to identify chemical-genetic interactions[5-8], high-copy expression libraries to identify phenotypic suppressors[9-11], and high-throughput complementation strategies using heterologous expression of barcoded open reading frames (ORFs)[12]. More recently, an ultra-diverse, barcoded "variomic" library containing thousands of alternate alleles for every yeast gene was used to identify drug resistance alleles which can point directly to drug targets[13]. Using these strategies, not only primary targets, but also "off-target" activities and alternate modes of action for a number of drugs have been identified in yeast[14].

In contrast to techniques that rely on genomic libraries of yeast strains and expression constructs, point mutations that confer drug resistance can be mapped directly to a drug's molecular target. This strategy was used, for example, to identify the targets of rapamycin, TOR1 and TOR2 in yeast[15-17], which ultimately helped to confirm the important homolog mTOR in humans[18]. In addition, targets of the antifungal compounds LY214352 (dihydroorotate dehydrogenase) [19] and UK-118005 (RNA Pol III)[20] were identified by cloning drug resistance genes. In general, classical genetic techniques are employed to characterize specific drug resistance mutations in yeast[20 21]. These methods require genetic crosses and the cloning of large numbers of

mutant alleles of genes, and also a plentiful supply of compound, which, in many cases, may be in limited supply and/or difficult to synthesize.

Next-generation sequencing (NGS) technology has made whole-genome sequencing a viable alternative to traditional genetic mapping approaches. Mutations that confer drug resistance can be pinpointed by simply comparing sequence reads of compound-resistant strains to those of the parental strain. Genes or pathways that display an enrichment in new mutations represent potential targets. For example, the target of a new anti-tuberculosis drug was identified by whole-genome sequencing of resistant clones[22], and NGS approaches have been used to identify mutations responsible for echinocandin resistance in *Candida galbrata*[23]. Deep sequencing was also used to identify mutations that confer resistance to oxidative stress in *S. cerevisiae*[24].

Although these studies point toward whole-genome sequencing as an attractive approach for characterizing drug resistant mutants in *S. cerevisiae*, the specific application of NGS toward the identification of small molecule targets has not been reported. Here we describe the use of NGS to identify drug targets in yeast using a straightforward approach that does not involve the use of tagged genomic libraries or require downstream genetic manipulations. We found that screening for resistance mutants in a *pdr1D* deletion strain minimized the selection of multi-drug resistant (MDR) mutants, and demonstrate that MDR false positives can be further limited by performing cross-resistance screens of candidate mutants in a panel of unrelated drugs. We identified the known targets of benomyl and rapamycin using this

approach (Figure 2-1), and show that NGS offers an orthogonal technique to other chemical genetic approaches available for studying small molecule MOAs in yeast.

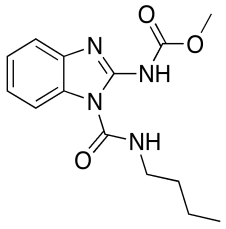

Benomyl

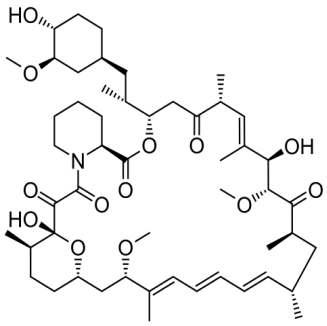

Rapamycin

compound	target	target (common name)	Resistance mutation	Reference
Benomyl	YML085C	TUB1		
	YFL037W	TUB2	R241H	Bostein,D.; et al, Genetics. 1985, 112, 715-734.
Rapamycin	YJR066W	TOR1	S1972*	
	YKL203C	TOR2	S1975R	Heitman J.; et al. J. Biol. Chem. 1995, 270, 46, 27531-27537
	YNL135C	FPR1	R49, F94	Heitman J.; et al. J. Biol. Chem. 1995, 270, 46, 27531-27537

Figure 2-1. Structures of benomyl and rapamycin. List of known targets of benomyl and rapamycin with references. * Heitman, J.; et al. *Science*. *1991*.

2.2. Methods

2.2.1. Resistant Mutant Selection

The *pdr1Δ* strain used for this study was created via homologous recombination from the background strain, BY4741, a derivative of S288C[25](see Supplemental Information for genotype). A preliminary growth study was conducted for both benomyl and rapamycin to determine an optimal drug screening concentration. YPD plates containing 1X, 5X, 10X, 20X, and 40X the IC_{50} of each compound (IC_{50} = 30 μM for benomyl; 25 nM for rapamycin) were inoculated with ~10^7 *pdr1Δ* cells and incubated for two days at 30˚C. The lowest concentration at which less than five colonies were observed was chosen as the dose for the selection of resistant mutants. The optimal selection concentrations for benomyl and rapamycin were determined to be 150 μM and 0.25 μM, respectively. To mutagenize cells with ethyl methanesulfonate (EMS), 1 mL of an overnight culture (~10^8 cells/mL) of *pdr1Δ* was added to a 1.5 mL microcentrifuge tube and pelleted by centrifugation. The supernatant was discarded and the pellet was resuspended in sterile water. The cells were pelleted again and then resuspended in 1 mL of 0.1 M sodium phosphate buffer at pH 7. Next, 30 μL of EMS was added to the EMS sample tube and the tube was vortexed for 15 s and then incubated with inversion at 30° C for 1 h. After incubation, the cells were pelleted and resuspended in 200 μL of 5% sodium thiosulfate to quench the remaining EMS, and then transferred to a clean tube. This thiosulfate wash step was repeated for a total of three times. After the final wash the pellet was resuspended in 1 mL of water, plated in 100 μl aliquots (~10^7 cells) onto 10

plates containing the selection dose determined above and incubated at 30^{o} C for 2 days. As a control, a second aliquot of cells treated identically except for the omission of EMS was selected for resistance in an attempt to discover spontaneous drug-resistant mutants.

2.2.2. Confirmation of Resistance and MDR Screening

EMS-treated and spontaneously resistant mutants from the initial selection were confirmed by re-streaking onto YPD/agar plates containing compound, along with the parental starting strain to serve as a non-viable control. Mutants that yielded colonies within 3 days were considered resistant and evaluated further in a multi-drug resistance cross-screen. This screen was performed using the 384 halo assay as previously reported [26]. Overnight cultures of resistant mutants were seeded in YPD top-agar at an OD_{600} of 0.06 and poured into OmniTrays. After the agar solidified, lethal doses of sixteen known anti-fungal compounds (see Supporting Information for a list of the anti-fungals used), dissolved in DMSO, were pinned into the agar. Plates were incubated at 30^{o} C overnight and then analyzed using an optical density plate reader to quantify growth inhibition by assigning each anti-fungal a 'halo score' for that particular resistant strain.

2.2.3. Genomic DNA Preparation

Mutants chosen for sequencing were grown overnight in 10 mL YPD liquid at 30°C. To pool samples, cultures of individual mutants were diluted to equal ODs and equal amounts of each strain were mixed to give a final volume of 10 mL. Cells were

pelleted by centrifugation, resuspended in 1 mL of sterile water and transferred to a 1.5 mL microcentrifuge tube. The cells were pelleted again and resuspended in 200 µl of lysis buffer (1% SDS, 2% Triton X 100, 100 mM NaCl, 10 mM Tris pH 8, 1 mM EDTA). Approximately 3 g of acid-washed glass beads and 200 µl of phenol:chloroform:isoamyl alcohol (25:24:1) were added to the resuspended cells, which were then vortexed for 3 min. An additional 200 ml of TE was added to the tube and the mixture was centrifuged for 5 min. Following centrifugation, 350 µl of the aqueous (top) layer was carefully removed with a pipette and transferred to a new tube with 1 mL of cold 100% ethanol. The DNA was allowed to precipitate at -20^{o} for at least 1 h (at most, overnight) and then centrifuged for 10 min to pellet the DNA. The DNA pellet was then resuspended in 400 µl of TE and 30 µg of RNase A was added and allowed to incubate at 37^{o} C for 2 h. The sample was then extracted with 400 µl of chloroform:isoamyl alcohol (24:1). Following centrifugation, 350 µl of the aqueous layer was removed and placed into a new tube containing 1 mL of cold 100% ethanol and allowed to precipitate for at least 1 h at 20^{o} C. After this second precipitation the DNA was pelleted and washed twice with 70% ethanol. The DNA pellet was air-dried at room temperature for 10 m and then resuspended in ultra pure water (80-100 µl). The quality and quantity of all samples were checked by gel electrophoresis.

2.2.4. Whole Genome Sequencing

For NGS, high-molecular weight genomic DNA (gDNA) was obtained from *pdr1*Δ benomyl and rapamycin resistant samples as described above. For the library

preparation, 500 ng of gDNA was first sheared to an average size of 300-400 bp using Covaris S2 (Woburn, Massachusettes) according to the manufacturers recommendations. A target insert size of 300-400 bp was then size-selected using an automated electrophoresis DNA fractionation system, LabChip XT (Caliper Life Sciences, Hopkinton, Massachusetts). Paired-end sequencing libraries were prepared using Illumina's TruSeq DNA Sample Preparation Kit (San Diego, California). Following DNA library construction, samples were quantified using the Agilent Bioanylzer per manufacturer's protocol (Santa Clara, California). DNA libraries were sequenced using the Illumina HiSEq2000 in one flow cell lane with sequencing paired-end read length at 2 x 100 bp. Reads were de-multiplexed using CASAVA (version 1.8.2).

2.2.5. Sequencing Data Analysis

Using the software tool Bowtie 2[27], we mapped the raw Illumina sequence data (as .fastq files representing all paired-end reads) from the drug-resistant mutants, as well as the parental strain *pdr1Δ*, to the most current *S. cerivisiae* reference genome assembly (sacCer3; April 2011). Sequencing was performed at a depth of 116 and 100 for the paired reads, and these were trimmed to 70 bases each for the mapping. We kept only the uniquely mapping reads to generate .bam files for each sample, including the parental strain. We found that 95% of the genome was covered by at least one read. These reads were then filtered to include only those that were inside the 1%-tile and 96%-tile in the read-depth distribution (see Supporting Information S2 2-7). We applied the genome analysis toolkit GATK[28,29] to the .bam files from

each mapped sample to produce SNP calls relative to the *sacCer3* reference genome. In order to generate SNP calls, the mapped files were processed using the GATK software to generate VCF files, using the following quality filters for calling SNPs: MQ < 30; FS > 60; ReadPosRankSum < -8.0. For each drug-resistant sample, we subtracted those SNPs that were also found in the *pdr1Δ* parental sample.

2.3. Results

2.3.1. Use of *pdr1*Δ as Parental Stain for Mutant Selection

In an earlier study, we had identified a number of novel cytotoxic compounds in *S. cerevisiae*[30] and had set out to identify their targets by selecting and sequencing drug-resistant mutants. In the first of these studies, we selected eight spontaneous mutants that were resistant to the drug of interest but remained sensitive to a panel of unrelated antifungal compounds. We anticipated that screening for cross-resistance against a diverse panel of unrelated drugs would allow us to eliminate any mutants that acquired resistance through multi-drug resistance (MDR) mechanisms, e.g., through up-regulation of drug efflux pumps or xenobiotic metabolism. Eight of the most promising drug-resistant mutants were selected based on a) resistance to the drug of interest and b) lack of resistance to the cross-screening panel. Sequencing the eight mutants plus the parental strain using NGS (SOLID) technology showed that, despite our efforts to eliminate MDR mutants, all eight of the resistant strains carried a mutation in the multidrug resistance gene *PDR1*. The *PDR1* gene encodes a

transcription factor that regulates the expression of multi-drug resistance genes including drug efflux pumps in the *PDR* family. A variety of point mutations in *PDR1* are known to confer the MDR phenotype[31] and are clustered in distinct regions within *PDR1*. All eight of the *pdr1* point mutations in our drug-resistant samples also clustered in these regions (data not shown).

Different point mutations in PDR1 are known to confer unique patterns of drug resistance, possibly due to the effect of each point mutation on the expression of specific ABC transporters[32]. Thus, while the drug resistance in these mutants appeared to be specific to our drug of interest, this specificity was probably due to the particular efficiency with which the drug was effluxed compared to the other drugs in the cross-screening panel, and not to a mechanism of resistance related to the drug's specific molecular target. These observations prompted us to select for resistance mutations in a *pdr1D* genetic background, which would not only eliminate *pdr1* mutations as sources of drug resistance, but would also make the yeast more drug sensitive in general. This enhanced sensitivity would allow us to use less compound in the selection experiments and could help to minimize other off-target effects. We next set out to test these hypotheses using two drugs whose targets are well established in yeast, benomyl and rapamycin.

2.3.2. Selection and MDR Cross-Screening of Benomyl and Rapamycin Mutants

Equal aliquots of EMS-treated and -untreated *pdr1Δ* cells were plated onto YPD/agar with an optimal lethal dose of either benomyl or rapamycin, determined based on preliminary growth experiments with the parental strain (See Methods). 65 benomyl resistant colonies were isolated from the EMS-treated cells, whereas no resistant colonies arose from the non-EMS-treated cells. All 65 EMS-derived benomyl resistant mutants formed substantial colonies when subjected to a second round of selection on benomyl media, while the parental control strain produced no colonies. Rapamycin selection yielded only six resistant colonies, one from EMS-treated cells and four from non-EMS-treated cells. In a second round of selection on rapamycin plates, all six mutants formed normal sized colonies while the parental formed none.

Using an automated yeast halo assay that we had developed previously[33], we screened the benomyl- and rapamycin-resistant mutants for multi-drug resistance in the presence of 14 antifungal drugs representing a variety of MOA classes (Figure 2-2). Each mutant was seeded in agar and poured into a 384-well-format "omni-tray", and DMSO stock solutions of benomyl, rapamycin, and the 14 drugs in the cross-resistance panel were pin-transferred to each mutant tray. Mutants were chosen for sequencing based on two criteria: 1) They showed no discernable halo for the drug of interest (benomyl or rapamycin); and 2) On average, they were as sensitive as the parental control to the 14-drug panel. Based on the above criteria, 9 of the 65

benomyl-resistant mutants and 5 of the 6 rapamycin-resistant mutants were pooled and genomic DNA from the pools were prepared for sequencing using Illumina HiSeq 2000 (San Diego, Ca).

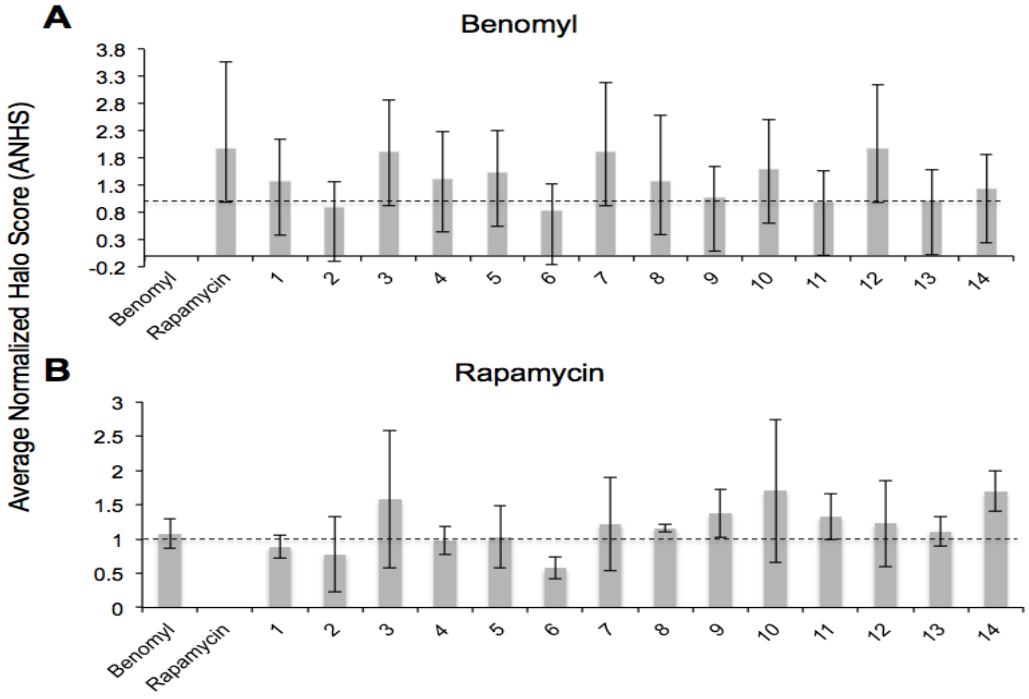

Figure 2-2. (A) Chart displaying the average normalized halo score (ANHS) of the nine benomyl resistant mutants for 16 antifungals, including benomyl (first entry). ANHS values below one (dotted line) indicate resistance, and those above the line indicate sensitivity. Benomyl ANHS values of zero corresponds to an IC_{50} > 2mM. (B) Chart displaying the ANHS of the five rapamycin resistant mutants for 16 antifugals including rapamycin (second entry). Rapamycin ANHS value of zero corresponds to an IC_{50} value of > 1M.

2.3.3. Sequencing of Benomyl and Rapamycin Mutants

We sequenced the pooled benomyl- and rapamycin-resistant mutants using the Illumina HiSeq 2000, and the reads were mapped onto the most current *S. cerevisiae* reference genome (sacCer3). The pool of 9 benomyl- and 5 rapamycin-resistant mutants were sequenced to average read depths of 211 and 199, respectively. When we compared the *pdr1D* sequence with that of the reference genome, ~20% of the 128 SNPs in the putatively haploid *pdr1D* appeared heterozygous. The detection of non-uniform SNPs in a haploid organism is consistent with reports from other genome-wide studies in yeast[24], in which spurious diploidization and transient polysomy has been known to occur during or prior to selection[34,35]. Indeed, all of the SNPs that appeared heterozygous in the parental strain were also found at a similar allele frequency in the drug-selected pools. For this reason, all SNPs that were called in the parental strain were discarded, including at loci that appeared to be diploid.

After subtracting SNPs that were inherited from the parental strain, we obtained 1401 SNPs unique to the benomyl pool, averaging to ~156 SNPs per strain. The vast majority (97%) of these mutations were G-to-A and C-to-T transitions and distributed roughly evenly among the chromosomes. The number and type of mutations were consistent with previous reports on the base change frequency and specificity observed in EMS-treated yeast[36]. The SNPs were further filtered to remove synonymous and non-coding mutations, yielding a final list of 700 exonic SNPs mapping to 639 unique genes (Figure 2-3).

For each SNP, an "allele frequency" (AF) was calculated as the proportion of total reads at that locus carrying the alternate allele. Since each mutant contributed roughly the same amount of DNA to the pool, the number of strains carrying a particular SNP within the pool, i.e., the "allele count" (AC), could be estimated using the GATK software package. We initially set out to determine the significance of

	A	C	G	T
A		1	12	5
C	8		2	799
G	561	0		5
T	1	6	1	

Mutations by Region	Count
Exon	1006
Intron	12
Intergenic modifier	383

Exonic mutation	Count
missense	686
nonsense	14
synonymous	306

Figure 2-3. Benomyl pool SNP statistics. Matrix with base changes (N=1401). List of mutations by region and types of exonic mutation.

obtaining a particular AC by estimating probabilities based on the known mutation frequency and effective EMS-sensitive genome, assuming a random distribution of SNPs among the 9 strains (see Supporting Information, *statistical analysis*). If all the SNPs in the pool were distributed randomly over the 9 genomes in the pool, we calculate that observing even one mutation shared by two or more strains in the pool

would occur in about 1 in 5 experiments. Finding three or more strains with the same mutation would occur by chance in only 2 in 10^5 experiments. And yet we observed 127 SNPs with AC values of 2, and 20 SNPs with AC values of 3. Many of these mutations were synonymous or occurred in non-coding regions, suggesting that they were not selective, and were most likely due to variations in the amount of DNA introduced per strain or variations among strains during the amplification of the DNA. Nonetheless, of the 700 SNPs in the benomyl-resistant pool, the SNP with the highest AC (AC = 4) was a C-to-T transition located in *TUB2*, the gene that encodes benomyl's known target, *b*-tubulin.

Multiple amino acid changes can confer drug resistance within the same target. Therefore, extending the allele count analysis to the gene level can, in principle, add another layer of confidence to the analysis by sidestepping the noise intrinsic to the calculated allele frequencies. For each of the 639 SNP-bearing genes from the benomyl pool, we created a new metric called the gene-level allele count (GL-AC), which represents the sum of the allele counts of all SNPs within a gene (see supplemental, information, *statistical analysis,* for formula). This gives us an upper bound on the number of strains with a mutation in a particular gene. The known benomyl target *TUB2* ranks highest among all genes with a GL-AC score of 8, which means that as many as 8 of the 9 strains might have mutations in that gene. The next-highest ranked genes were two genes with GL-AC scores of 5 (Table 2-1).

gene	position	alternate reads/ total reads	AC	p-value (AC)	GL-AC	p-value (GL-AC)	mutation
TUB2	chrVI:57056	105/223	4	1.20E-09	8	0.008	**R241C**
	chrVI:57371	69/250	3	1.80E-05			P346S
	chrVI:56403	17/214	1	1			T23S
SCJ1	chrXIII:695582	38/125	3	1.80E-05	5	0.65	P78L
	chrXIII:696377	18/186	1	1			G343D
	chrXIII:6964	22/180	1	1			V359I
SPE4	chrXII:433410	58/195	3	1.80E-05	5	0.65	V106I
	chrXII:433661	51/209	2	0.17			S22N

Table 2-1. Benomyl pool sequencing. Top-ranked genes based on gene-level allele count (GL-AC).

In the histogram of GL-AC scores presented in Figure 2-4, *TUB2* stands out among the other genes with its GL-AC score of 8. To determine if the GL-AC scores we observe are evidence of selection, we estimated the probability of observing any genes with GL-AC scores as large or larger than the ones we observe under non-selective conditions (i.e., the GL-AC distribution that one would expect if the 9 strains had been selected at random from a pool of EMS-treated strains under nonselective conditions). We did this by simulating the distribution of GL-ACs under the assumption that the SNPs are distributed randomly over the genes, taking into account gene length and base pair composition (based on the specificity of EMS-treatment for G and C (Supporting Information, *statistical analysis*)). This simulation showed that without selective pressure, from a pool of 9 EMS-treated strains finding even one gene with a GL-AC of 8 or higher would occur in only 8 out of 1000 experiments. On the other hand, finding at least a single gene with a GL-AC of 5 or

higher would occur in 650 out of 1000 experiments. Therefore, *TUB2* is the only gene with a GL-AC value that is highly unlikely to have occurred by chance.

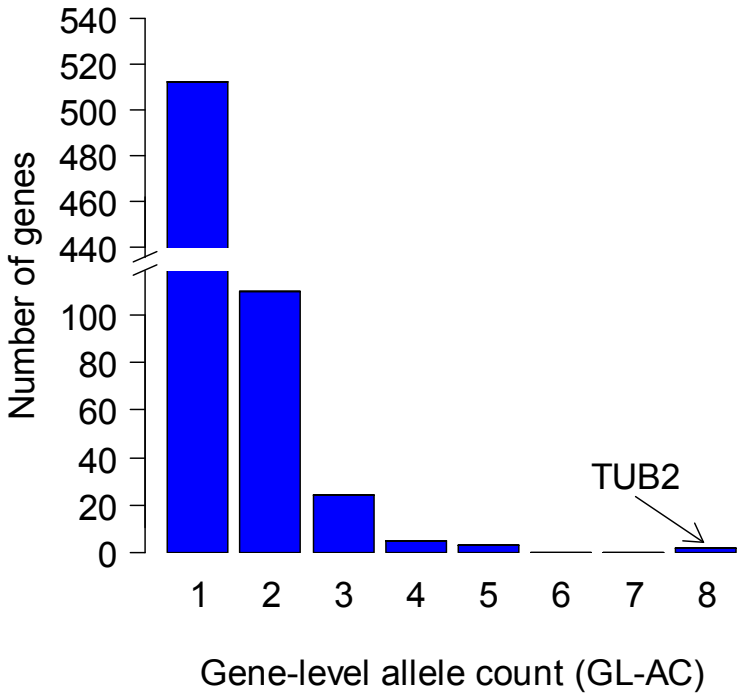

Figure 2-4. Distribution of gene-level allele counts for benomyl pool (GL-AC ≥ 1)

For the 5 pooled rapamycin mutants, one was derived from an EMS-treated line and the other four were spontaneous mutants. The genomic DNA of the 5 mutants were pooled in equal amounts and sequenced in the same manner as described above, to an average read depth of 199**.** SNP calls were performed using the

same parameters as for the benomyl pool, yielding 116 SNPs that were not inherited from the parent.

	A	C	G	G/T	T
A		**1**	**4**	**1**	**2**
C	**6**		**1**	**0**	**44**
G	**35**	**0**			**8**
T	**1**	**2**	**1**		

Mutations by Region	Count
Exon	64
Intron	0
Intergenic modifier	42

Exonic mutations	Count
missense	46
nonsense	4
synonymous	14

Figure 2-5. Rapamycin pool SNP statistics. Matrix with base changes (N=116). List of mutations by region and types of exonic mutation.

After filtering out synonymous and non-coding SNPs, 50 exonic, non-synonymous SNPs remained (Figure 2-5), each mapping to a unique gene. All but one of these SNPs had allele frequencies near 1/5 as depicted in the histogram in figure 6. The only SNP with an AC > 1 was located in the gene *FPR1* (AC=3), which encodes the yeast homolog of the human FK506-binding protein FKBP12, a well-known target of rapamycin (Table 2). Furthermore, there were two unique, non-parental alleles found *at the same locus* (an A-to-G and an A-to-T transition at position chrXIV:372100) proving that, at the very least, there were two strains harboring FPR1 SNPs. The probability of observing three or more strains with a mutation at the same base by

chance is very low (p-value = 1.4 x 10^{-9}) given the low level of mutations in the genome and the fact that there are only 5 strains in the pool (Table 2). The two SNPs

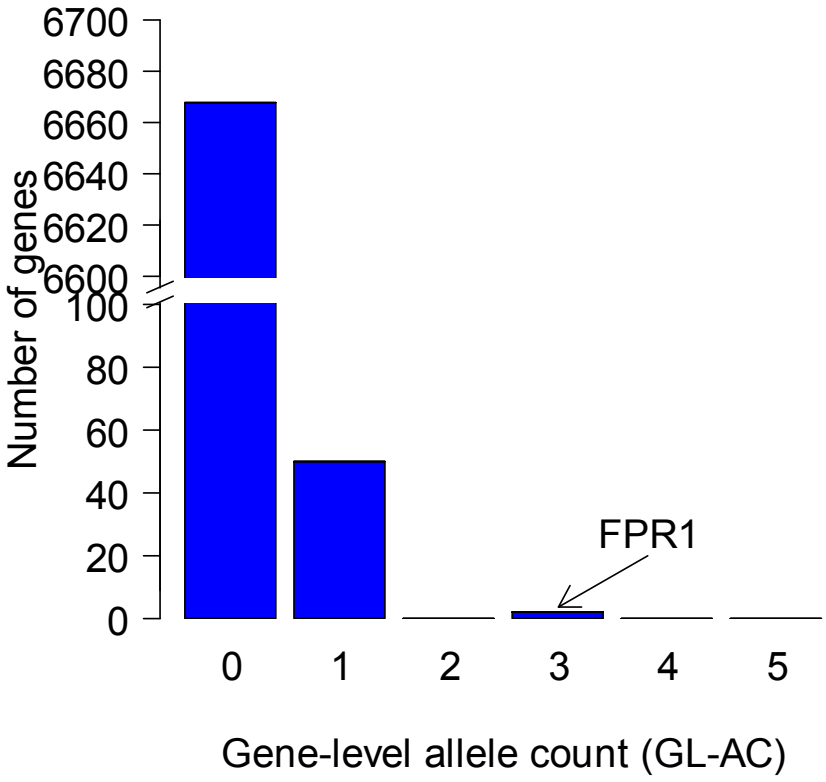

Figure 2-6. Distribution of gene-level allele counts for rapamycin, including those with GL-AC = 0.

represent different but similar amino acid changes: Phe^{43}-to-Ile and Phe^{43}-to-Leu, located near the rapamycin binding pocket in the crystal structure (PDB 1FKB)[37]. Fpr1p binds rapamycin with high affinity, forming a toxic complex that binds and

inhibits target of rapamycin proteins Tor1 and Tor2. Indeed, *TOR1* was among the 50 genes in the rapamycin-resistant pool that carried a mutation.

	gene	position	alternate reads/ total reads	AC	p-value (AC)	GL-AC	p-value (GL-AC)	mutation
1	**FPR1**	chrXIV:372100	38/63	3	1.40E-09	3	0.002	**F43I, F43L**
2	MZM	chrIV:1436553	38/177	1	1	1	1	A113S
3	DCR2	chrXII:847561	33/156	1	1	1	1	G522R
4	ITC1	chrVII:258208	44/212	1	1	1	1	R168C
5	ARO2	chrVII:226630	26/136	1	1	1	1	P78S
:	:							
:	:							
:	:							
16	TOR1	chrX:565331	33/204	1	1	1	1	S1972R
:	:							
:	:							
:	:							
50	NTE1	chrXIII:157425	12/221	1	1	1	1	D278E

Table 2-2. Sequencing results for rapamycin pool. Highest ranking genes based on (gene level allele count) GL-AC.

2.4. Discussion

This proof-of-concept study provides a demonstration of the use of MUTseq for identifying drug targets in yeast. Analysis of the sequencing data from pools of benomyl- and rapamycin-resistant mutants resulted in a ranked list of genes for each drug, at the top of which were their known targets, *TUB2* and *FPR1*. Using MUTseq to confirm the target(s) of benomyl revealed three genes with GL-AC counts of five or more, with *TUB2*, the gene that encodes benomyl's known target, *b*-tubulin, at the top of the list. Interestingly, the most frequent alternate allele in *TUB2* that we

identified corresponds to an Arg-to-Cys mutation at position 241 in *b*-tubulin, which is at the same site as a mutation (Arg to His) previously found in a screen for benomyl resistance[38].

Applying MUTseq to the antifungal, rapamycin revealed the gene *FPR1* (GL-AC=2), which encodes the homolog of the rapamycin- and FK506 binding protein FKBP12. Since four of the five strains in the rapamycin-resistant pool were selected from a set of spontaneous mutants, there were considerably fewer SNPs than in the benomyl pool. While the mutations that we identified in *FPR1* (F43I/L) has not been reported previously, in the crystal structure of the complex with FKBP12 (PDB 1FKB)[37], Phe[43] projects directly into the FK506/rapamycin binding pocket. The SNP that we found in *TOR1* corresponds to the same mutation at Ser[1972] that had been shown previously to confer resistance to rapamycin in yeast[16].

In the absence of selection, the likelihood of finding any SNP with an AC of greater than 2 in non-exonic bases in a pool of 9 strains is very low. It is unlikely that two or more of the benomyl mutants are clones since the EMS protocol used to introduce mutations does not allow for a recovery time after EMS treatment, precluding the cells from replicating and producing clones. A more likely explanation for unexpectedly large number of alternate alleles with AC = 2 and AC = 3 is that during pooling and library preparation prior to sequencing, one of the mutants had become disproportionately represented in the pool (e.g., from differential PCR amplification). Such differences in the relative contributions of strains within the pool, however, would have less of an impact on the interpretation of SNPs with

higher AC values, especially ones that are rare. The only SNP with an AC = 4 in the benomyl pool was the R241C mutation in *TUB2*. If any such high-AC SNPs had arisen from an overrepresented strain, we would have expected other SNPs from this strain with similarly high AC values. GL-AC metric helps to mitigate against this source of error by providing an independent, gene-level analysis of SNPs based on the fact that multiple amino acid changes in the same protein can confer resistance to a drug.

In our selection of resistant mutants we found that the optimal selection conditions, as well as the mutation rates under each condition, were different for the two drugs tested. We obtained no spontaneous benomyl-resistant mutants, but isolated many EMS-derived mutants. In contrast, the majority of the rapamycin-resistant mutants that we identified were spontaneous, and the mutation rate for rapamycin was about 10-fold less than that of benomyl. This suggests that a variety of mutagenesis methods should be employed for each new drug to increase the likelihood of finding a constellation of resistance alleles for each drug. For example, UV-irradiation and proofreading-deficient *pold* mutants show different mutation specificities that are both somewhat orthogonal to that of EMS. Pools of resistant mutants derived from a variety of mutagens would increase the effective genome size available to absorb neutral mutations, while increasing the significance of any genes identified with high GL-AC values.

Of course the use of MUTseq requires that the compound of interest is lethal toward *S. cerevisiae*. While a given drug of interest may not be lethal toward wt

yeast, or even toward classic MDR mutants like *pdr1D*, it may be possible to identify a yeast deletion mutant that is sensitive to the drug. An initial genome-wide search for sensitive haploid deletion mutants could be performed for a given compound using available techniques; such deletion mutants would provide the necessary genetic background for mutant selection, and in addition, the genome-wide sensitivity data could be useful in downstream MOA studies. In order to mitigate against identifying MDR resistance mutations in such cases, it would be advisable to knock out the gene that confers specific resistance in a *pdr1D* background. Our results show that the sequencing of resistant strains of *S. cerevisiae* using NGS shows promise as a general method for identifying small molecule targets in this organism. The unbiased approach of prioritizing mutations, and the known targets that were uncovered in doing so, shows that this MUTseq can be applied to the discovery of new targets of novel compounds. In addition we show that by using the *pdr1D* background strain and screening for multi-drug resistance, we can minimize the occurrence of confounding MDR mutations.

2.5. Supplementary Information

2.5.1. Yeast Genotype: BY4741 MATa his3Δ1 leu2Δ0 met15Δ0 ura3Δ0 pdr1Δ0::kanMX4

2.5.2. Table S2-1. MDR cross screen compounds and concentrations

Compound	Concentration
Hexachlorophene	1mM
Bifonazole	0.5mM
Benzalkonium chloride	2mM
Cetylpyridinium chloride	2mM
Procloroperazine edisylate	100uM
Tetrachloroisophthalonitrile	0.5mM
Chlorhexidine	10mM
Cycloheximide	1mM
Trifluoroperazine HCl	10mM
Chloroxine	10mM
Dihydocelastrol	10mM
Tioconazole	100uM
Cetrimonium Bromide	5mM
Clotrimazole	35mM

2.5.3. Sequencing Coverage Distribution

Figure S2-1

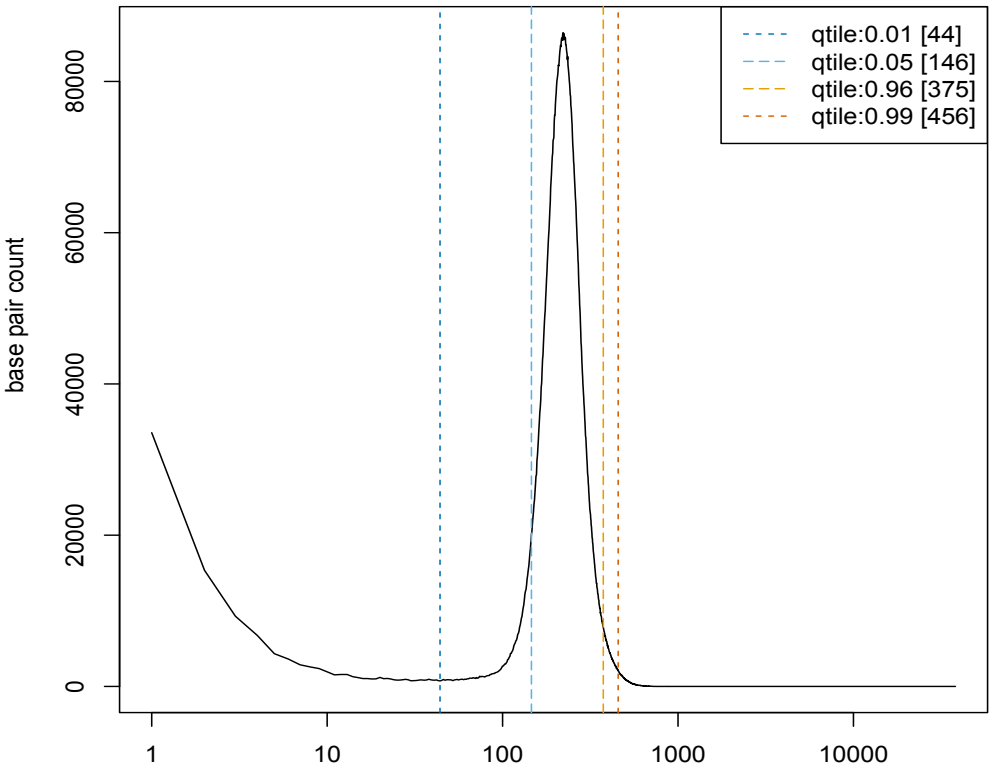

Genome-wide coverage distribution for pdr1 knockout parental control. Log scale read depth values (x axis) for all bases with at least one read (95% of genome). These were filtered further to include only those within the 1% (44 reads) and 96% (375 reads) boundries.

Figure S2-2

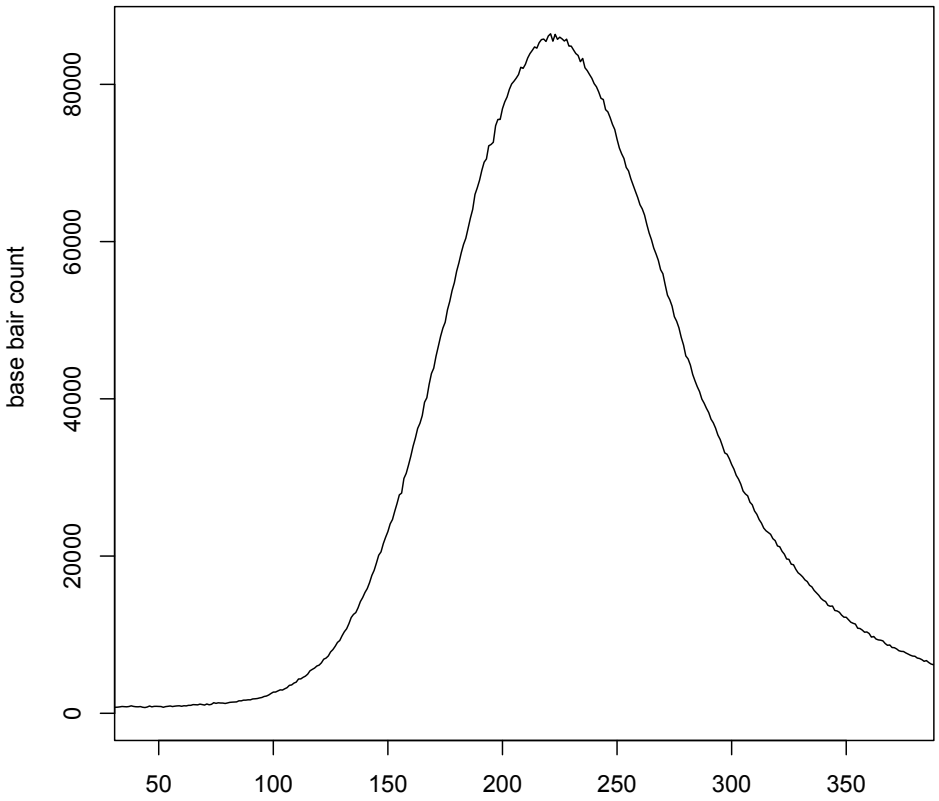

Pdr1 trimmed coverage distribution. Linear scale read depth values (x axis) for all bases between the 1% and 96% boundries for the parental control. Median=229, mean=232, standard deviation=53.7.

Figure S2-3

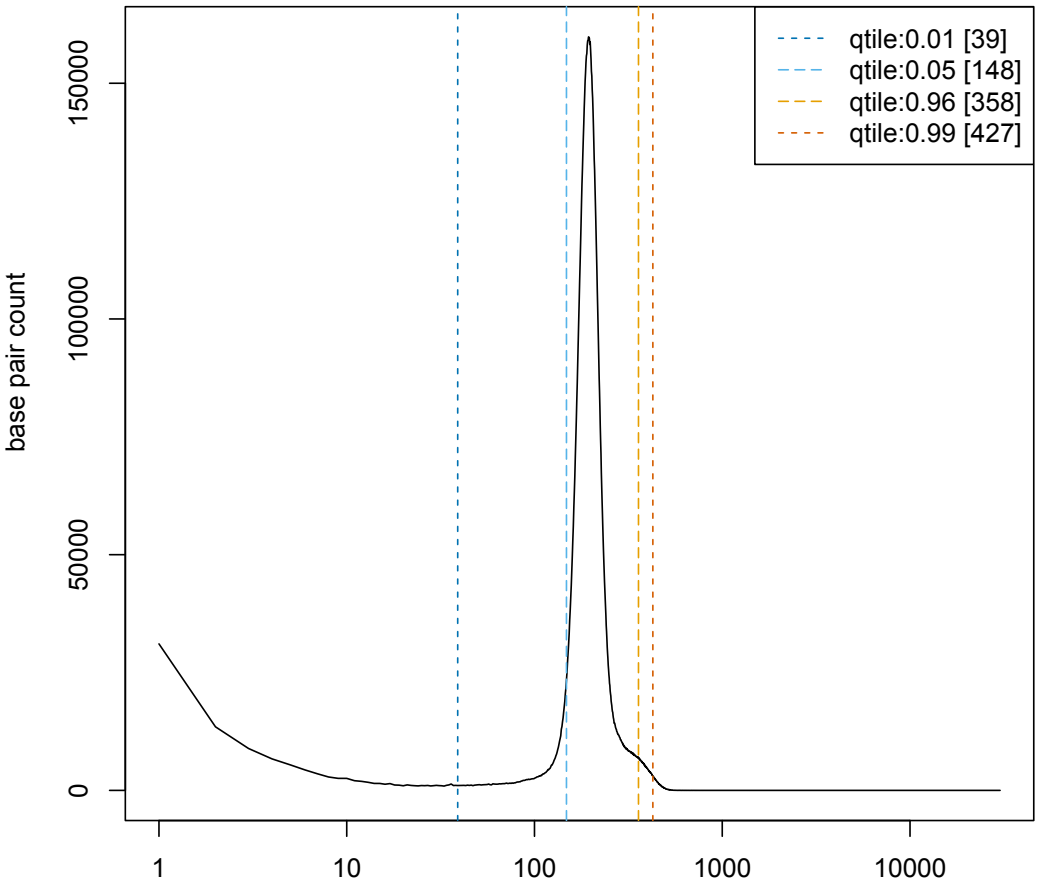

Genome-wide coverage distribution for the benomyl pool. Log scale read depth (x axis) values for all bases with at least one read (95% of genome). These were filtered further to include only those within the 1% (39 reads) and 96% (358 reads) boundries.

Figure S2-4

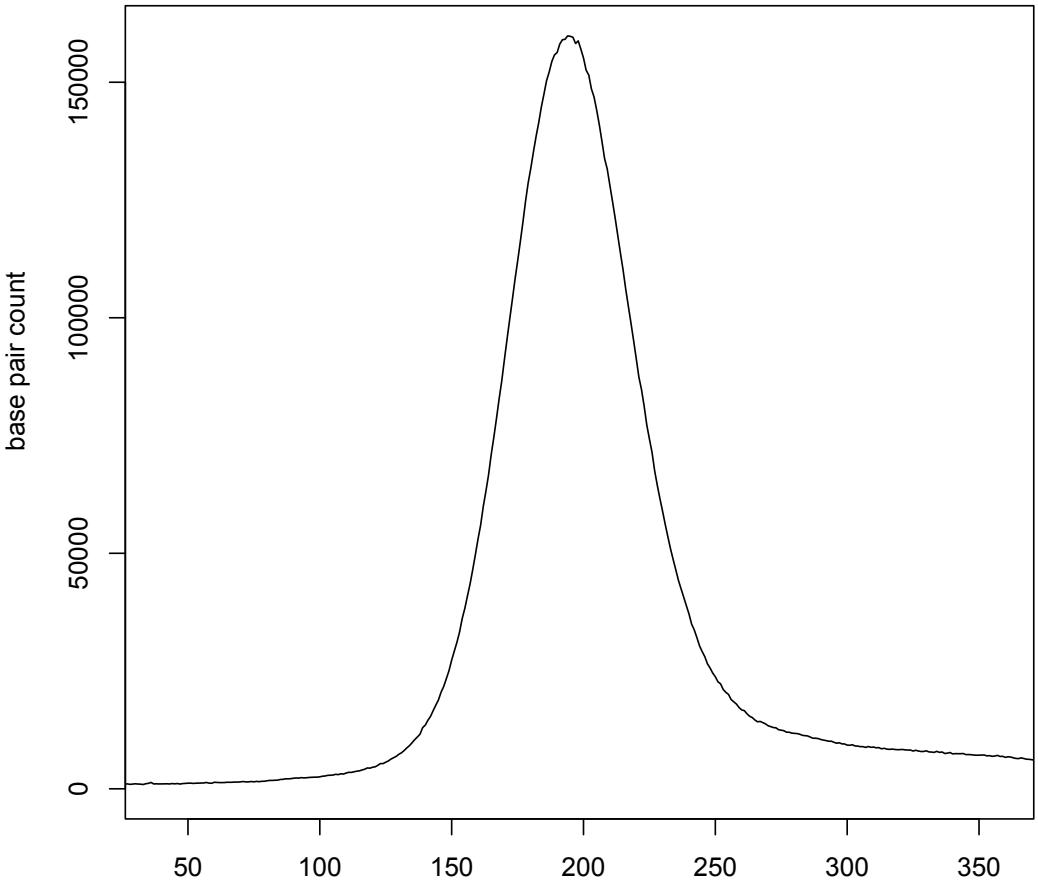

Benomyl trimmed coverage distribution. Linear scale read depth values (x axis) for all bases between the 1% and 96% boundries for the benomyl pool. Median=198, mean=204 and standard deviation=41.9.

Figure S2-5

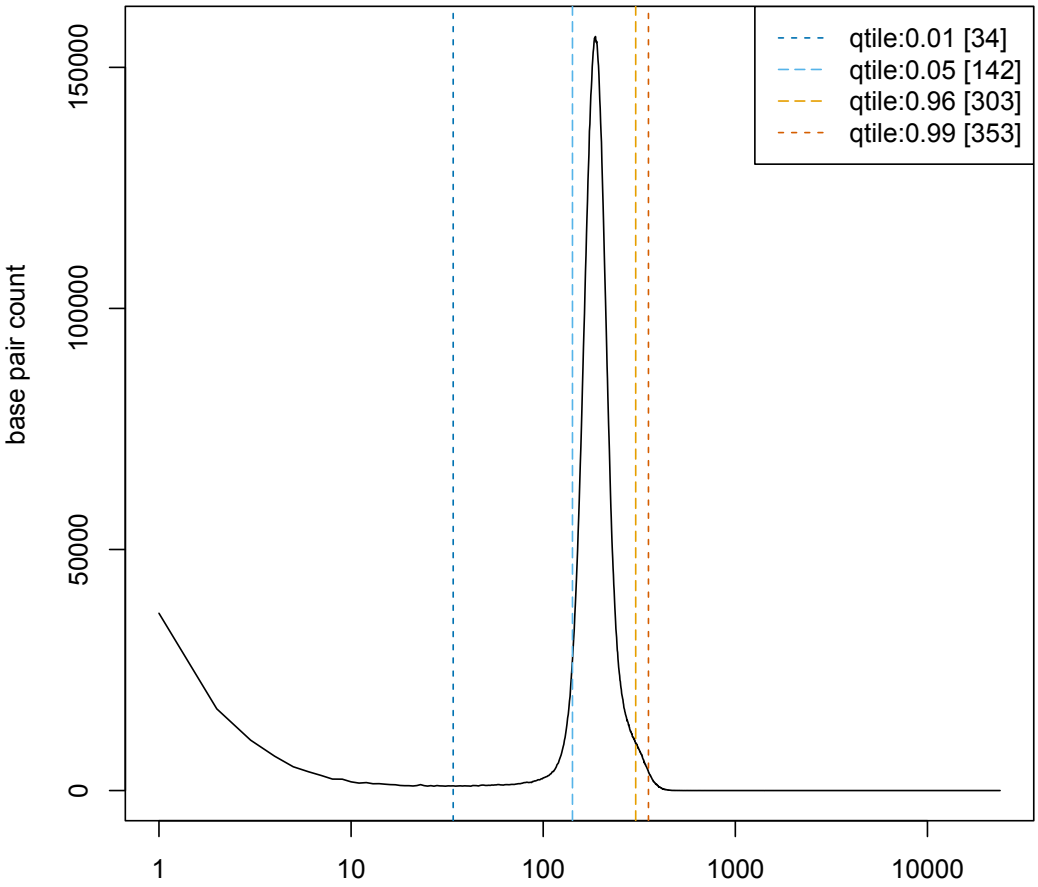

Genome-wide coverage distribution for the rapamycin pool. Log scale read depth (x axis) values for all bases with at least one read (95% of genome). These were filtered further to include only those within the 1% (34 reads) and 96% (303) boundries.

Figure S2-6

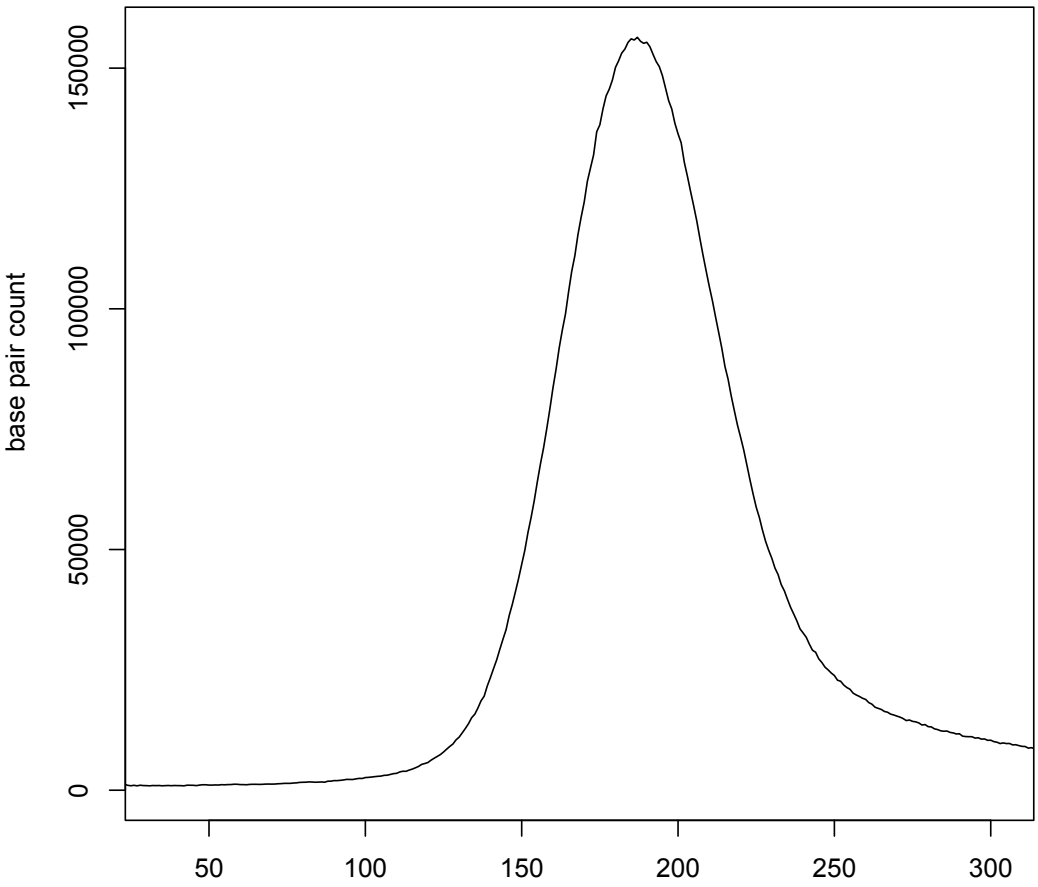

Rapamycin trimmed coverage distribution. Linear scale read depth values (x axis) for all bases between the 1% and 96% boundries for the rapamycin pool. Median=191, mean=194 and standard deviation=35.4.

2.5.4. Statistical Analysis

S2

Probability that x or more strains in a pool have SNPs at a single base

In this section we describe how we estimate the probability that x or more strains have SNPs at a single base somewhere in the genome in the absence of selection. We do this under the assumption that the mutations we observe occur with equal probability at every base. Finding more strains with mutations at a particular base than are likely to occur by chance suggests that the mutation is being selected for. Let S to be the total number of strains included in the pool (in the benomyl pool S=9 and in the rapamycin pool S=5). Define X_A to be the total number of strains with a mutation at a particular base where the reference strain is an A and p_A the probability of a mutation at a base A. The probability of getting X_A strains with a mutation at a single base is

$$P(X_A) = (1-p_A)^{(S-X_A)} p_A^{X_A} \binom{S}{X_A}.$$

The probability of having x or more strains with a SNP at particular location where the reference strain has an A base is $\sum_{j=x}^{S} P(j)$. As a result the probability that the maximum value that X_A takes at any base in the genome ($X_{A,max}$) is greater than or equal to x is

$$P(X_{A,max} \geq x) = 1 - \left(1 - \sum_{j=x}^{S} P(j)\right)^b$$

where b is the number of exonic A bases in the reference genome. A similar formula will generate the estimates for the other three bases. To determine the probability of getting x or more mutations at a base somewhere in the genome we estimate the probability of the complement of that event (getting less than x for all four bases) then subtract it from one.

$$P(X_{max} \geq x) = 1 - P(X_{A,max} < x) * P(X_{G,max} < x) * P(X_{C,max} < x) * P(X_{T,max} < x) \quad (1)$$

For both the benomyl and rapamycin the probability of getting three or more strains with a SNP at a single base anywhere in the genome is very low as can be seen from the estimates of equation 1 in the table below. The estimates differ substantially between the two pools due to the fact that the Rapamycin pool is smaller and has a much lower mutation rate. The estimates are not very sensitive to reducing the number of bases on which a mutation can fall to simulate hot spots.

2.6. References

(1) Swinney, D. C.; Anthony, J. How were new medicines discovered? *Nature reviews. Drug discovery* **2011**, *10*, 507-519.

(2) Wacker, S. A.; Houghtaling, B. R.; Elemento, O.; Kapoor, T. M. Using transcriptome sequencing to identify mechanisms of drug action and resistance. *Nature Chemical Biology* **2012**, *8*, 235-237.

(3) Lomenick, B.; Hao, R.; Jonai, N.; Chin, R. M.; Aghajan, M.; Warburton, S.; Wang, J.; Wu, R. P.; Gomez, F.; Loo, J. A.; Wohlschlegel, J. A.; Vondriska, T. M.; Pelletier, J.; Herschman, H. R.; Clardy, J.; Clarke, C. F.; Huang, J. Target identification using drug affinity responsive target stability (DARTS). *Proceedings of the National Academy of Sciences of the United States of America* **2009**, *106*, 21984-21989.

(4) Menacho-Marquez, M.; Murguia, J. R. Yeast on drugs: Saccharomyces cerevisiae as a tool for anticancer drug research. *Clinical & translational oncology : official publication of the Federation of Spanish Oncology Societies and of the National Cancer Institute of Mexico* **2007**, *9*, 221-228.

(5) Lopez, A.; Parsons, A. B.; Nislow, C.; Giaever, G.; Boone, C. Chemical-genetic approaches for exploring the mode of action of natural products. *Progress in drug research. Fortschritte der Arzneimittelforschung. Progres des recherches pharmaceutiques* **2008**, *66*, 237, 239-271.

(6) Giaever, G.; Shoemaker, D. D.; Jones, T. W.; Liang, H.; Winzeler, E. A.; Astromoff, A.; Davis, R. W. Genomic profiling of drug sensitivities via induced haploinsufficiency. *Nat Genet* **1999**, *21*, 278-283.

(7) Giaever, G.; Chu, A. M.; Ni, L.; Connelly, C.; Riles, L.; Veronneau, S.; Dow, S.; Lucau-Danila, A.; Anderson, K.; Andre, B. Functional profiling of the Saccharomyces cerevisiae genome. *nature* **2002**, *418*, 387-391.

(8) Parsons, A. B.; Lopez, A.; Givoni, I. E.; Williams, D. E.; Gray, C. A.; Porter, J.; Chua, G.; Sopko, R.; Brost, R. L.; Ho, C.-H. Exploring the mode-of-action of bioactive compounds by chemical-genetic profiling in yeast. *Cell* **2006**, *126*, 611-625.

(9) Hoon, S.; Smith, A. M.; Wallace, I. M.; Suresh, S.; Miranda, M.; Fung, E.; Proctor, M.; Shokat, K. M.; Zhang, C.; Davis, R. W.; Giaever, G.; St Onge, R. P.; Nislow, C. An integrated platform of genomic assays reveals small-molecule bioactivities. *Nat Chem Biol* **2008**, *4*, 498-506.

(10) Luesch, H.; Wu, T. Y.; Ren, P.; Gray, N. S.; Schultz, P. G.; Supek, F. A genome-wide overexpression screen in yeast for small-molecule target identification. *Chem. Biol.* **2005**, *12*, 55-63.

(11) Butcher, R. A.; Schreiber, S. L. A small molecule suppressor of FK506 that targets the mitochondria and modulates ionic balance in Saccharomyces cerevisiae. *Chem Biol* **2003**, *10*, 521-531.

(12) Ho, C. H.; Magtanong, L.; Barker, S. L.; Gresham, D.; Nishimura, S.; Natarajan, P.; Koh, J. L.; Porter, J.; Gray, C. A.; Andersen, R. J.; Giaever, G.; Nislow, C.; Andrews, B.; Botstein, D.; Graham, T. R.; Yoshida, M.; Boone, C. A molecular barcoded yeast ORF library enables mode-of-action analysis of bioactive compounds. *Nat Biotechnol* **2009**, *27*, 369-377.

(13) Huang, Z.; Chen, K.; Zhang, J.; Li, Y.; Wang, H.; Cui, D.; Tang, J.; Liu, Y.; Shi, X.; Li, W.; Liu, D.; Chen, R.; Sucgang, R. S.; Pan, X. A functional variomics tool for discovering drug-resistance genes and drug targets. *Cell reports* **2013**, *3*, 577-585.

(14) Lum, P. Y.; Armour, C. D.; Stepaniants, S. B.; Cavet, G.; Wolf, M. K.; Butler, J. S.; Hinshaw, J. C.; Garnier, P.; Prestwich, G. D.; Leonardson, A.; Garrett-Engele, P.; Rush, C. M.; Bard, M.; Schimmack, G.; Phillips, J. W.; Roberts, C. J.; Shoemaker, D. D. Discovering modes of action for therapeutic compounds using a genome-wide screen of yeast heterozygotes. *Cell* **2004**, *116*, 121-137.

(15) Heitman, J.; Movva, N. R.; Hall, M. N. Targets for cell cycle arrest by the immunosuppressant rapamycin in yeast. *Science* **1991**, *253*, 905-909.

(16) Cafferkey, R.; Young, P. R.; McLaughlin, M. M.; Bergsma, D. J.; Koltin, Y.; Sathe, G. M.; Faucette, L.; Eng, W. K.; Johnson, R. K.; Livi, G. P. Dominant missense mutations in a novel yeast protein related to mammalian phosphatidylinositol 3-kinase and VPS34 abrogate rapamycin cytotoxicity. *Mol. Cell. Biol.* **1993**, *13*, 6012-6023.

(17) Kunz, J.; Henriquez, R.; Schneider, U.; Deuter-Reinhard, M.; Movva, N. R.; Hall, M. N. Target of rapamycin in yeast, TOR2, is an essential phosphatidylinositol kinase homolog required for G1 progression. *Cell* **1993**, *73*, 585-596.

(18) Brown, E. J.; Albers, M. W.; Shin, T. B.; Ichikawa, K.; Keith, C. T.; Lane, W. S.; Schreiber, S. L. A mammalian protein targeted by G1-arresting rapamycin-receptor complex. *Nature* **1994**, *369*, 756-758.

(19) Inokoshi, J.; Tomoda, H.; Hashimoto, H.; Watanabe, A.; Takeshima, H.; Omura, S. Cerulenin-resistant mutants of Saccharomyces cerevisiae with an altered fatty acid synthase gene. *Molecular & general genetics : MGG* **1994**, *244*, 90-96.

(20) Wu, L.; Pan, J.; Thoroddsen, V.; Wysong, D. R.; Blackman, R. K.; Bulawa, C. E.; Gould, A. E.; Ocain, T. D.; Dick, L. R.; Errada, P.; Dorr, P. K.; Parkinson, T.; Wood, T.; Kornitzer, D.; Weissman, Z.; Willis, I. M.; McGovern, K. Novel small-molecule inhibitors of RNA polymerase III. *Eukaryotic cell* **2003**, *2*, 256-264.

(21) Gustafson, G.; Davis, G.; Waldron, C.; Smith, A.; Henry, M. Identification of a new antifungal target site through a dual biochemical and molecular-genetics approach. *Current genetics* **1996**, *30*, 159-165.

(22) Andries, K.; Verhasselt, P.; Guillemont, J.; Gohlmann, H. W.; Neefs, J. M.; Winkler, H.; Van Gestel, J.; Timmerman, P.; Zhu, M.; Lee, E.; Williams, P.; de Chaffoy, D.; Huitric, E.; Hoffner, S.; Cambau, E.; Truffot-Pernot, C.; Lounis, N.; Jarlier, V. A diarylquinoline drug active on the ATP synthase of Mycobacterium tuberculosis. *Science* **2005**, *307*, 223-227.

(23) Singh-Babak, S. D.; Babak, T.; Diezmann, S.; Hill, J. A.; Xie, J. L.; Chen, Y. L.; Poutanen, S. M.; Rennie, R. P.; Heitman, J.; Cowen, L. E. Global analysis of the evolution and mechanism of echinocandin resistance in Candida glabrata. *PLoS pathogens* **2012**, *8*, e1002718.

(24) Timmermann, B.; Jarolim, S.; Russmayer, H.; Kerick, M.; Michel, S.; Kruger, A.; Bluemlein, K.; Laun, P.; Grillari, J.; Lehrach, H.; Breitenbach, M.; Ralser, M. A new dominant peroxiredoxin allele identified by whole-genome re-sequencing of random mutagenized yeast causes oxidant-resistance and premature aging. *Aging* **2010**, *2*, 475-486.

(25) Brachmann, C. B.; Davies, A.; Cost, G. J.; Caputo, E.; Li, J.; Hieter, P.; Boeke, J. D. Designer deletion strains derived from Saccharomyces cerevisiae S288C: a useful set of strains and plasmids for PCR-mediated gene disruption and other applications. *Yeast* **1998**, *14*, 115-132.

(26) Woehrmann, M. H.; Gassner, N. C.; Bray, W. M.; Stuart, J. M.; Lokey, S. HALO384: a halo-based potency prediction algorithm for high-throughput detection of antimicrobial agents. *J Biomol Screen* **2010**, *15*, 196-205.

(27) Langmead, B.; Salzberg, S. L. Fast gapped-read alignment with Bowtie 2. *Nature Methods* **2012**, *9*, 357-359.

(28) McKenna, A.; Hanna, M.; Banks, E.; Sivachenko, A.; Cibulskis, K.; Kernytsky, A.; Garimella, K.; Altshuler, D.; Gabriel, S.; Daly, M.; DePristo, M. A. The Genome Analysis Toolkit: a MapReduce framework for analyzing next-generation DNA sequencing data. *Genome Research* **2010**, *20*, 1297-1303.

(29) DePristo, M. A.; Banks, E.; Poplin, R.; Garimella, K. V.; Maguire, J. R.; Hartl, C.; Philippakis, A. A.; del Angel, G.; Rivas, M. A.; Hanna, M.; McKenna, A.; Fennell, T. J.; Kernytsky, A. M.; Sivachenko, A. Y.; Cibulskis, K.; Gabriel, S. B.; Altshuler, D.; Daly, M. J. A framework for variation discovery and genotyping using next-generation DNA sequencing data. *Nature Genetics* **2011**, *43*, 491-498.

(30) Gassner, N. C.; Tamble, C. M.; Bock, J. E.; Cotton, N.; White, K. N.; Tenney, K.; St Onge, R. P.; Proctor, M. J.; Giaever, G.; Nislow, C.; Davis, R. W.; Crews, P.; Holman, T. R.; Lokey, R. S. Accelerating the discovery of biologically active small molecules using a high-throughput yeast halo assay. *J. Nat. Prod.* **2007**, *70*, 383-390.

(31) Carvajal, E.; van den Hazel, H. B.; Cybularz-Kolaczkowska, A.; Balzi, E.; Goffeau, A. Molecular and phenotypic characterization of yeast PDR1 mutants that show hyperactive transcription of various ABC multidrug transporter genes. *Molecular & general genetics : MGG* **1997**, *256*, 406-415.

(32) Balzi, E.; Goffeau, A. Yeast multidrug resistance: the PDR network. *Journal of Bioenergetics and Biomembranes* **1995**, *27*, 71-76.

(33) Woehrmann, M. H.; Gassner, N. C.; Bray, W. M.; Stuart, J. M.; Lokey, S. HALO384: a halo-based potency prediction algorithm for high-throughput detection of antimicrobial agents. *J Biomol Screen*, *15*, 196-205.

(34) Lynch, M.; Sung, W.; Morris, K.; Coffey, N.; Landry, C. R.; Dopman, E. B.; Dickinson, W. J.; Okamoto, K.; Kulkarni, S.; Hartl, D. L.; Thomas, W. K. A genome-wide view of the spectrum of spontaneous mutations in yeast. *Proceedings of the National Academy of Sciences of the United States of America* **2008**, *105*, 9272-9277.

(35) Gerstein, A. C.; Chun, H. J.; Grant, A.; Otto, S. P. Genomic convergence toward diploidy in Saccharomyces cerevisiae. *PLoS Genetics* **2006**, *2*, e145.

(36) Shiwa, Y.; Fukushima-Tanaka, S.; Kasahara, K.; Horiuchi, T.; Yoshikawa, H. Whole-Genome Profiling of a Novel Mutagenesis Technique Using Proofreading-Deficient DNA Polymerase delta. *International journal of evolutionary biology* **2012**, *2012*, 860797.

(37) Van Duyne, G. D.; Standaert, R. F.; Schreiber, S. L.; Clardy, J. Atomic Structure of the Rapamycin Human Immunophilin FKBP-12 Complex. *J. Am. Chem. Soc.* **1991**, *113*, 7433-7434.

(38) Thomas, J. H.; Neff, N. F.; Botstein, D. Isolation and characterization of mutations in the beta-tubulin gene of Saccharomyces cerevisiae. *Genetics* **1985**, *111*, 715-734.

3. SEQUENCING OF RESISTANT MUTANTS IMPLICATE CATIONIC AMPHIPHILIC DRUGS (CADS) AS MODULATORS OF FLIPPASE ACTIVITY IN *RCY1Δ S. CEREVISIAE*

3.1. Introduction

Cationic amphiphilic drugs (CADs) are small molecules comprised of hydrophobic aromatic moieties and a charged amine separated by aliphatic linkers. CADs have long been known to cause drug-induced phospholipidosis (DIPL) in animals[1,2]. DIPL is characterized by the accumulation of polar phospholipids in the lysosome; it was described initially as "foam cell syndrome" in patients with hyperlipidemia and hepatosplenomegaly[3]. This accumulation of intracellular phospholipids in the lysosome is accompanied by the formation of lamellar bodies (Figure 3-1) and has been reported in kidney, liver, spleen, lung and cornea tissues among others[4,5]. According to the FDA, more than 380 different drugs are known to cause DIPL, including a wide range of therapeutics such as antibiotics, antidepressants, antipsychotics and antiarrythmic drugs[6,7]. The potential adverse consequences of DIPL is a serious concern for drug developers, and efforts have been made to predict DIPL-causing agents[7,8]. Recently, a chemogenomics study showed that CADs induced NEO1 haploinsufficiency in yeast and that this fitness signature may be an effective biomarker for identifying DIPL-causing drugs[9]. Another study

used *in vitro* high content screening and *in silico* modeling to study and screen against DIPL-causing compounds[10]. Although a number of theories have been proposed, the

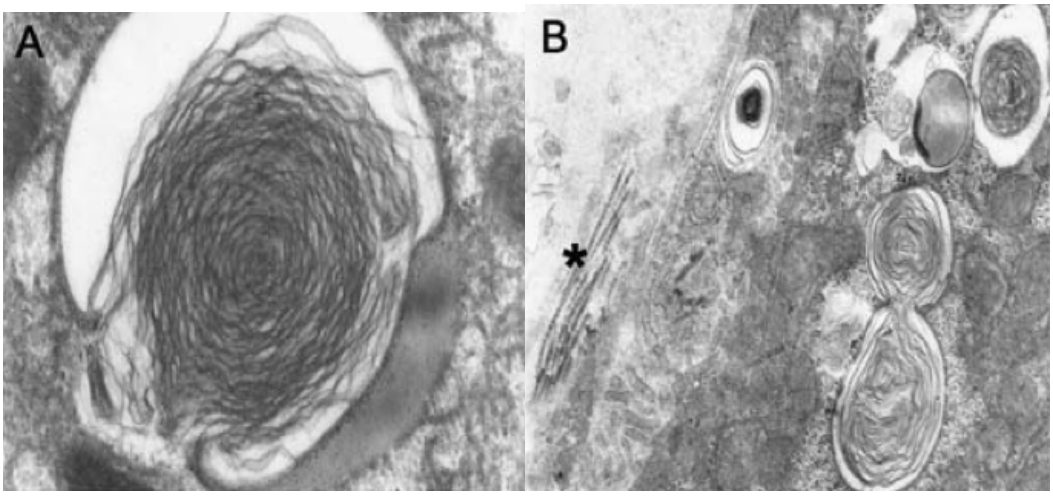

Figure 3-1. A) Lamellar Body. B) Two lamellar bodies fusing in a

exact mechanism by which CADs cause phospholipidosis remains unclear [11-13]. It is thought that CADs form complexes with phospholipids resulting in reduced enzymatic degradation and the creation of an influx gradient of additional phospholipids into the membrane. A second proposal is that CADs directly bind and inhibit phospholipases, thus attenuating the breakdown of phospholipids and perpetuating accumulation.

CADs have also been found to induce hepatitis and intrahepatic cholestasis[14], the impairment of bile salt secretion into the liver canaliculi and then into the duodenum. Cholestasis can cause minimal injury to individual cells[15] and is frequently asymptomatic, and as such the ability to identify CADs that may induce liver injury is of paramount importance when examining drug candidates. The

mechanisms proposed for drug induced liver cholestasis are focused on interference with bile salt transport (such as blockage of BSEP, a bile salt export pump[16], disruption of the lipid bilayer, or disruption of the intracellular actin filaments that help mediate bile salt vesicle transport[15]). The relationship between phospholipidosis and liver cholestasis is not well understood, but intrahepatic cholestasis can also be caused by an inherited mutation in the human gene ATP8B1[17]. This gene encodes a type IV P-type ATPase (a phospholipid transporter (PLT) or "flippase"). Instead of transporting specific cations like other subfamilies of P-type ATPases, PLTs create phospholipid asymmetry by flipping phospholipids from the extracelluar to the cytosolic leaflet[18,19]**.** Several members of the subfamily are important for vesicle budding in the secretory and endocytic pathways [20-22]. Although the actual mechanism by which mutation of this enzyme leads to cholestasis is unknown, these results make it clear that Atp8b1p activity is essential for bile salt transport[23,24].

In a screen of ~24,000 compounds we identified a set of compounds that showed strong chemical synthetic lethality with *RCY1*, a gene that encodes an F-box containing protein involved in membrane protein recycling and vesicular trafficking[25,26]. Many of these compounds were known CADs or were very similar in structure to known CADs including the anti-psychotic haloperidol, a compound known to cause DIPL. These compounds were highly potent in *rcy1*Δ but virtually inactive in wild type, suggesting that their MOAs might be related to the function of Rcy1p in vesicle trafficking. We selected resistant mutants to a novel CAD, **3346-2086**, in the *rcy1*Δ background and sequenced their genomes *via* next generation

sequencing (NGS). The sequencing revealed a cluster of resistance-conferring single nucleotide polymorphisms (SNPs) in genes coding for the phospholipid translocases (PLTs): Drs2p, Dnf1p, and Dnf2p. These results suggest that there is a functional relationship between CADs, Rcy1p and flippases, which may be related to previous studies suggesting that Rcy1p and Drs2p physically interact[27]. Sensitivity profiles in *rcy1*Δ may help predict chemotypes that are prone to causing DIPL and/or drug-induced cholestasis.

3.2. Methods

3.2.1. Strains and Plasmids *(Supplemental Information Table S3-1)*

3.2.2. Synthesis *(Supplemental Information)*

3.2.3. Mutant Selection and Confirmation

Optimal drug concentration for the selection of resistance mutants was determined in a preliminary screen in which ~10^7 cells were plated onto YPD agar containing **3346** at 5X, 10X, 20X and 40X its IC_{50} in *rcy1*Δ (~1 μM). The optimal screening concentration is defined as the lowest concentration on which less than 5 colonies grew. This concentration was determined to be 40 μM. To mutagenize cells with ethyl methanesulfonate (EMS), 1 mL of an overnight culture (~10^8 cells/mL) of *pdr1Δ* was added to a 1.5 mL microcentrifuge tube and pelleted by centrifugation. The supernatant was discarded and the pellet was resuspended in sterile water. The cells were pelleted again and then resuspended in 1 mL of 0.1 M sodium phosphate

buffer at pH 7. Next, 30 µL of EMS was added to the EMS sample tube and the tube was vortexed for 15 s and then incubated with inversion at 30° C for 1 h. After incubation, the cells were pelleted and resuspended in 200 µL of 5% sodium thiosulfate to quench the remaining EMS, and then transferred to a clean tube. This thiosulfate wash step was repeated for a total of three times. After the final wash the pellet was resuspended in 1 mL of water, plated in 100 µl aliquots (~10^7 cells) onto 10 plates containing the selection dose determined above and incubated at 30° C for 2 days. As a control, a second aliquot of cells treated identically, except for the omission of EMS, was selected for resistance in an attempt to discover spontaneous drug-resistant mutants. Apparent EMS-treated and spontaneous mutants from the initial selection were reselected to confirm resistance by re-streaking onto plates containing **3346**. The parental strain was also struck out on every confirmation plate as a non-viable control.

3.2.4. High Throughput Screening

Chemical libraries and mutants were screened using the Halo384 assay developed previously[28,29] . Overnight cultures of the strains to be screened were seeded into YPD agar at a concentration of 0.06 OD_{600} and poured into OmniTrays. After agar solidification, the chemical libraries (as 10mM stock solutions in DMSO) were pin-transferred into the seeded YPD agar plates (approx. 0.2 ul). The ChemDiv and Spectrum collections were pinned from 384 well stock plates at 10mM. The inoculated and drug-treated plates were then incubated at 30° C overnight and subsequently analyzed using an optical density plate reader to quantify growth

inhibition by assigning each compound a 'halo score' for that particular resistant strain. We used an algorithm based on a set of known compounds which allows for the extrapolation of IC_{50} values from halo scores[29].

3.2.5. Sequencing of 3346-resistant Mutants

For pooled samples, liquid cultures of each mutant were diluted to the same OD and mixed in equal parts to a final volume of 15 mL. Genomic DNA (gDNA) was then extracted using the protocol described previously[30]. For the DNA library preparation, 500 ng of gDNA was first sheared down to 300–450 bp using the Covaris S2 (Woburn, MA) per the manufacturer's recommendations. A target insert size of 300–400 bp was then size-selected using the automated electrophoretic DNA fractionation system LabChip XT (Caliper Life Sciences). Paired-end sequencing libraries were prepared using Illumina's TruSeq DNA Sample Preparation Kit (San Diego, CA). Following DNA library construction, samples were quantified using the Agilent Bioanalyzer per the manufacturer's protocol (Santa Clara, CA). DNA libraries were sequenced using the Illumina HiSeq. 2000 in one lane of the flow cell with sequencing paired-end read length at 2 × 100 bp. Reads were demultiplexed using CASAVA (version 1.8.2). Using the software tool Bowtie2[31] the raw Illumina sequence data (as .fastq files representing all paired-end reads) from the 3 pools of drug-resistant mutants , as well as the parental strain *pdr1Δ rcy1Δ*, were mapped to the most current *S. cerevisiae* reference genome assembly (sacCer3; April 2011). Sequencing was performed to a length of 100 bases for each end of the paired-end reads, and these were trimmed from the 3' end to 70 bases each for the mapping.

Only the uniquely mapping reads were kept to generate alignment files in the *bam* format[32] for each sample, including the parental strain. The genome analysis toolkit GATK[33,34] was applied to the *bam* files from each mapped sample to produce SNP calls for each sample relative to sacCer3 reference genome. When calling SNPs in the drug-resistant pools, the GATK "ploidy" parameter was set to 6, 5, or 8, corresponding to the number of haploid strains included in the pool, allowing the program to estimate the allele frequency of each SNP. For each drug-resistant pool, we subtracted those SNPs that were also found in the parental sample. SNPs were also filtered out whose loci had read depths outside the 1%-ile and 96%-ile in the read-depth distribution. The mean read depth for the parental and 3 drug-resistant pools was 174, 262, 259, 64, respectively. The lower 1%-ile limit was 53, 17, 18, 24 respectively and the upper 96%-ile limit was 318, 479, 473, 130, respectively. (S3 6-9).

3.2.6. Flippase Activity Assay

Liquid yeast cultures were grown to early-mid log phase in SD medium (complete). Aliquots (10-200 μL, depending on cell density) of the growing cultures were diluted into 1 ml of SD containing 1 ug/mL propidium iodide. Drugs were added from a 10 mM stock in DMSO, incubated for various periods of time (5 min to overnight) at 20 ^{o}C, and then C14/C6-7-nitro-benz-2-oxa-1,3-diazol-4-yl (NBD) analogues of phosphatidylcholine (PC) was added from a 1 mM stock in $CHCl_3$ or from a 100 μM micelle suspension in saline to a final concentration of 1.2 μM. The suspension was immediately introduced into the cytometer and data taken for 2-5

min. The flow cytometer output files (Listmode files) from these runs were then analyzed, and the level of green fluorescence determined as a function of time for phospholipid-negative cells of a size just larger than single cells (corresponding to growing/budding cells). The slope of the resulting linear uptake of probe was then determined by least squares fit, and reported a rate. At V_{max} conditions, that rate is only dependent on the activity of enzyme in the cell plasma membrane, which was reproducible for a given strain under these conditions.

3.2.7. Dithionite Scrambling Assay

This procedure was adopted from that described by Zhou et al[35]. The phospholipid scrambling effects of CADs was quantified by observing the rate of NBD-PL quenching by dithionite. Phospholipids (PLs) and fluorescent derivatives (NBD-PLs) were purchased from Avanti Polar Lipids. These included 1,2-dioleoyl-*sn*-glycero-3-phosphocholine (DOPC), 1-palmitoly-2-[6-(NBD-amino)hexanoyl]-*sn*-glycero-3-phospho-L-serine (NBD-PS), 1-palmitoly-2-[6-(NBD-amino)hexanoyl]-*sn*-glycero-3-phosphocholine (NBD-PC) and1-palmitoly-2-[6-(NBD-amino)hexanoyl]-*sn*-glycero-3-phosphoethanolamine (NBD-PE). NBD-PL containing liposomes were prepared by dissolving DOPC in 1-2 ml of chloroform which was then blown down and stored overnight in a desiccator. The dry film was then hydrated by resuspending the lipids in 10mM phosphate 100mM NaCl buffer (liposome buffer) followed by gentle vortexing for 1 h. The hydrated lipids were the extruded through a 0.2 μm Nucleopore track etch membrane to afford 1% NBD-PL DOPC liposomes. To preform the assay, 40μl of liposomes were suspended in liposome buffer (20mg

lipid/ml). The liposome suspensions were monitored on a fluorometer for 60 s, to establish a baseline fluorescence, at which time drug or DMSO (10µl) was added. The drug-treated liposomes were read on the fluorometer for 540 s, to ensure that quenching due to the drug had plateaued. At this time 10µl of 1M tris 1M dithionite was added to the cuvette and fluorescence readings were taken for an additional 480s. Rates of fluorescence decrease due to phospholipid scrambling were calculated from fluorometer readings in a 3 min time interval between 3 and 8 min after the addition of dithionite to ensure that outer leaflet NBD-PL quenching had plateaued.

3.3. Results

3.3.1. High-Throughput Screening of the ChemDiv Library in *S. cerevisiae*

The biological basis for multidrug resistance in yeast is poorly understood. While the MDR phenotype can sometimes be ascribed to drug efflux pumps and transcription factors that control their expression (e.g. *PDR1, PDR3, PDR5, SNQ2* and *YOR1*)[36-38], there are other MDR pathways that are more indirect and less well understood, such as aromatic amino acid biosynthesis, and vesicle trafficking[39]. We set out to study the chemical sensitivity profiles of less well-characterized MDR pathways. To this end, we screened a 23,000-member diversity library of drug-like molecules and a 1500 member library of known drugs for their effect on eight yeast MDR mutants in addition to WT. The yeast mutants included *ARO2* (aromatic amino acid biosynthesis[40]), *ERG4* (ergosterol biosynthesis[41]), *COG7* (protein trafficking[42]),

VPS3 (vacuolar protein sorting[43]), *PEP12* (vesicular trafficking[44]), *PDR1* (drug response[45]), *PDR5* (drug pump[46]) and *RCY1* (membrane trafficking and recycling[25]).

Of the 23,000 compounds screened, 1,268 showed measurable halos in at least one of the mutants. As expected, the mutants were sensitive to a larger number of compounds than WT and were, on average, more sensitive to compounds that

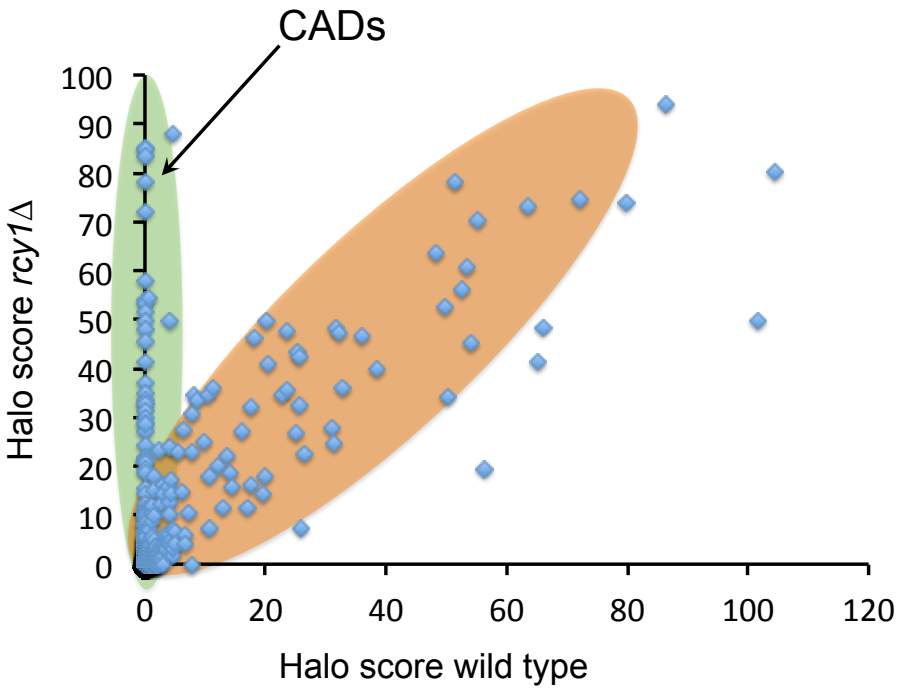

Figure 3-2. Plot of halo scores in wild type versus *rcy1*Δ from a screen of the ChemDiv library. Data points highlighted in green represent compounds that are active in *rcy1*Δ but not in wild type. Data points highlighted in orange represent compounds that are active in wild type and are as or more sensitive in *rcy1*Δ.

effected both. Surprisingly, the classic drug pump mutants *pdr1*Δ and *pdr5*Δ were the least sensitive among the 8 MDR mutant strains compared to wild type, while the

A

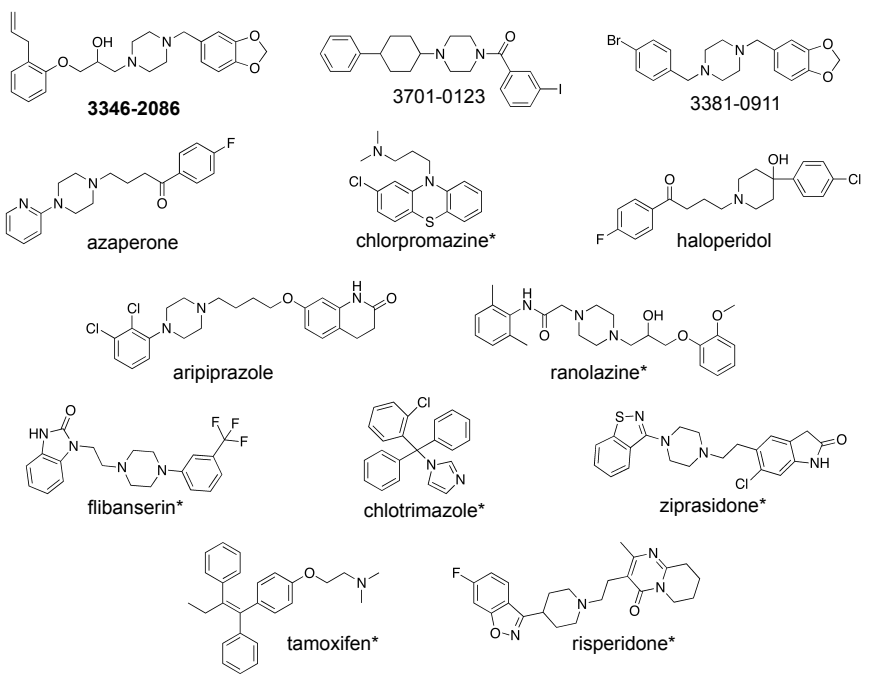

B

compound	WT	*rcy1*Δ	*erg4*Δ	*pdr5*Δ	DIPL	reference
3346-2086	>200	0.78	>200	>200	unknown	n/a
3381-0911	>200	0.97	>200	>200	unknown	n/a
3701-0123	>200	1.9	>200	14.4	unknown	n/a
azaperone	>200	0.4	>200	>200	unknown	n/a
haloperidol	>200	0.91	>200	>200	yes	Reasor
chlorpromazine	>100	27.1	n/a	n/a	yes	Kodavanti
tamoxifen	18.8	8	n/a	n/a	yes	Reasor
ziprasidone	37	2.8	n/a	n/a	unknown	n/a
clotrimazole	5.1	1.7	n/a	n/a	yes	Ribelin
aripiprazole	53.5	53.7	n/a	n/a	unknown	n/a
flibraserine	>100	>100	n/a	n/a	unknown	n/a
ranolazine	>100	>100	n/a	n/a	no**	Scheurel
risperidone	>100	>100	n/a	n/a	no	Mesens

Figure 3-3. A) Structures of CAD hits from screens of the ChemDiv and Spectrum libraries. B) Estimated IC_{50} (μM) values for the CADs in figure A in wild type, *rcy1*Δ, *erg4*Δ and *pdr5*Δ dermined by extrapolation of halo scores using an algorithm developed previously. IC_{50} values for ziprasidone, filbraserine, chlorpromazine and ranolazine were determined via concentration dependent growth inhibition in liquid and were not screened against *erg4*Δ or *pdr5*Δ. * Not library compounds. **Speculated causative agent. References

recycling mutant *rcy1*Δ was the most sensitive strain. Notably, there was a subset of drugs that induced very large halos in *rcy1*Δ cells, but had no effect at all on wild type yeast, suggesting that these compounds act by a mechanism specifically blocked by Rcy1p (Figure 3-2). In the screen of over 1500 known drugs we found additional compounds that displayed chemical/genetic synthetic lethality with *rcy1*Δ, including the anti-psychotics haloperidol, chlorpromazine, azaperone and ziprasidone (Figure 3-3, references[2,11,47-49]), all of which can be classified as CADs. To investigate this unexpected relationship of CADs to RCY1, we used the potent novel CAD, **3346-2086** (hereafter referred to as **3346**) to screen for resistant mutants.

3.3.2. Selection of 3346-resistant Mutants

In order to avoid selecting classic MDR mutants we generated the *rcy1*Δ *pdr1*Δ background to select 3346-resistant mutants. This screen produced many colonies (>50) of which 20 were isolated for further investigations. Of these 20, one strain had lost the kanMX6 cassette used to disrupt the RCY1 gene; the remaining 19 were confirmed by liquid growth inhibition experiments to be resistant to **3346** (S3 1-5). We then cross-screened several of the mutants against other compounds to test whether resistance was specific to CADs. The mutants that were tested were all significantly resistant to the anti-psychotics haloperidol, chlorpromazine and ziprasidone, (IC_{50} values 2-30μM) (Figure 3-4), but retained their sensitivity to the anti- psychotic, aripiprazole. Clotrimazole, a structurally unrelated azole antifungal agent that was also more toxic to *rcy1*Δ than WT, but displayed a distinct sensitivity profile across the different strains (selected mutants, wild type and *rcy1*Δ). This

result suggests that the MDR effect of *rcy1*Δ toward azoles is mechanistically distinct from its hypersensitivity to CADs.

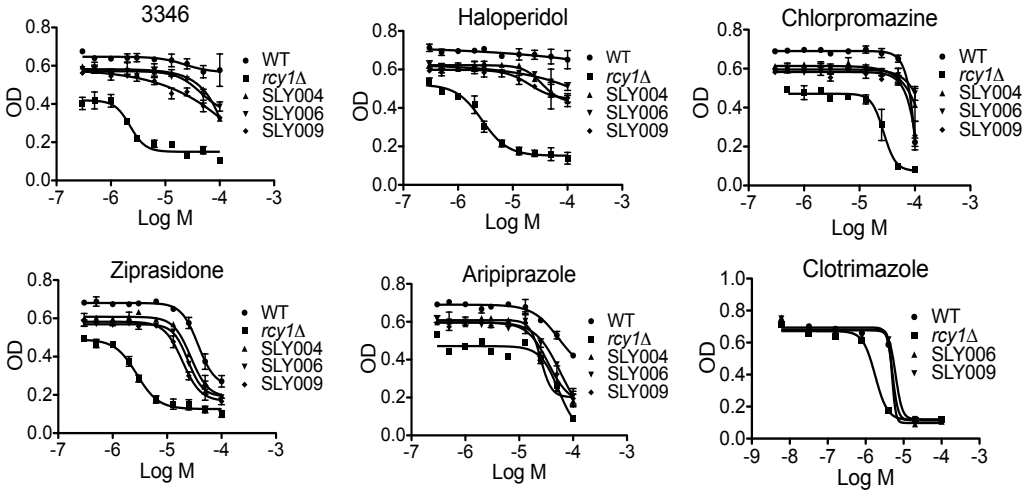

Figure 3-4. Growth inhibition curves for 3346 and five FDA approved drugs against wild type, *rcy1*Δ and three 3346-resistant mutants; SLY004, SLY006 and SLY009. Ziprasidone, haloperidol, chlorpromazine and aripiprazole are anti-psychotic CADs. Clotrimazole is an over the counter anti-fungal. IC_{50} values for the six compounds in *rcy1*Δ are: 3346 ~2 μ M, ziprasidone ~3 μ M, haloperidol ~3 μ M, chlorpromazine ~27 μ M, aripiprazole ~54 μ M, clotrimazole ~9 μ M, respectively.

3.3.3. Sequencing of 3346-resistant Mutants

Four bar-coded libraries were prepared (3 pools of mutants and the *rcy1*Δ *pdr1*Δ parental strain) and sequenced using the Illumina HiSeq 2000. Reads for each were mapped to the most current *S. cerevisiae* consensus sequence (SacCer 3) and a list of annotated SNPs was generated for each pool. SNPs that were inherited from

the *rcy1*Δ *pdr1*Δ parental strain were filtered out, leaving a total of 1493 newly acquired mutations across the three pools, averaging to ~80 SNPs per mutant. Removal of synonymous mutations and mutations in non-coding regions reduced the SNP list to 679 exonic, non-synonymous mutations in 627 unique genes (S3-10).

Genes that are enriched in SNPs are potentially either targets of **3346** or genes that function in its mode of action (MOA). We previously developed a simple ranking system to aid in identifying potential gene targets for a given drug[30]. This system is based on two metrics, allele count (AC) and gene level-allele count (GL-AC). AC is an estimate of the number of mutants in a pool that are mutated at a specific nucleotide and is calculated by the genome analysis toolkit (GATK). The GL-AC metric identifies genes that acquire resistance by mutation at more than one locus by calculating the sum of all the ACs in a given gene. Applied to the list of SNPs from the pool of 19 mutant genomes, this method identified the two highest scoring genes encoded the aminophospholipid translocases (flippases), *DRS2* and *DNF1*. *DNF1* incurred SNPs at five different loci, one with an AC of three, two positions each with ACs of 2 and another two positions with ACs of 1, resulting in an overall GL-AC of 9 (Table 3-1). *DRS2* had SNPs at four distinct positions, resulting in a GL-AC of 7. The p-values for these GL-AC values were 0.0001 and 0.001 for *DNF1* and *DRS2* respectively, confirming that these mutations are specifically favored by selective pressure from **3346.** In addition, mutations also appeared in one other member of the family, *DNF2*, a paralog of *DNF1,* with a GL-AC value of 3.

	gene	position	AC	GL-AC	p-value (GL-AC)	mutation
1	DNF1	chrV:513063	1	9	1.00E-04	P107L
	DNF1	chrV:514356	2			T538K
	DNF1	chrV:514693	3			K650N
	DNF1	chrV:516207	1			A1155V
	DNF1	chrV:516214	2			M1157I
2	DRS2	chrI:98906	1	7	0.0013	K264N
	DRS2	chrI:98908	2			K264E
	DRS2	chrI:98155	3			E515K
	DRS2	chrI:98064	1			S545F
3	YMR317W	chrXIII:908138	2	4	0.54	P259S
	YMR317W	chrXIII:908564	2			S401T
1 of 12	DNF2	chrIV:632353	1	3	1	A358T
	DNF2	chrIV:634879	1			M1200V
	DNF2	chrIV:635195	1			R1305K

Table 3-1. Highest ranking genes by gene-level allele count (GL-AC) across all 19 mutants including chromosome position, mutation, GL-AC value with corresponding p-value.

Since the mutations were found in pools, we used Sanger sequencing to identify several mutant clones containing specific mutations. The results confirmed all of the DRS2 mutations and the AC values that were predicted by the NGS results. Out of eleven examined, three separate clones contained K264 mutations: clone SLY006 (*drs2-K264N*) and clones SLY007 and SLY008 (*drs2-K264E*) (figure S3-11). Three other clones harbored the E515K mutation in Drs2: clones SLY005, SLY016 and SLY017 and the *drs2-S545F* mutation was found in clone SLY004. One of the DNF1

mutations (*dnf1-K650N*) was recovered in clone SLY009. The remaining *DNF1* and all of the *DNF2* mutations presumably reside in the eight mutants that have not yet been individually sequenced.

3.3.4. Genetic Studies

Since the synthetic lethality between **3346** and *rcy1*Δ can be relieved by mutation of these phospholipid transporters, we tested the **3346** sensitivity of strains harboring deletions of these proteins. As shown in Fig 3-5D, deletion of Drs2 results in high sensitivity to **3346**; moreover, this sensitivity was not enhanced in the *rcy1*Δ *drs2*Δ double mutant, suggesting that the genes are epistatic.

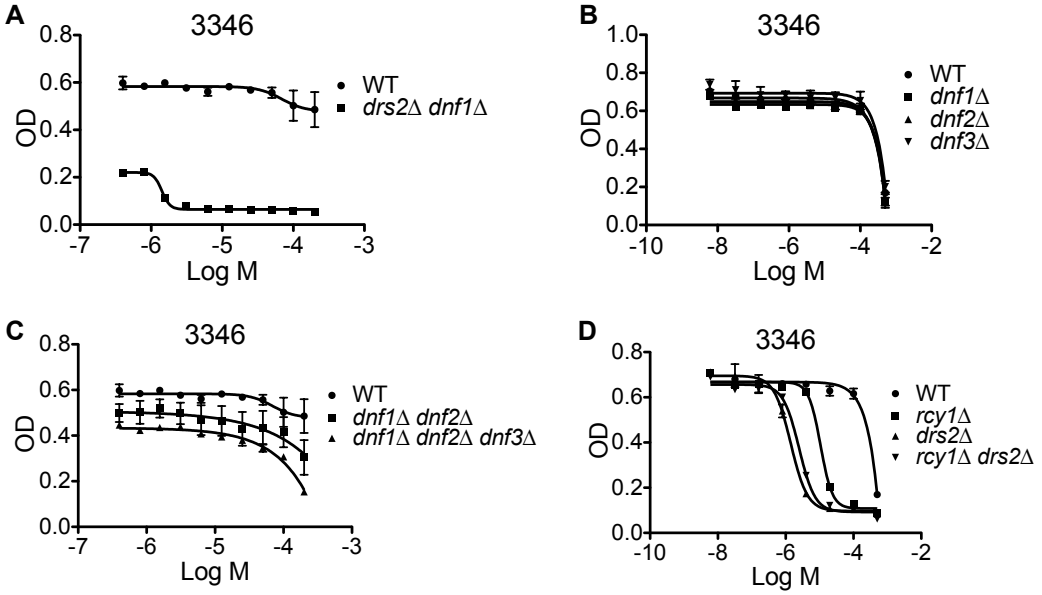

Figure 3-5. 3346 growth inhibition curves for flippase null-mutants.

In keeping with this observation, co-overexpression of *DRS2* and its associated subunit *CDC50* in an *rcy1*Δ background (SLY038) almost completely

suppresses the effects of 3346-lethality (figure 3-6A). In contrast, deletion of Dnf1, Dnf2, or (Dnf3) did not result in sensitivity to **3346** and the combined deletions *dnf1*Δ *dnf2*Δ and *dnf1*Δ *dnf2*Δ *dnf3*Δ mutants were only marginally sensitive (Figure 3-5 B-C). The *drs2*Δ *dnf1*Δ double mutant, however, was barely viable at low 3346 concentrations, over a 48 h period, and was essentially non-viable at concentrations > 1 μM (Figure 3-5A).

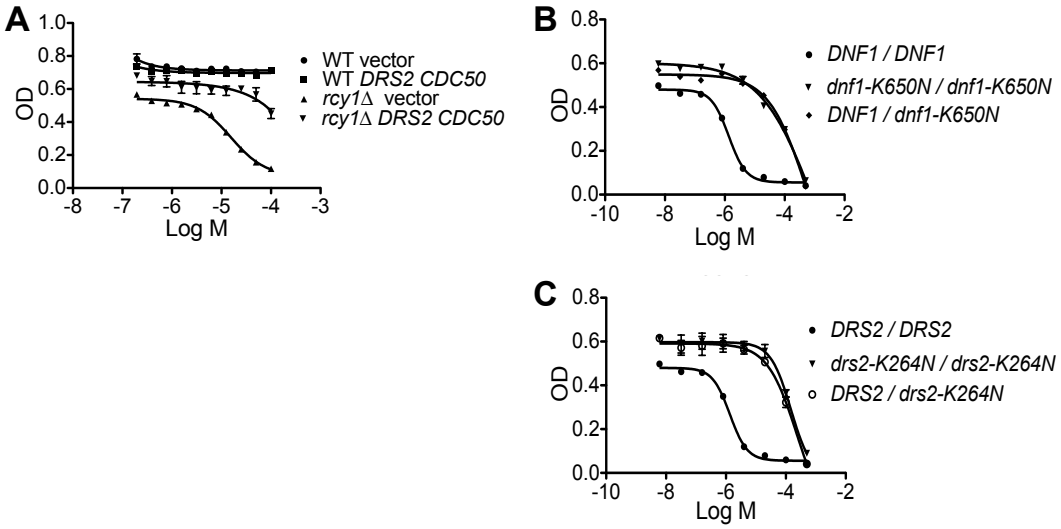

Figure 3-6. A) Growth inhibition curves for wild type empty vector transformant (WT vector), wild type *DRS2 CDC50* high-copy vector transformant (WT *DRS2 CDC50*), *rcy1*Δ empty vector transformant (*rcy1*Δ vector) and *rcy1*Δ *DRS2 CDC50* high-copy vector transformant (*rcy1*Δ *DRS2 CDC50*). B) Growth inhibition curves for the *DRS2* wild type homozygous diploid (*DRS2 / DRS2*), *drs2* mutant homozygous diploid (*drs2-K264N / drs2-K264N*) and the *DRS2* heterozygous diploid (*DRS2 / drs2-K264N*). C) Growth inhibition curves for the *DNF1* wild type homozygous diploid (*DNF1 / DNF1), dnf1* mutant homozygous diploid (*dnf1-K650N / dnf1-K650N*) and the *DNF1* heterozygous diploid (*DNF1 / dnf1-K650N*).IC_{50} for both wild type homozygous diploids (*DRS2 / DRS2*, *DNF1 / DNF1)* is ~ 1μM.

To determine whether the flippase mutations are dominant or recessive, we compared 3346-sensitivity of *rcy1*Δ homozygous diploids with heterozygotes containing *rcy1*Δ and either *drs2-K264N* (SLY035) or *dnf1-K650N* (SLY036). As expected, a homozygous *rcy1*Δ diploid (SLY032) is **3346**-sensitive and the *drs2-K264N* and *dnf1-K650N* homozygous diploids (SLY033, SLY034) are **3346** resistant. The *drs2-K264N* and *dnf1-K650N* heterozygotes both displayed **3346** resistance identical to that of the homozygous mutant diploids (figure 3-6 B-C), showing that the mutations are dominant and suggesting that they are not loss of function mutations.

The residues altered by these mutations are scattered across the sequence, but are largely conserved, cytoplasmic, and located near transmembrane domains (Figure S3-12). An idea of the three dimensional distribution of the relevant residues can be gained by noting the positions of the corresponding residues in the Ca-ATPase, a homologous P-type ATPase whose structures at various stages in the reaction of cycle of these transporters is known in considerable detail[50]. This analysis shows that in the folded protein the mutated residues are clustered in a cytoplasmic patch that forms part of the exposed surface of the enzyme in the conformations adopted at the E2P and E2 stages of the reaction cycle (Figure S3-13). The latter are the stages at which the transported phospholipid become irreversibly bound to the transporter and flipped from the external to the internal leaflet of the membrane.

3.3.5. Flippase Assays

In yeast, these transporters are not essential – mutants harboring deletions of any member of the family other than Neo1 grow readily. However, it is possible that inhibition of these activities might be deleterious in an *rcy1*Δ background, so that mutations in the phospholipid transporters that are no longer inhibited can survive in this background. To investigate this possibility, yeast cells harboring only one transporter (Drs2, Dnf1, or Dnf2) were treated with **3346** and the effect on transport of phospholipid analogues was measured. In no case was any inhibition of uptake observed (data not shown).

These experiments suggest that CADs do not directly affect phospholipid transport, but do not rule out the possibility of indirect effects, particularly in an *rcy1*Δ background. To investigate this possibility, we measured the effect of continued exposure to **3346** on phospholipid transport by *rcy1*Δ cells. As shown in Figure 6C there is no immediate effect of the drug on PC uptake (transported primarily by Dnf1 and Dnf2). Beginning about 90 minutes after addition of drug, however, there is a dramatic decrease in PC transport when compared to untreated control *rcy1*Δ cells. This effect of the drug on transport is considerably reduced in *rcy1*Δ cells harboring a resistance mutation in either Dnf1 (Figure 7D) or Drs2 (not shown). A similar dramatic drop in PS transport is observed at about the same time (Figure 7E), an effect which was reduced in cells containing a resistance mutation in either Dnf1 (Figure 7F) or Drs2 (not shown). It should be noted that the rates of PS transport are somewhat higher in *rcy1*Δ cells in comparison to cells with a functional

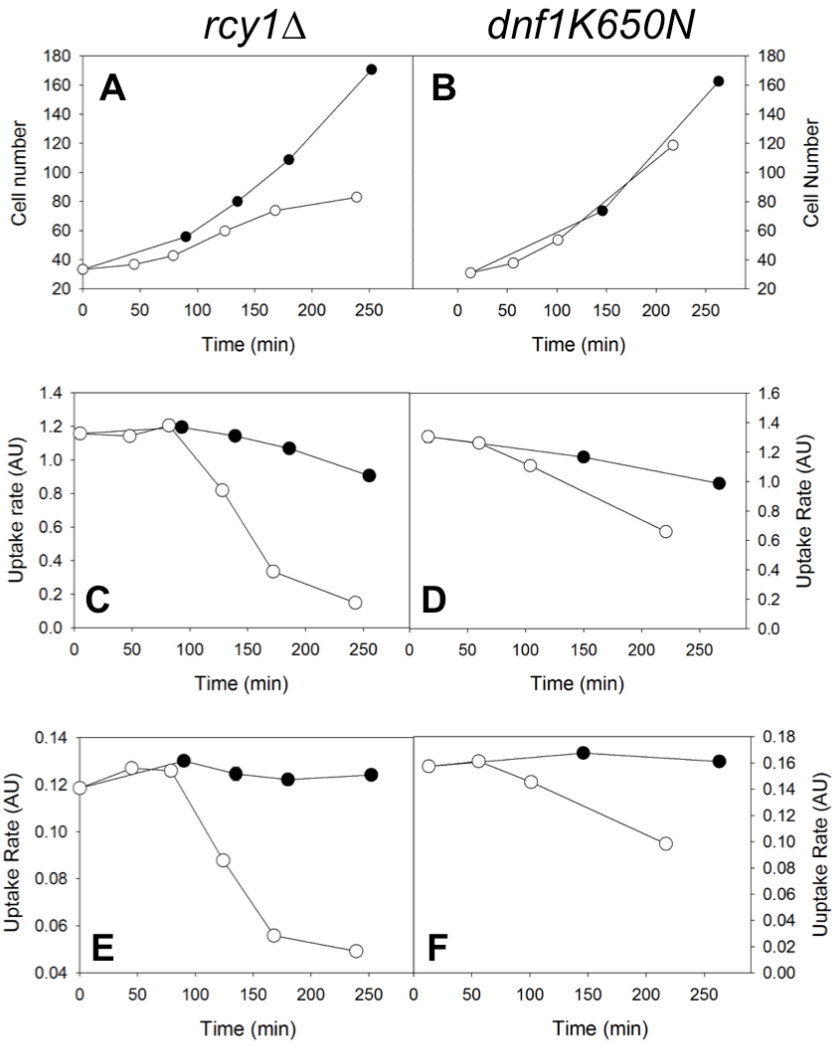

Figure 3-7. A and B) Growth curves for both *rcy1*Δ (right) and *dnf1*Δ (left) in the presence of 3346 (10uM). C and D) Phospholipid (PS) uptake rates for both *rcy1*Δ (right) and *dnf1*Δ (left) in the presence of 3346 (10uM). E and F) Phospholipid (PE) uptake rates for both *rcy1*Δ (right) and *dnf1*Δ (left) in the presence of 3346 (10uM).

copy of Rcy1. One possible explanation for these reductions in transport is that the cells are dying from the drug treatment. As shown Figure 7A, however, the growth rate of drug treated cells is not altered until well after the onset of the drop in phospholipid transport. Yeast in which Dnf1p, Dnf2p, and Drs2p have all been eliminated by mutation grow very poorly, suggesting that the broad drop in phospholipid transport activity observed in cells lacking the resistance mutations may be responsible for the subsequent reduction in growth rate.

3.3.6. Dithionite Scrambling Assays

Based on the broad structure-activity relationship of these drugs in yeast (and in human transporters. *See SI*) as well as the fact that flippases don't appear to be the direct target, we sought out other possible MOAs. It has been long been suggested that DIPL is caused by the binding of drugs, CADs in particular, to phospholipids rendering them less susceptible to degradation by phopholipases[5,51,52]. In another study surface plasmon resonance was used to measure CAD-lipid affinities which were then correlated with a given CAD's ability to cause DIPL. Additionally, it has been reported that certain drugs, CADs included, cause a disruption in the membrane asymmetry of PC and PE in erythrocytes[53,54]. Given this information we postulated that the MOA of CADs could be attributed to a scrambling of membrane phospholipids that works against the efforts of flippases to maintain PL asymmetry and that this equilibrating effect becomes toxic in the absence of Rcy1. To test this we employed a dithionite quenching assay that has been previously used to measure phospholipid transport across liposome membranes[35,55]. Fluorescence of liposomes

containing 1% NBD-PL was monitored during a 540 s drug-incubation period which was followed by addition of dithionite to quench the NBD-PLs in the outer leaflet. In order to measure NBD-PL scrambling we quantified the rate at which fluorescence decreased over a 3 min period after dithionite addition. We observed that fluorescence of NBD-PS and NBD-PE containing liposomes treated with 3346 and haloperidol decreased at a higher rate than those treated with DMSO (figure 3-8). The decease seen with 3346 amounted to about 0.5% of the total fluorescence over the 3 min. These rates are comparable to those observed in reconstituted proteoliposomes containing purified Drs2[35]. These studies showed a fluorescence decrease of about 8% of the total fluorescence, over a 30 min period, due to active transport of NBD-PLs. In an attempt to correlate PL scrambling with *rcy1*Δ activity we tested several other CADs exhibiting a range of *rcy1*Δ activity (Table S3-2). Tamoxifen and 3701, compounds that are selectively active in *rcy1*Δ, exhibited rates of fluorescence decrease comparable to those seen with 3346. Conversely, ranolazine and aripiprazole, compounds with little to no *rcy1*Δ activity exhibited lower rates of fluorescence decrease. Interestingly, azaperone and ziprasidone, compounds that are *rcy1*Δ-active preformed poorly in the liposome assay. We noticed that the compounds that are *rcy1*Δ active but did not significantly decrease fluorescence in the dithionite

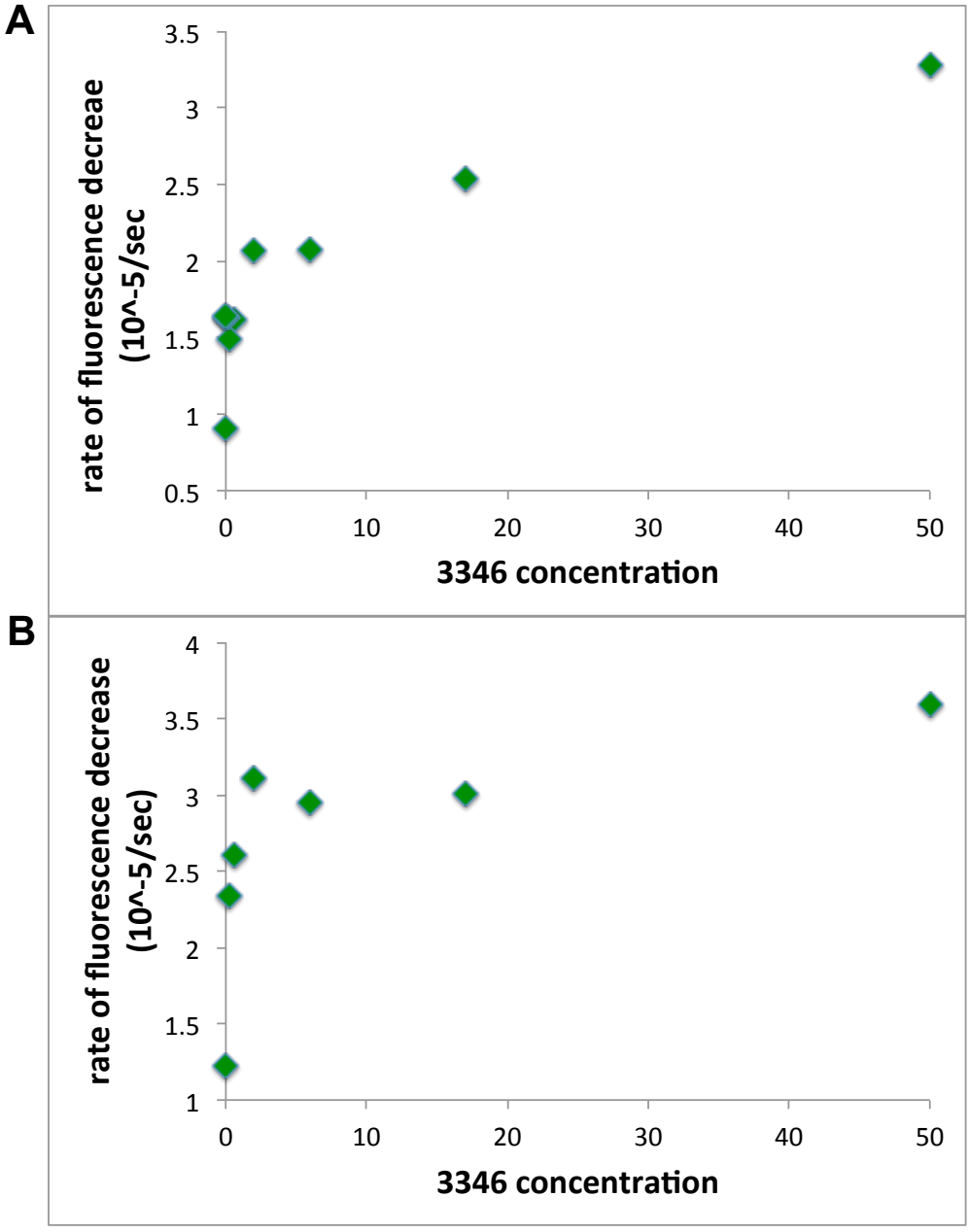

Figure 3-8. Dithionite quenching assay A) Plot of rate of fluorescence decrease vs 3346 concentration (uM) for PS. B) Plot of rate of fluorescence decrease vs 3346 concentration (uM) for PE.

assay (azaperone, ziprasidone and aripiprazole to some extent) are aryl amines, which are susceptible to N-oxidation. It is reasonable to postulate that the N-oxy metabolite is the active agent *in vivo* and in liposomes they are not oxidized rendering them less able to interact with PLs. To test this we extracted the organic contents of an overnight wild type yeast culture treated with ziprasidone and analyzed it *via* HPLC. Indeed, in addition to an M + 1 peak at 313 m/z there was a significant amount of the oxidized M + 1 + 16 peak at 329 m/z. There was no oxidized adduct in cultures containing 3346.

3.4. Discussion

3.4.1. Flippase Mutations are the Cause of CAD Resistance

Based on the significance of their AC and GL-AC scores, mutations in at least two of the five phospholipid transporters in yeast, *DRS2* and *DNF1*, confer CAD resistance in *rcy1*Δ yeast. The appearance of mutations in more than one member of this transporter family, and their clustering in the folded structure, argues that they all participate in the same mechanism in rescuing CAD sensitivity. The fact that the mutations are dominant, and that resistance is conferred by mutation in any one transporter in a background where the other potential target transporters are wt, suggests that **3346** does not form a lethal complex with its target, and that sensitivity results from a failure of some function in an *rcy1*Δ background which can be rescued by any mutated transporter. The loss of viability that follows the general disruption of phospholipid transport from the cell surface after a generation in the presence of

the drug suggests that the eventual disappearance of phospholipid transport at the plasma membrane may be the final cause of drug toxicity in yeast. Significantly, Dnf1, Dnf2, and Drs2 are the three members of the family that function in the plasma membrane – Dnf3 and Neo1 functions are likely to be intracellular.

3.4.2. Rcy1 is Known to Interact with Flippases in *S. cerevisiae*

The striking feature of CAD toxicity is its dependence on the absence of Rcy1p. Moreover, loss of Drs2p also confers sensitivity to CADS, while the *rcy1*Δ *drs2*Δ double mutant is no more sensitive than either of the individual deletions, suggesting that Rcy1p and Drs2p act in the same pathway on which the mechanism of CAD sensitivity depends. In fact, similar epistatic interactions between these two proteins in the endocytic and recycling pathways were observed earlier by Tanaka's group[27], who have also shown that these two proteins physically interact[56] and that the absence of this interaction is detrimental to Drs2p function. The nature of this interaction and its role in membrane trafficking and homeostasis are unclear, and no similar interactions of Rcy1p with Dnf1p or Dnf2p have been observed. It is also unlikely that Rcy1p binding is obscuring the site identified by the CAD resistance mutations, since the Rcy1p binding site is on the opposite side of the transporter from the location of these mutations[56]. Because Rcy1p is an F-box protein, it might also be expected that Rcy1p functions in an SCF-E3 ubiquitin ligase complex, which might then target Drs2p for destruction, a conclusion that is weakly supported by the slight increase in PS transport observed in *rcy1*Δ cells. However, there is no agreement that Rcy1p functions in any such SCF complex[25,26], and ubiquitination can be a regulatory

rather than a targeting signal. However, the discovery of this connection between Rcy1p and Drs2p in studies of vesicle trafficking pathways, and the appearance of defects in these pathways when either of these proteins is deleted, suggests that the target(s) of **3346** may work in these pathways as well. Moreover, the resistance conferred by mutations in Dnf1, Dnf2, or Drs2 suggests that these proteins are relatively directly affected by the absence, inhibition, or activation of the **3346** targets, either in their ability to persist at the plasma membrane or in their ability to reach it in the first place.

3.4.3. CADs and Flippase Mutations Cause Cholestasis

The connection between CAD toxicity and phospholipid transporters revealed in this work may provide an important clue to the origin of adverse side effects seen in humans treated with CADs, particularly liver cholestasis and phospholipidosis. While overt liver injury is rare and complete recovery is common upon drug withdrawal, drug-induced cholestasis is a serious side effect that can cause permanent damage requiring a liver transplant[57]. Haloperidol is a CAD that is known to cause both liver cholestasis and phospholipidosis[2]. This fact coupled with our findings provides a connection between the Rcy1-Drs2 (Dnf1 and Dnf2) pathway and drug-induced liver disease. The results presented here provide two potential insights into this process. One is that these toxic effects may be linked to effects on phospholipid transporters. In fact, it is known that heritable cholestasis results from mutations to a liver-specific phospholipid transporter ATP8B1. An interesting question is therefore whether administration of CADs that induce liver cholestasis and phospholipidosis do so

because of altered phospholipid transport. The second insight is that this toxic effect is enhanced by reduced levels of either a phospholipid transporter (Drs2p) or an F-box protein (Rcy1p). That discovery raises the question of whether, for example, harboring particular isotypes of ATP8B1 or some other member of the P4 ATPase family enhances the risk associated with CADs. There is no mammalian homolog of Rcy1p, nor enough information on the function of this interaction to enable a hypothesis about whether corresponding functions are present for mammalian P4 ATPases. Information on this subject might shed light on other potential risk factors for toxic liver effects of CADs. In the absence of this information, structure/activity relationships in *rcy1*Δ yeast may provide useful information on the potential of compounds for liver toxicity.

3.4.4. Potential Models

The mechanism by which CADs induce toxicity in *rcy1*Δ remains unclear. We can, however propose possible explanations for our observations using what others have discovered. We have shown in this study that CADs seem to have the ability to scramble aminophospholipids (PLs) in liposomes. If we assume that they have similar effects *in vivo,* perhaps in the *rcy1*Δ mutant there is a disruption that renders the cell unable to counter this uncoupling of PL asymmetry, which results in lethality. What could this disruption be? Studies have shown that in *rcy1*Δ cells, Cdc50-EGFP accumulates, along with Snc1-mRFP in large structures near the tip or neck of the bud[27]. This suggests that Cdc50-Drs2 is not properly localized and that this disruption may enhance the toxic effect of CADs. For instance, maybe Drs2 is being

mislocalized to the PM. Under this scenario, trans-golgi and endosomal membranes would be lacking a PS transporter to maintain asymmetry at these locales, which could cause lethality. As for what the mutations are doing to rescue the cell from this situation; 1) the *DRS2* mutations could have a hyper-activating effect on Drs2 at the TGN to compensate for the low levels present there, 2) the *DNF1* and *DNF2* mutations could be causing a relaxation of substrate specificity where even low levels of Dnf1 and Dnf2 present at the TGN could compensate for the lack of Drs2. Baldridge *et al* have shown that mutations in *DNF1*, specifically Tyr618Phe, allow for the transport of PS while retaining the ability or transport PC[58]. A third effect of the mutations could be that they give the flippases the ability to properly localize in the absence of Rcy1. One obvious hole in the mislocalization theory is that we would expect to see reduced transport in untreated *rcy1*Δ cells when in fact *rcy1*Δ transports just as well as wild type.

Another theory could be that Rcy1 plays an MDR role, perhaps in concert with Drs2. Previously, it was demonstrated that Rcy1 was necessary for recycling of the fluorescent lipid FM 4-64[26]. Our results suggest that CADs are membrane active and probably accumulate in them. It is plausible that the membrane recycling actions of Rcy1 play a cleansing role in the cell and that in its absence CAD accumulation becomes toxic, unless hyper-activation mutations in flippases are incurred to mitigate against this.

In conclusion, this body of work has provided significant insights into the mechanisms by which CADs act in yeast and how these drugs cause disease in

humans, particularly phospholipidosis and liver cholestatsis. Additionally, we have demonstrated the utility of MUTseq to characterize the MOAs of bioactive compounds. MUTseq was used to clearly identify the celluar targets of benomyl and rapamycin and even recover exact resistance-conferring residues found in prior studies. While it did not explicitly elucidate the MOA of CADs, it has provided solid evidence for their involvement in membrane homeostasis, weather it be by disrupting membrane asymmetry, which may cause downstream problems, (endocytosis, vesicular trafficking, etc.) or by other mechanisms that are still yet to be determined. Undoubtedly, the resistance conferring mutations that we have isolated will be of interest and hopefully assistance to those who study flippases, especially in yeast. Further studies will be required to fully understand how CADs behave in cells. A final observation worth noting is with regard to phenotypic screening. The unbiased nature of this type of screen can lead one down paths they may never thought they would go down. I for one didn't think I would have had to learn so much about membranes and flippases. The compounds lead the way. And this is the beauty of the phenotypic screen: it samples all cellular entities including proteins, DNA and even lipids.

3.5. Supplemental Information

3.5.1. Genetics

Table S3-1- Strains

	genotype	source
BY4741 YJL20	*Mat a his3Δ1 leu2Δ0 met15Δ0 ura3Δ0 rcy1Δ::KanMX6*	Open Biosystems
BY4741 YGL0	*Mat a his3Δ1 leu2Δ0 met15Δ0 ura3Δ0 pdr1Δ::KanMX6*	Open Biosystems
SLY001	*Mat α his3Δ1 leu2Δ0 ura3Δ0 lys2Δ0 rcy1Δ::KanMX6*	this study
SLY002	*Mat a his3Δ1 leu2Δ0 met15Δ0 ura3Δ0 pdr1Δ::KanMX6 rcy1Δ::KanMX6*	this study
SLY004	*Mat a his3Δ1 leu2Δ0 met15Δ0 ura3Δ0 pdr1Δ::KanMX6 rcy1Δ::KanMX6 drs2-S545F*	this study
SLY005	*Mat a his3Δ1 leu2Δ0 met15Δ0 ura3Δ0 pdr1Δ::KanMX6 rcy1Δ::KanMX6 drs2-E515K*	this study
SLY016	*Mat a his3Δ1 leu2Δ0 met15Δ0 ura3Δ0 pdr1Δ::KanMX6 rcy1Δ::KanMX6 drs2-E515K*	this study
SLY017	*Mat a his3Δ1 leu2Δ0 met15Δ0 ura3Δ0 pdr1Δ::KanMX6 rcy1Δ::KanMX6 drs2-E515K*	this study
SLY006	*Mat a his3Δ1 leu2Δ0 met15Δ0 ura3Δ0 pdr1Δ::KanMX6 rcy1Δ::KanMX6 drs2-K264N*	this study
SLY007	*Mat a his3Δ1 leu2Δ0 met15Δ0 ura3Δ0 pdr1Δ::KanMX6 rcy1Δ::KanMX6 drs2-K264E*	this study
SLY008	*Mat a his3Δ1 leu2Δ0 met15Δ0 ura3Δ0 pdr1Δ::KanMX6 rcy1Δ::KanMX6 drs2-K264E*	this study
SLY009	*Mat a his3Δ1 leu2Δ0 met15Δ0 ura3Δ0 pdr1Δ::KanMX6 rcy1Δ::KanMX6 dnf1-K650N*	this study
SLY022	*Mat α his3Δ1 leu2Δ0 met15Δ0 ura3Δ0 pdr1Δ::KanMX6 rcy1Δ::KanMX6 drs2-K264N*	this study
SLY023	*Mat α his3Δ1 leu2Δ0 met15Δ0 ura3Δ0 pdr1Δ::KanMX6 rcy1Δ::KanMX6 dnf1-K650N*	this study
SLY024	*Mat α his3Δ1 leu2Δ0 ura3Δ0 lys2Δ0 drs2Δ::KanMX6*	Hua et al. 2002
SLY025	*Mat α his3Δ1 leu2Δ0 ura3Δ0 lys2Δ0 dnf1Δ::KanMX6*	from Todd Graham
SLY026	*Mat α his3Δ1 leu2Δ0 ura3Δ0 lys2Δ0 dnf2Δ::KanMX6*	from Todd Graham
SLY027	*Mat α his3Δ1 leu2Δ0 ura3Δ0 lys2Δ0 dnf3Δ::KanMX6*	from Todd Graham
SLY028	*Mat α his3Δ1 leu2Δ0 ura3Δ0 lys2Δ0 drs2Δ::KanMX6 dnf1Δ::KanMX6*	Hua et al. 2002
SLY029	*Mat α his3Δ1 leu2Δ0 ura3Δ0 met15Δ0 dnf1Δ::KanMX6 dnf2Δ::KanMX6*	Hua et al. 2002
SLY030	*Mat α his3Δ1 leu2Δ0 ura3Δ0 met15Δ0 dnf1Δ::KanMX6 dnf2Δ::KanMX6 dnf3Δ::KanMX6*	Hua et al. 2003
SLY031	*Mat a his3Δ1 leu2Δ0 met15Δ0 ura3Δ0 rcy1Δ::nat drs2Δ::KanMX6*	this study
SLY032	*Mat a/α his3Δ1/his3Δ1 leu2Δ0/leu2Δ0 met15Δ0/Met15Δ0 ura3Δ0/ura3Δ0 Lys2Δ0/lys2Δ0 rcy1Δ/rcy1Δ*	this study
SLY033	*a/α his3Δ1/his3Δ1 leu2Δ0/leu2Δ0 met15Δ0/met15Δ0 ura3Δ0/ura3Δ0 rcy1Δ/rcy1Δ drs2-K264N/drs2-K2*	this study
SLY034	*a/α his3Δ1/his3Δ1 leu2Δ0/leu2Δ0 met15Δ0/met15Δ0 ura3Δ0/ura3Δ0 rcy1Δ/rcy1Δ dnf1-K650N/dnf1-K6*	this study
SLY035	*Mat a/α his3Δ1/his3Δ1 leu2Δ0/leu2Δ0 met15Δ0/met15Δ0 ura3Δ0/ura3Δ0 rcy1Δ/rcy1Δ DRS2/drs2-K264*	this study
SLY036	*Mat a/α his3Δ1/his3Δ1 leu2Δ0/leu2Δ0 met15Δ0/met15Δ0 ura3Δ0/ura3Δ0 rcy1Δ/rcy1Δ DNF1/dnf1-K650*	this study
SLY037	*Mat a his3Δ1 leu2Δ0 met15Δ0 ura3Δ0 (DRS2 CDC50 URA3 2 μm)*	this study
SLY038	*Mat a his3Δ1 leu2Δ0 met15Δ0 ura3Δ0 rcy1Δ::KanMX6 (DRS2 CDC50 URA3 2 μm)*	this study

3.5.2. Growth Inhibition

DMSO/drug stock solutions were serially diluted, in triplicate with YPD culture (OD_{600}=0.06), in a 96 well format. Growth was monitored for 24 h using an automatic plate reader at 30^{o} C. Inhibitory concentrations were then calculated by analyzing late log-phase OD_{600} readings in Prism GraphPad. IC_{50} values were also calculated via extrapolation of halo scores utilizing an algorithm described in a previous publication[30].

Figure S3-1

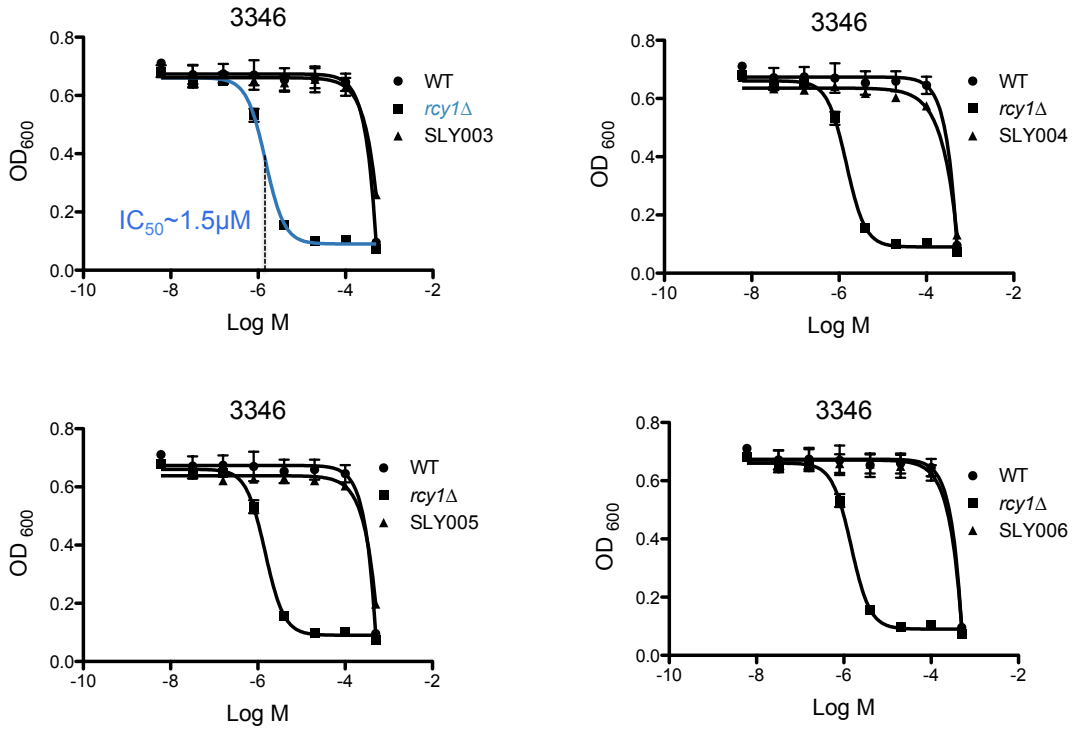

Growth inhibition curves for 3346 resistant mutants SLY003-006.

Figure S3-2

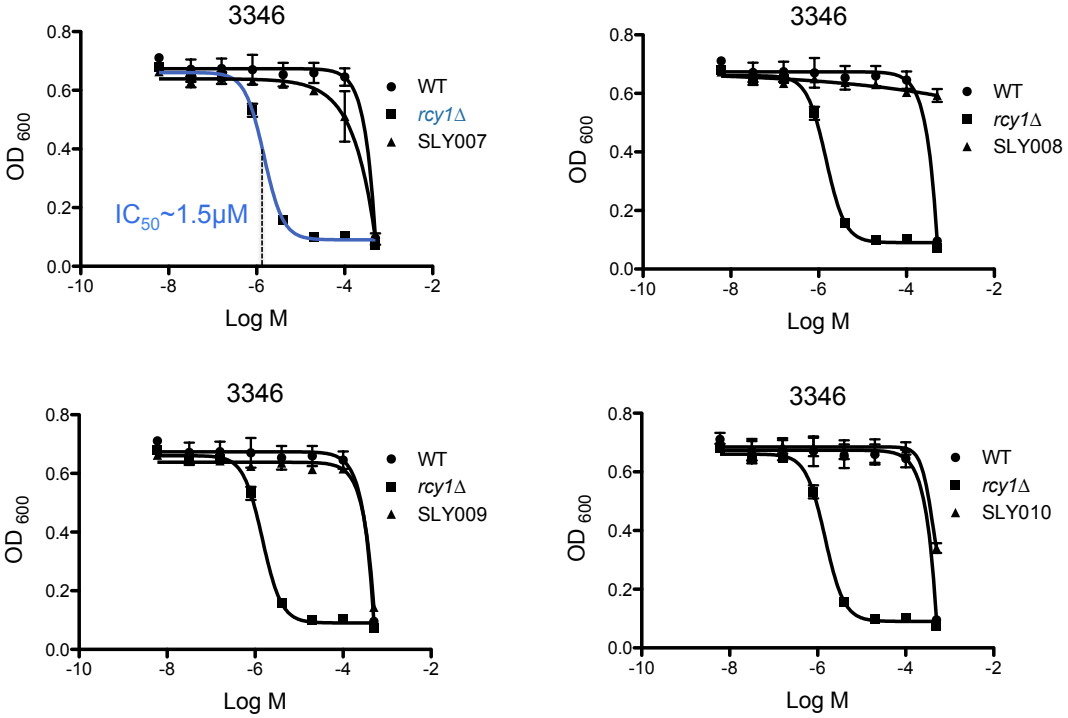

Growth inhibition curves for 3346-resistant mutants SLY007-010.

Figure S3-3

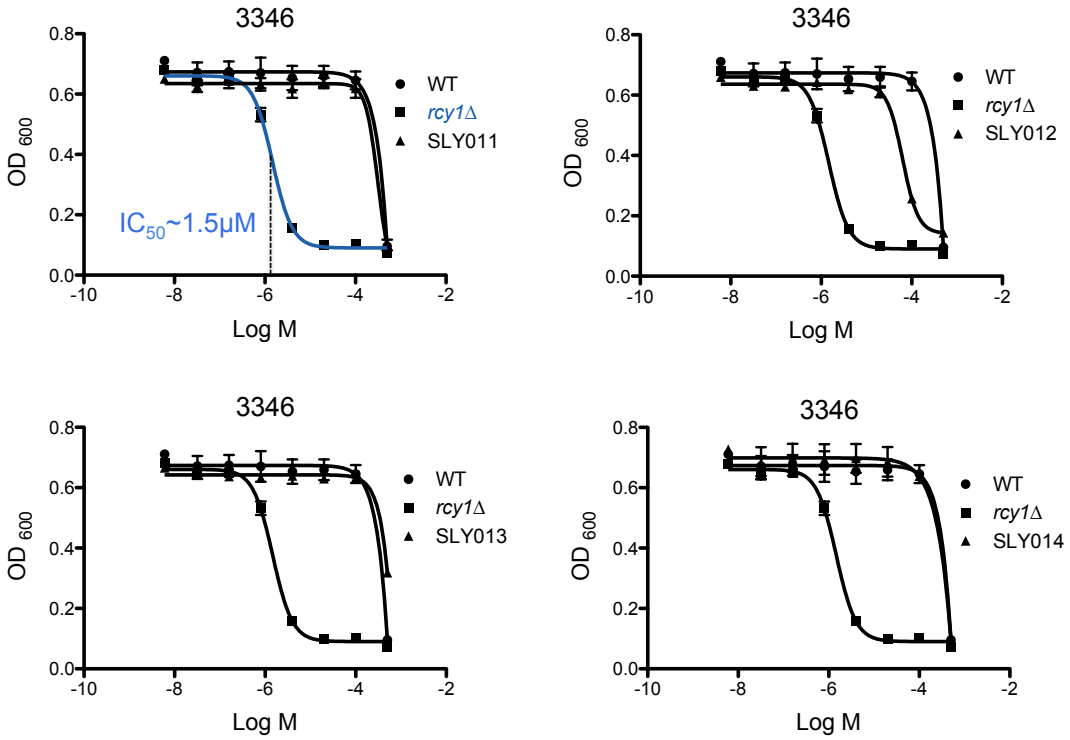

Growth inhibition curves for 3346-resistant mutants SLY011-014.

Figure S3-4

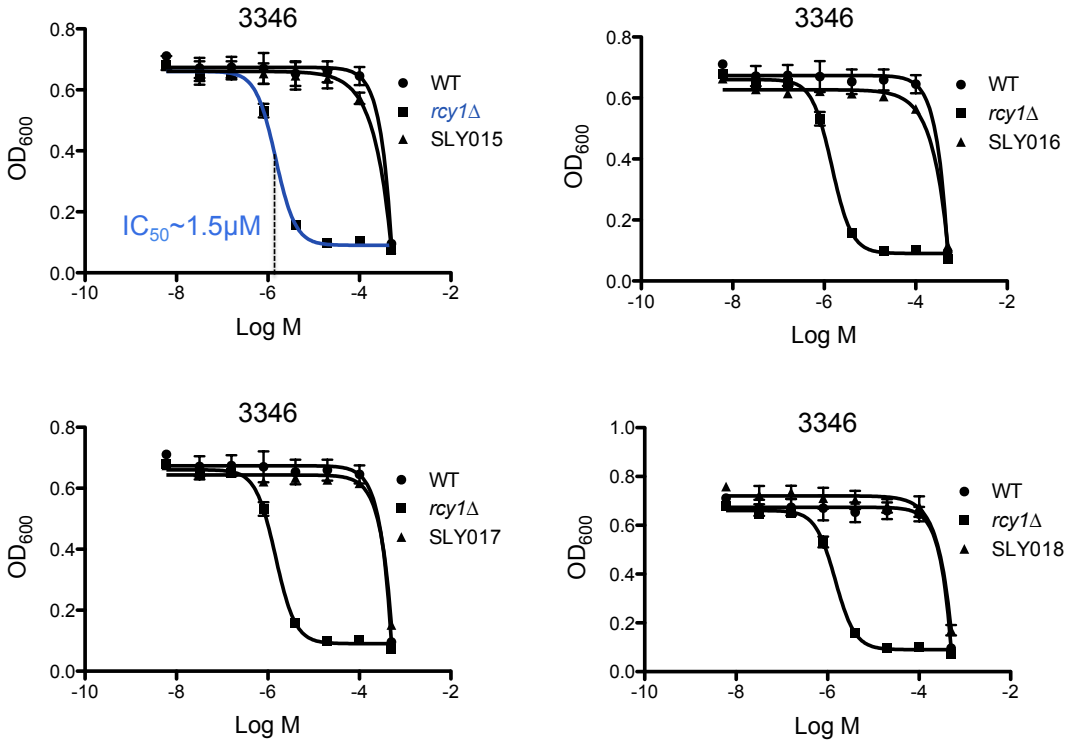

Growth inhibition curves for 3346-resistant mutants SLY015-018.

Figure S3-5

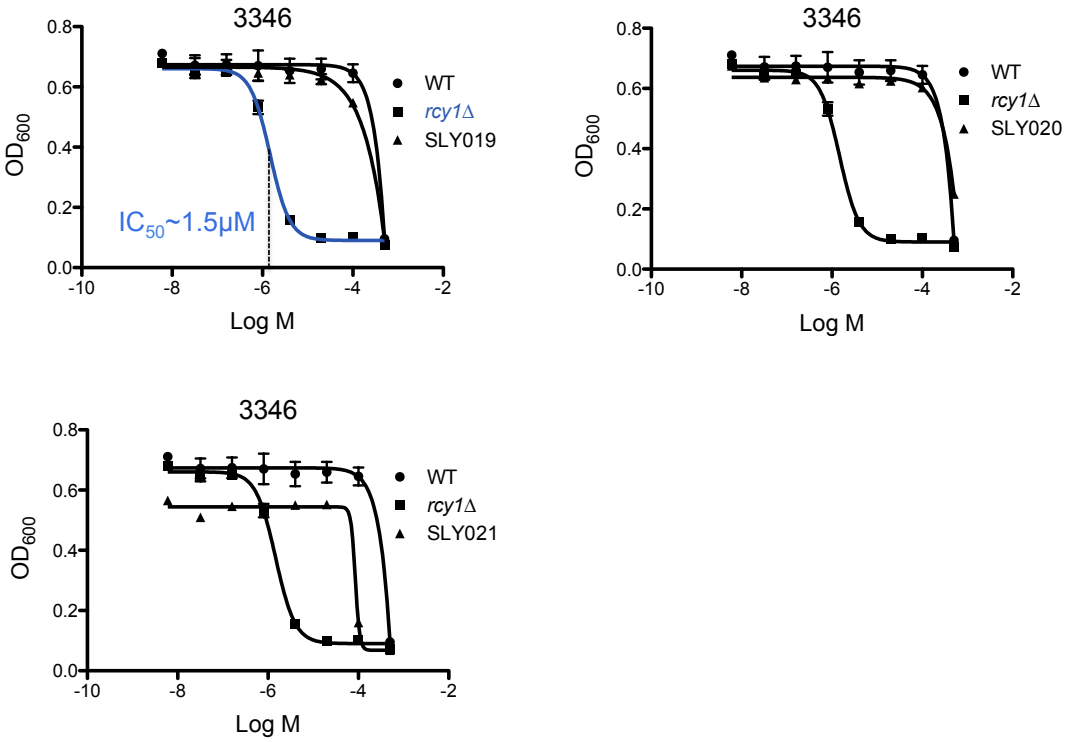

Growth inhibition curves for 3346-resistant mutants SLY019-021.

3.5.3. Sequencing Information

Figure S3-6

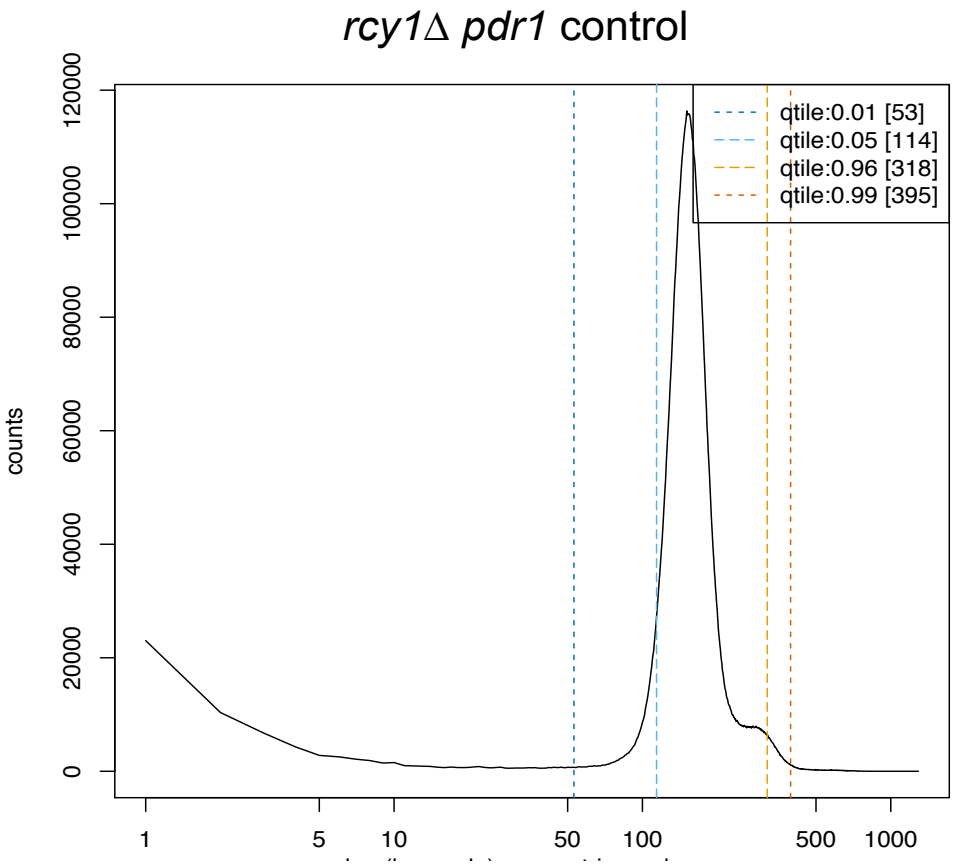

Coverage distribution on genes only. Value (log scale) over untrimmed range. Median = 160; mean = 174; stdev = 64.2

Figure S3-7

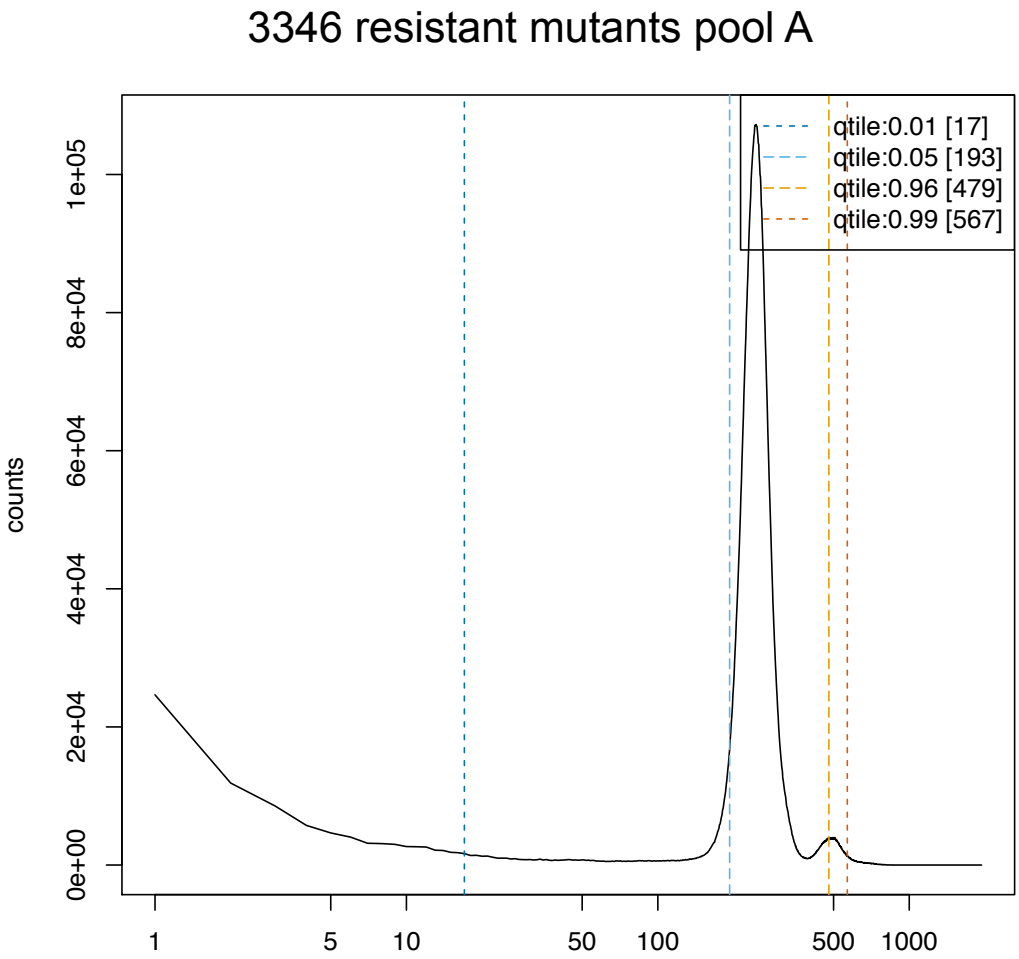

Pool A consists of 6 spontaneous mutants. Coverage distribution on genes only. Value (log scale) over untrimmed range. Median = 250; mean = 262; stdev = 80.3

Figure S3-8

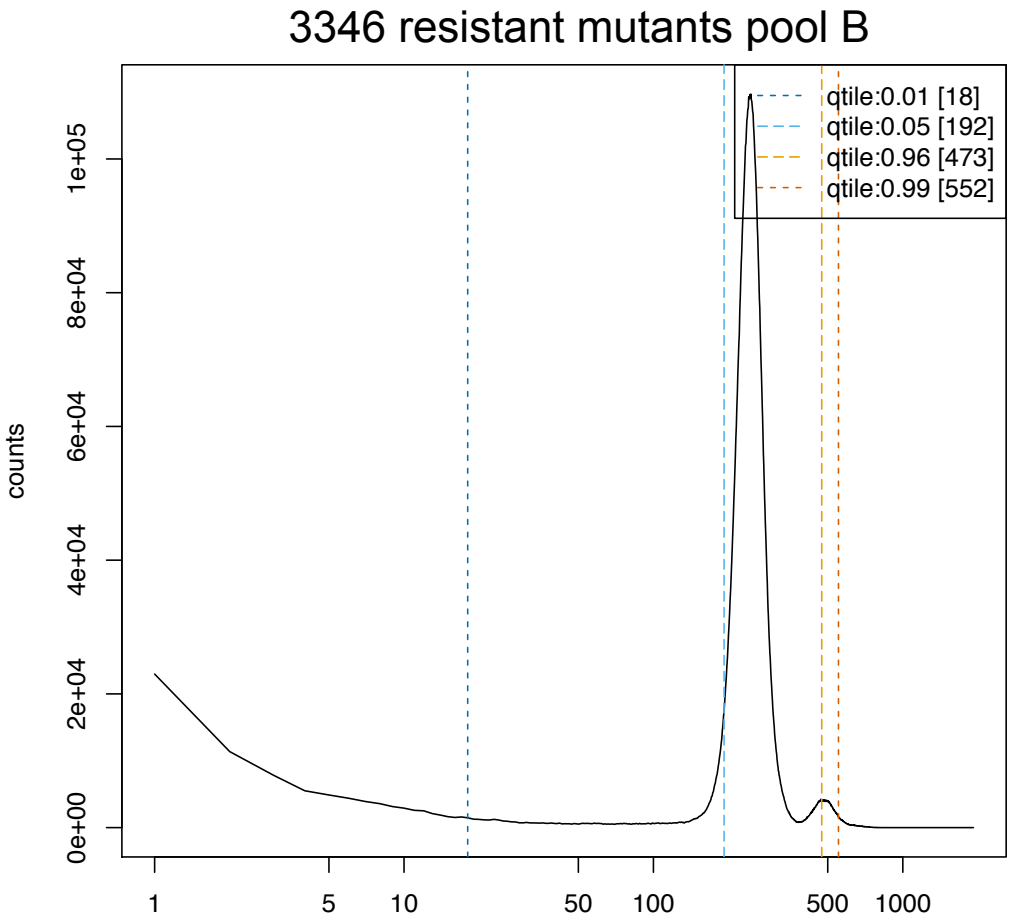

Pool B consists of 5 EMS-treated mutants. Coverage distribution on genes only. Value (log scale) over untrimmed range. Median = 247; mean = 259; stdev = 77.4

Figure S3-9

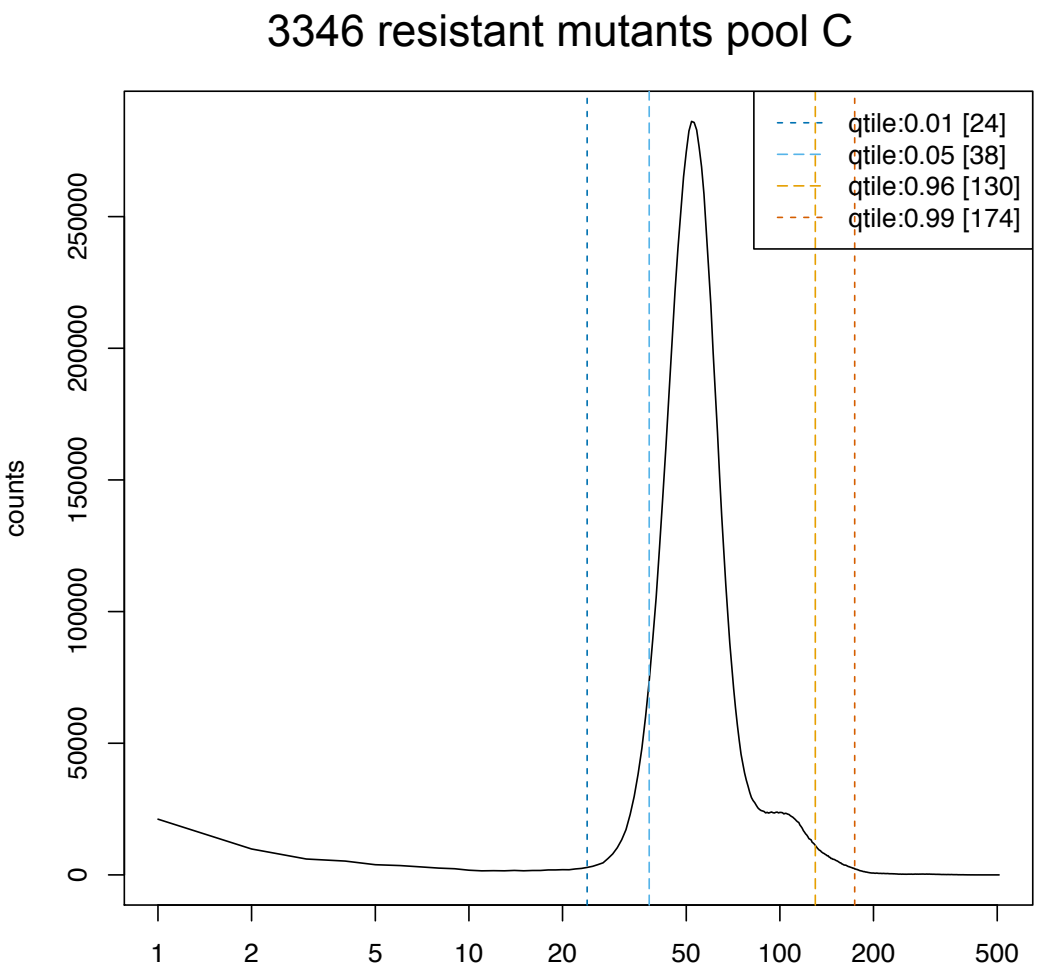

Pool B consists of 4 EMS-treated mutants and 4 non-EMS treated mutants. Coverage distribution on genes only. Value (log scale) over untrimmed range. Median = 56; mean = 64; stdev = 30.5

Figure S3-10

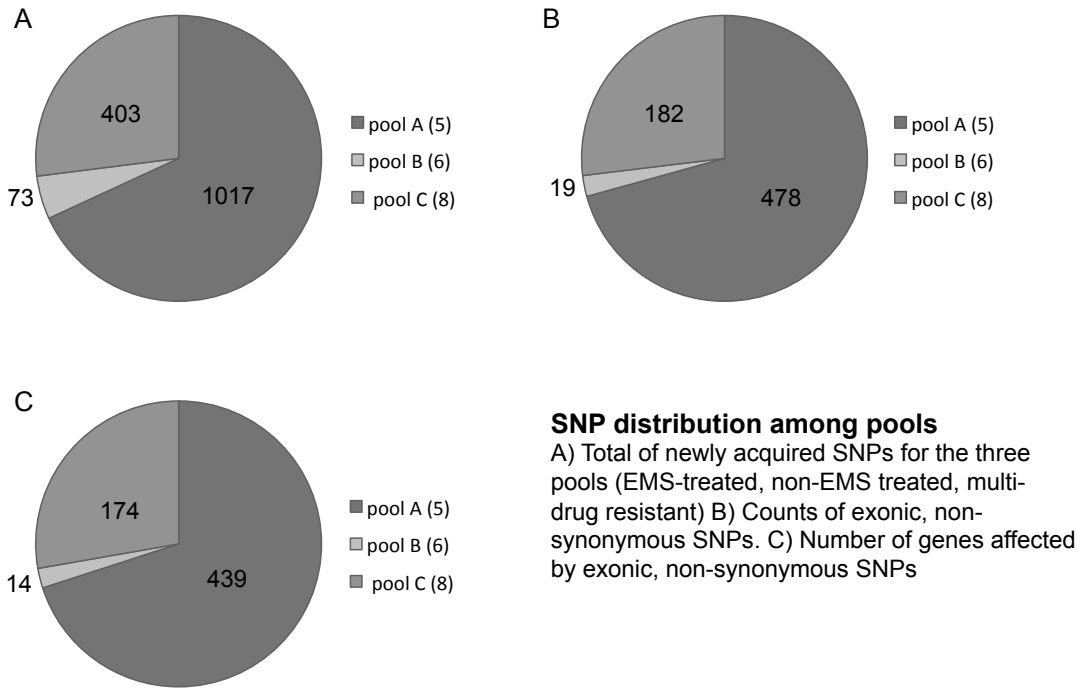

SNP distribution among pools
A) Total of newly acquired SNPs for the three pools (EMS-treated, non-EMS treated, multi-drug resistant) B) Counts of exonic, non-synonymous SNPs. C) Number of genes affected by exonic, non-synonymous SNPs

3.5.4. Synthesis

All other compounds used in this project were obtained commercially. Compound libraries screened include ChemDiv and Spectrum collections. Other compounds that were screened were purchased as individual orders.

To produce the epoxide intermediate **(3)**, 4 ml of dioxane, 13 mmol of allyl phenol **(2)** and 26 mmol of NaOH (12M) was added to a reaction bomb and stirred at 80-90 C^{o} for one hour. Next, 32 mmol of epichlorohydrin **(1)** was slowly added along with enough dioxane to bring the volume of the reaction mixture up to 10 ml. The

Scheme S3-1

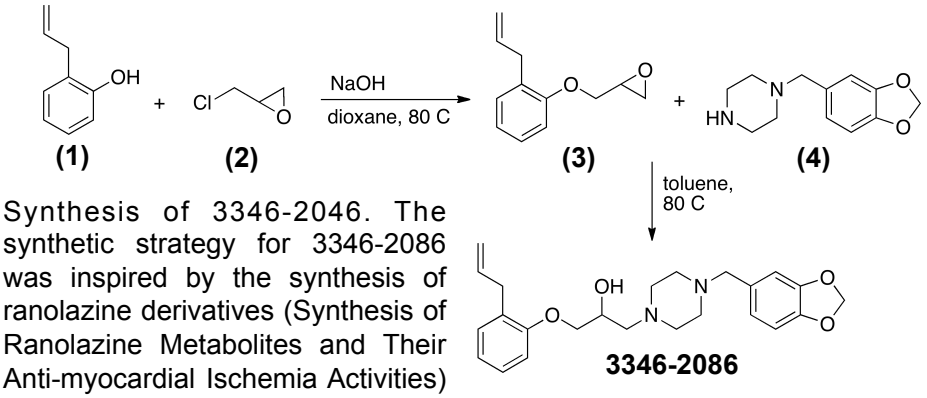

Synthesis of 3346-2046. The synthetic strategy for 3346-2086 was inspired by the synthesis of ranolazine derivatives (Synthesis of Ranolazine Metabolites and Their Anti-myocardial Ischemia Activities) in a study by Hongbin Sun et al.

reaction was allowed to proceed over night with stirring at 80-90 C^{o}. The reaction was checked by TLC (12% ethyl acetate/hexane), which confirmed the presence of the desired epoxide **(3)**. The reaction mixture was then diluted by a factor of four with ethyl acetate, gravity filtered and extracted with water twice and once with brine. The crude solution was then condensed under reduced pressure and purified on a silica column (12% ethyl acetate/hexane) yielding 1.145g (46%). The purified epoxide **(3)** was checked by TLC and NMR. To obtain 3346, 6 mmol of the epoxide **(3)** was dissolved in 4 ml of MeOH and added to a reaction bomb containing a solution of 6 mmol of the piperazine **(4)** in 8 ml of toluene. The mixture was allowed to react over night at 80-90 C^{o} while stirring. The reaction mixture was checked the next day by TLC (15:1 DCM:MeOH), which confirmed to formation of the desired product (3346). The reaction mixture was then concentrated down to a yellow oil *via* reduced pressure and washed with MeOH. This solution was again reduced to a crude oil and silica column purified (15:1 DCM:MeOH) yielding 2.134g (85%). The desired product was confirmed by LCMS and NMR.

H[1] NMR- 3346

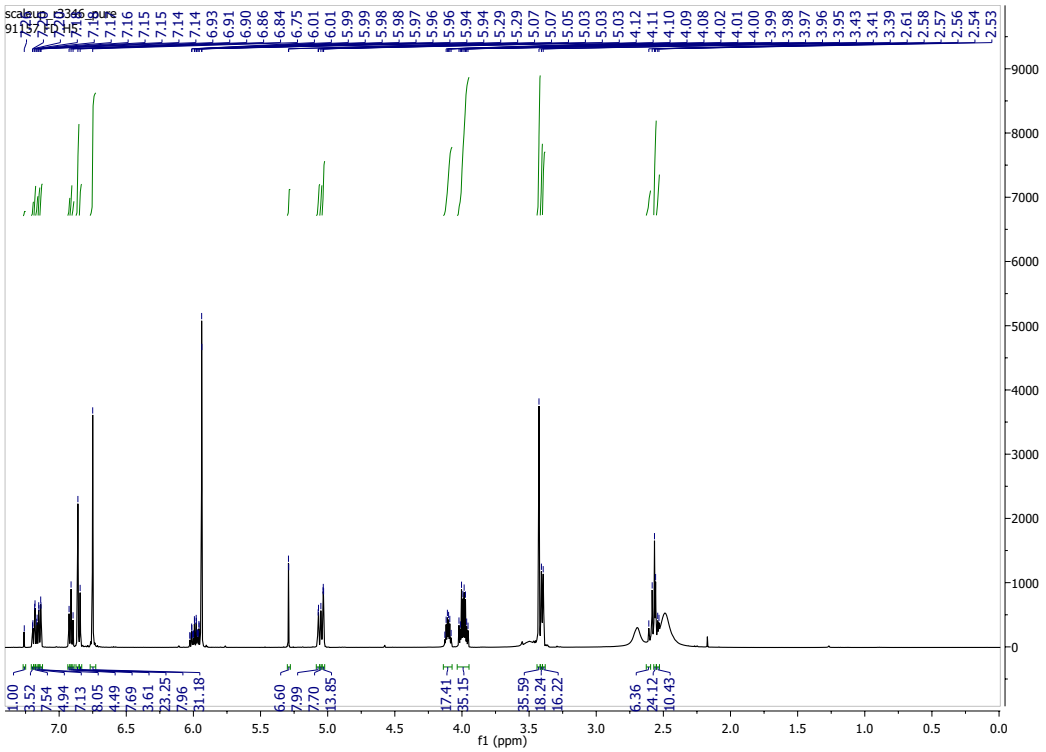

[1]H NMR: (500 MHz, CDCl3) δ7.18 (1H, t, *J* = 7.8 Hz), δ7.14 (1H, d, *J* = 7.7 Hz), δ6.91 (1H, t, *J* = 7.6 Hz), δ6.85 (2H, m), δ6.75 (2H, m), δ5.98 (1H, m), δ5.94 (2H, d, 0.7 Hz), δ5.05 (2H, m), δ4.10 (1H, m), δ3.99 (2H, m), δ3.43 (2H, s), δ3.40 (2H, d, *J* = 6.7 Hz), δ2.70 (1H, bs), δ2.56 (4H, m), δ2.49 (6H, bs)

LCMS- 3346

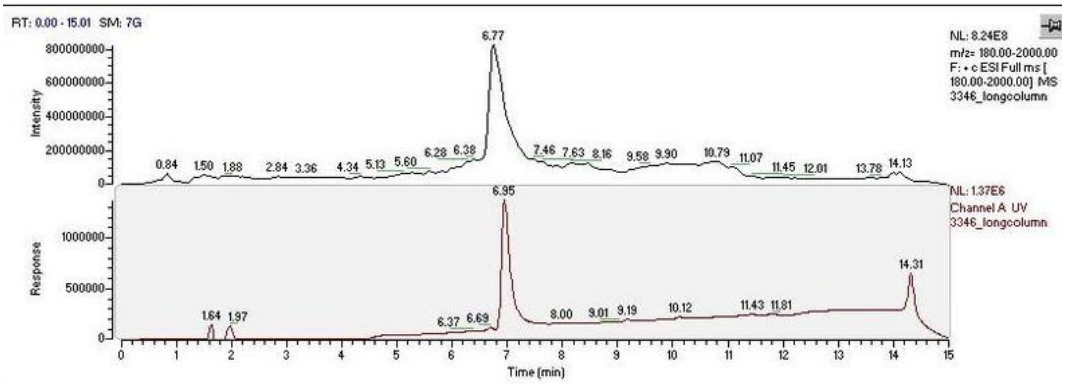
RT: 0.00 - 15.01 SM: 7G
NL: 8.24E8
m/z= 180.00-2000.00
F: + c ESI Full ms [
180.00-2000.00] MS
3346_longcolumn
Intensity
6.77
0.84 1.50 1.88 2.84 3.36 4.34 5.13 5.60 6.28 6.38 7.46 7.63 8.16 9.58 9.90 10.79 11.07 11.45 12.01 13.78 14.13
NL: 1.37E6
Channel A UV
3346_longcolumn
Response
6.95
14.31
1.64 1.97 6.37 6.69 8.00 9.01 9.19 10.12 11.43 11.81
Time (min)

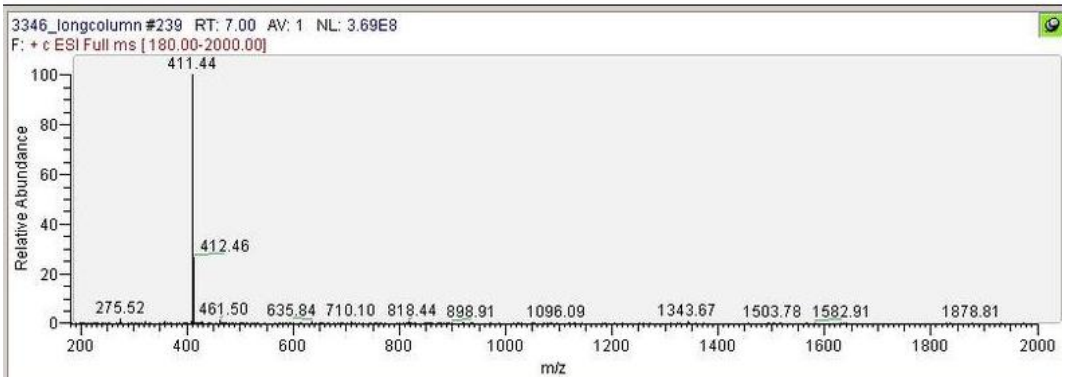
3346_longcolumn #239 RT: 7.00 AV: 1 NL: 3.69E8
F: + c ESI Full ms [180.00-2000.00]
Relative Abundance
411.44
412.46
275.52 461.50 635.84 710.10 818.44 898.91 1096.09 1343.67 1503.78 1582.91 1878.81
m/z

3.5.5. Sanger Sequencing

Figure S3-11

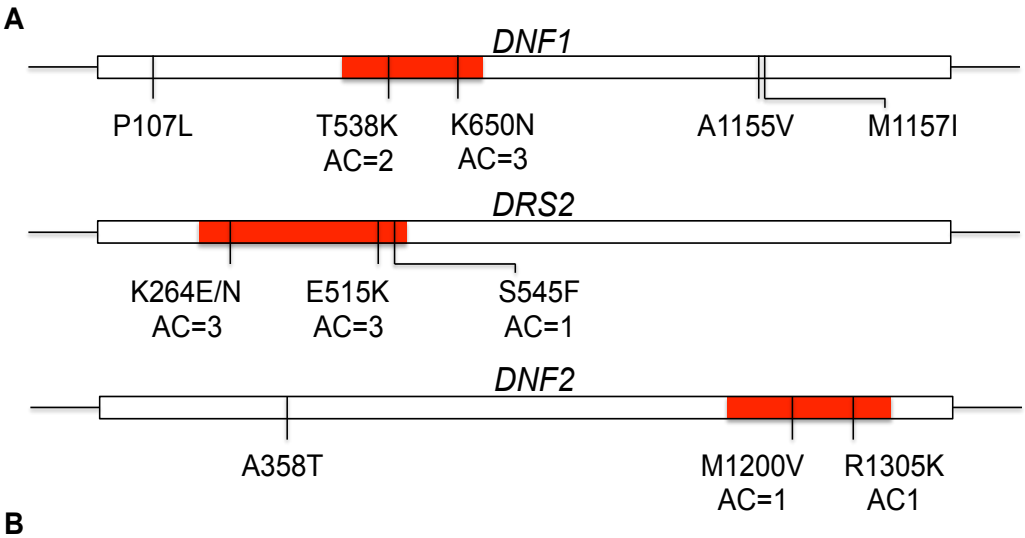

B

	SYL004	SLY005	SLY016	SLY017	SLY006	SLY007	SLY008	SLY009	Total AC	NGS AC
DNF1 T538									0	2
DNF1 K650								N	1	3
DRS2 K264					N	E	E		3	3
DRS2 E515		K	K	K					3	3
DRS2 S545	F								1	1
DNF2 M1200									0	1
DNF2 R1305									0	1

(A) Schematic of the regions of *DRS2, DNF1* and *DNF2* to be amplified and sequenced. (B) Table of mutations found.

3.5.6. Structural Analysis

Figure S3-12

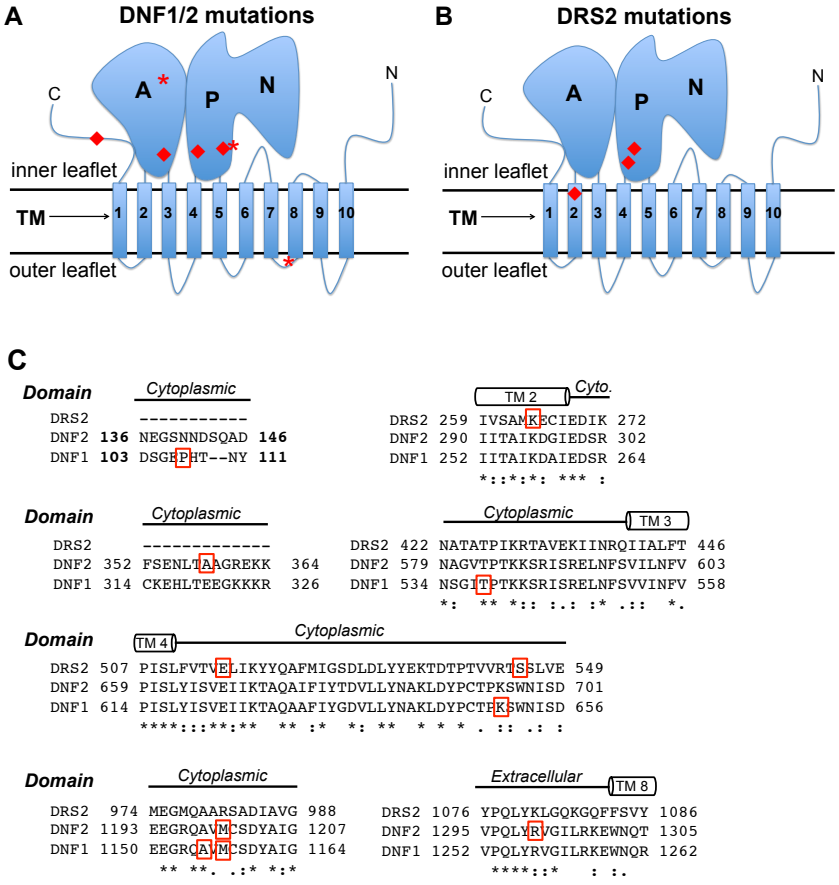

A/B) Schematic of Drs2 and Dnf1 showing general locations of the mutations incurred in the pool of 19 3346-resistant pool. In A, diamonds represent Dnf1p mutations and asterisks represent Dnf2p mutaions. C) Sequence homology diagram showing all *DRS2, DNF1* and *DNF2* mutations (designated with red squares).

Figure S3-13

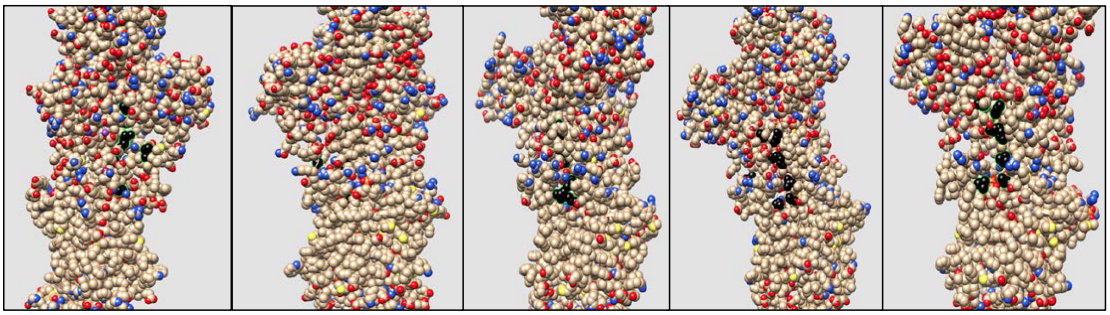

3.5.7. Scrambling Assay

Table S3-2

compound	*rcy1Δ* IC50 (uM)	rate at 50uM
3346	0.78	3.28
azaperone	0.4	1.29
haloperidol	0.91	3.56
3701	1.9	2.28
ziprasidone	2.8	0.43
tamoxifen	8	3.18
chlorpromazine	27.1	0.479
aripiprazole	53.7	1.07
ranolazine	>100	1.66

Table showing *rcy1*Δ activity and rate of fluorescent decrease in the dithionite assay for the CADs tested.

3.6. References

(1) Halliwell, W. H. Cationic amphiphilic drug-induced phospholipidosis. *Toxicologic Pathology* **1997**, *25*, 53-60.

(2) Reasor, M. J. A review of the biology and toxicologic implications of the induction of lysosomal lamellar bodies by drugs. *Toxicology and applied pharmacology* **1989**, *97*, 47-56.

(3) Yamamoto, A.; ADACHI, S.; KITANI, T.; SHINJI, Y.; Seki, K.-i.; NASU, T.; NISHIKAWA, M. Drug-induced lipidosis in human cases and in animal experiments. *The Journal of Biochemistry* **1971**, *69*, 613-615.

(4) Dake, M. D.; Madison, J. M.; Montgomery, C. K.; Shellito, J. E.; Hinchcliffe, W. A.; Winkler, M. L.; Bainton, D. F. Electron microscopic demonstration of lysosomal inclusion bodies in lung, liver, lymph nodes, and blood leukocytes of patients with amiodarone pulmonary toxicity. *The American journal of medicine* **1985**, *78*, 506-512.

(5) Lullmann, H.; Lullmann-Rauch, R.; Wassermann, O. Lipidosis induced by amphiphilic cationic drugs. *Biochemical pharmacology* **1978**, *27*, 1103-1108.

(6) Anderson, N.; Borlak, J. r. Drug-induced phospholipidosis. *FEBS letters* **2006**, *580*, 5533-5540.

(7) Wang, T.; Feng, Y.; Jin, X.; Fan, X.; Crommen, J.; Jiang, Z. Liposome electrokinetic chromatography based in vitro model for early screening of the drug-induced phospholipidosis risk. *Journal of pharmaceutical and biomedical analysis* **2014**, *96*, 263-271.

(8) Hamaguchi, R.; Tanimoto, T.; Kuroda, Y. Putative biomarker for phospholipid accumulation in cultured cells treated with phospholipidosis-inducing drugs: Alteration of the phosphatidylinositol composition detected using high-performance liquid chromatography-tandem mass spectrometry. *Journal of Chromatography B* **2014**, *967*, 110-117.

(9) Lee, A. Y.; Onge, R. P. S.; Proctor, M. J.; Wallace, I. M.; Nile, A. H.; Spagnuolo, P. A.; Jitkova, Y.; Gronda, M.; Wu, Y.; Kim, M. K. Mapping the cellular response to small molecules using chemogenomic fitness signatures. *Science* **2014**, *344*, 208-211.

(10) Bauch, C.; Bevan, S.; Woodhouse, H.; Dilworth, C.; Walker, P. Predicting in vivo phospholipidosis-inducing potential of drugs by a combined high content screening and in silico modelling approach. *Toxicology in Vitro* **2015**, *29*, 621-630.

(11) Kodavanti, U. P.; Mehendale, H. M. Cationic amphiphilic drugs and phospholipid storage disorder. *Pharmacological Reviews* **1990**, *42*, 327-354.

(12) Hanumegowda, U. M.; Regueiro-Ren, A.: Drug-Induced Phospholipidosis: Prediction, Detection, and Mitigation Strategies. In *Tactics in Contemporary Drug Design*; Springer, 2015; pp 261-281.

(13) Seydel, J. K.; Wassermann, O. NMR-studies on the molecular basis of drug-induced phospholipidosis,ÄîII. Interaction between several amphiphilic drugs and phospholipids. *Biochemical pharmacology* **1976**, *25*, 2357-2364.

(14) Nathwani, R. A.; Kaplowitz, N. Drug hepatotoxicity. *Clinics in liver disease* **2006**, *10*, 207-217.

(15) Navarro, V. J.; Senior, J. R. Drug-related hepatotoxicity. *New England Journal of Medicine* **2006**, *354*, 731-739.

(16) Stieger, B.; Fattinger, K.; Madon, J.; Kullak-Ublick, G. A.; Meier, P. J. Drug-and estrogen-induced cholestasis through inhibition of the hepatocellular bile salt export pump (Bsep) of rat liver. *Gastroenterology* **2000**, *118*, 422-430.

(17) van Mil, S. W.; Klomp, L. W.; Bull, L. N.; Houwen, R. H. In *Tilte*2001.

(18) Axelsen, K. B.; Palmgren, M. G. Evolution of substrate specificities in the P-type ATPase superfamily. *Journal of Molecular Evolution* **1998**, *46*, 84-101.

(19) Tang, X.; Halleck, M. S.; Schlegel, R. A.; Williamson, P. A subfamily of P-type ATPases with aminophospholipid transporting activity. *Science* **1996**, *272*, 1495-1497.

(20) Chen, C.-Y.; Ingram, M. F.; Rosal, P. H.; Graham, T. R. Role for Drs2p, a P-type ATPase and potential aminophospholipid translocase, in yeast late Golgi function. *The Journal of cell biology* **1999**, *147*, 1223-1236.

(21) Hua, Z.; Fatheddin, P.; Graham, T. R. An essential subfamily of Drs2p-related P-type ATPases is required for protein trafficking between Golgi complex and endosomal/vacuolar system. *Molecular biology of the cell* **2002**, *13*, 3162-3177.

(22) Pomorski, T.; Lombardi, R.; Riezman, H.; Devaux, P. F.; van Meer, G.; Holthuis, J. C. Drs2p-related P-type ATPases Dnf1p and Dnf2p are required for phospholipid translocation across the yeast plasma membrane and serve a role in endocytosis. *Molecular biology of the cell* **2003**, *14*, 1240-1254.

(23) Pawlikowska, L.; Groen, A.; Eppens, E. F.; Kunne, C.; Ottenhoff, R.; Looije, N.; Knisely, A.; Killeen, N. P.; Bull, L. N.; Elferink, R. P. O. A mouse genetic model for familial cholestasis caused by ATP8B1 mutations reveals perturbed bile salt homeostasis but no impairment in bile secretion. *Human molecular genetics* **2004**, *13*, 881-892.

(24) van der Woerd, W. L.; van Mil, S. W.; Stapelbroek, J. M.; Klomp, L. W.; van de Graaf, S. F.; Houwen, R. H. Familial cholestasis: progressive familial intrahepatic cholestasis, benign recurrent intrahepatic cholestasis and intrahepatic cholestasis of pregnancy. *Best Practice & Research Clinical Gastroenterology* **2010**, *24*, 541-553.

(25) Wiederkehr, A.; Avaro, S.; Prescianotto-Baschong, C.; Haguenauer-Tsapis, R.; Riezman, H. The F-box protein Rcy1p is involved in endocytic membrane traffic and recycling out of an early endosome in Saccharomyces cerevisiae. *The Journal of cell biology* **2000**, *149*, 397-410.

(26) Galan, J.-M.; Wiederkehr, A.; Seol, J. H.; Haguenauer-Tsapis, R.; Deshaies, R. J.; Riezman, H.; Peter, M. Skp1p and the F-box protein Rcy1p form a non-SCF complex involved in recycling of the SNARE Snc1p in yeast. *Molecular and cellular biology* **2001**, *21*, 3105-3117.

(27) Furuta, N.; Fujimura-Kamada, K.; Saito, K.; Yamamoto, T.; Tanaka, K. Endocytic recycling in yeast is regulated by putative phospholipid translocases and the Ypt31p/32p‚ÄìRcy1p pathway. *Molecular biology of the cell* **2007**, *18*, 295-312.

(28) Gassner, N. C.; Tamble, C. M.; Bock, J. E.; Cotton, N.; White, K. N.; Tenney, K.; St. Onge, R. P.; Proctor, M. J.; Giaever, G.; Nislow, C. Accelerating the Discovery of Biologically Active Small Molecules Using a High-Throughput Yeast Halo Assay‚ä•. *Journal of natural products* **2007**, *70*, 383-390.

(29) Woehrmann, M. H.; Gassner, N. C.; Bray, W. M.; Stuart, J. M.; Lokey, S. HALO384 A Halo-Based Potency Prediction Algorithm for High-Throughput Detection of Antimicrobial Agents. *Journal of biomolecular screening* **2010**, *15*, 196-205.

(30) Wride, D. A.; Pourmand, N.; Bray, W. M.; Kosarchuk, J. J.; Nisam, S. C.; Quan, T. K.; Berkeley, R. F.; Katzman, S.; Hartzog, G. A.; Dobkin, C. E. Confirmation of the cellular targets of benomyl and rapamycin using next-generation

sequencing of resistant mutants in S. cerevisiae. *Molecular BioSystems* **2014**, *10*, 3179-3187.

(31) Langmead, B.; Salzberg, S. L. Fast gapped-read alignment with Bowtie 2. *Nature Methods* **2012**, *9*, 357-359.

(32) Li, H.; Handsaker, B.; Wysoker, A.; Fennell, T.; Ruan, J.; Homer, N.; Marth, G.; Abecasis, G.; Durbin, R. The sequence alignment/map format and SAMtools. *Bioinformatics* **2009**, *25*, 2078-2079.

(33) McKenna, A.; Hanna, M.; Banks, E.; Sivachenko, A.; Cibulskis, K.; Kernytsky, A.; Garimella, K.; Altshuler, D.; Gabriel, S.; Daly, M.; DePristo, M. A. The Genome Analysis Toolkit: a MapReduce framework for analyzing next-generation DNA sequencing data. *Genome Research* **2010**, *20*, 1297-1303.

(34) DePristo, M. A.; Banks, E.; Poplin, R.; Garimella, K. V.; Maguire, J. R.; Hartl, C.; Philippakis, A. A.; del Angel, G.; Rivas, M. A.; Hanna, M.; McKenna, A.; Fennell, T. J.; Kernytsky, A. M.; Sivachenko, A. Y.; Cibulskis, K.; Gabriel, S. B.; Altshuler, D.; Daly, M. J. A framework for variation discovery and genotyping using next-generation DNA sequencing data. *Nature Genetics* **2011**, *43*, 491-498.

(35) Zhou, X.; Graham, T. R. Reconstitution of phospholipid translocase activity with purified Drs2p, a type-IV P-type ATPase from budding yeast. *Proceedings of the National Academy of Sciences* **2009**, *106*, 16586-16591.

(36) Carvajal, E.; Van Den Hazel, H.; Cybularz-Kolaczkowska, A.; Balzi, E.; Goffeau, A. Molecular and phenotypic characterization of yeast PDR1 mutants that show hyperactive transcription of various ABC multidrug transporter genes. *Molecular and General Genetics MGG* **1997**, *256*, 406-415.

(37) Balzi, E.; Goffeau, A. Yeast multidrug resistance: the PDR network. *Journal of bioenergetics and biomembranes* **1995**, *27*, 71-76.

(38) Monk, B. C.; Goffeau, A. Outwitting multidrug resistance to antifungals. *Science* **2008**, *321*, 367-369.

(39) Hillenmeyer, M. E.; Fung, E.; Wildenhain, J.; Pierce, S. E.; Hoon, S.; Lee, W.; Proctor, M.; Onge, R. P. S.; Tyers, M.; Koller, D. The chemical genomic portrait of yeast: uncovering a phenotype for all genes. *Science* **2008**, *320*, 362-365.

(40) Braus, G. H. Aromatic amino acid biosynthesis in the yeast Saccharomyces cerevisiae: a model system for the regulation of a eukaryotic biosynthetic pathway. *Microbiological reviews* **1991**, *55*, 349-370.

(41) Lai, M. H.; Bard, M.; Pierson, C. A.; Alexander, J. F.; Goebl, M.; Carter, G. T.; Kirsch, D. R. The identification of a gene family in the Saccharomyces cerevisiae ergosterol biosynthesis pathway. *Gene* **1994**, *140*, 41-49.

(42) Loh, E.; Hong, W. The binary interacting network of the conserved oligomeric Golgi tethering complex. *Journal of Biological Chemistry* **2004**, *279*, 24640-24648.

(43) Robinson, J. S.; Klionsky, D. J.; Banta, L. M.; Emr, S. D. Protein sorting in Saccharomyces cerevisiae: isolation of mutants defective in the delivery and processing of multiple vacuolar hydrolases. *Molecular and cellular biology* **1988**, *8*, 4936-4948.

(44) Gerrard, S. R.; Levi, B. P.; Stevens, T. H. Pep12p is a multifunctional yeast syntaxin that controls entry of biosynthetic, endocytic and retrograde traffic into the prevacuolar compartment. *Traffic* **2000**, *1*, 259-269.

(45) Mamnun, Y. M.; Pandjaitan, R.; Mahe, Y.; Delahodde, A.; Kuchler, K. The yeast zinc finger regulators Pdr1p and Pdr3p control pleiotropic drug resistance (PDR) as homo‚Äêand heterodimers in vivo. *Molecular microbiology* **2002**, *46*, 1429-1440.

(46) Balzi, E.; Wang, M.; Leterme, S.; Van Dyck, L.; Goffeau, A. PDR5, a novel yeast multidrug resistance conferring transporter controlled by the transcription regulator PDR1. *Journal of Biological Chemistry* **1994**, *269*, 2206-2214.

(47) Ribelin, W. E. The effects of drugs and chemicals upon the structure of the adrenal gland. *Toxicological Sciences* **1984**, *4*, 105-119.

(48) Scheurle, C.; D√ § mmrich, M.; Becker, J. U.; Baumg√ § rtel, M. W. Renal phospholipidosis possibly induced by ranolazine. *Clinical kidney journal* **2013**, sft141.

(49) Mesens, N.; Steemans, M.; Hansen, E.; Verheyen, G. R.; Van Goethem, F.; Van Gompel, J. Screening for phospholipidosis induced by central nervous drugs: comparing the predictivity of an in vitro assay to high throughput in silico assays. *Toxicology in Vitro* **2010**, *24*, 1417-1425.

(50) Morth, J. P.; Pedersen, B. P.; Buch-Pedersen, M. J.; Andersen, J. P.; Vilsen, B.; Palmgren, M. G.; Nissen, P. A structural overview of the plasma membrane Na+, K+-ATPase and H+-ATPase ion pumps. *Nature Reviews Molecular Cell Biology* **2011**, *12*, 60-70.

(51) Pappu, A.; Hostetler, K. Y. Effect of cationic amphiphilic drugs on the hydrolysis of acidic and neutral phospholipids by liver lysosomal phospholipase A. *Biochemical pharmacology* **1984**, *33*, 1639-1644.

(52) Seydel, J. K.; Wassermann, O. NMR-studies on the molecular basis of drug-induced phospholipidosis—II. Interaction between several amphiphilic drugs and phospholipids. *Biochemical pharmacology* **1976**, *25*, 2357-2364.

(53) 田村明; 守脇尚子; 藤井達三. Disturbing effect of cationic amphiphilic drugs on phospholipid asymmetry of the membrane lipid bilayer of human erythrocytes. *Chemical and pharmaceutical bulletin* **1983**, *31*, 1692-1697.

(54) Bradford, P.; Marinetti, G. Effects of local anesthetics on phospholipid topology and dopamine uptake and release in rat brain synaptosomes. *The Journal of membrane biology* **1982**, *67*, 211-218.

(55) McIntyre, J. C.; Sleight, R. G. Fluorescence assay for phospholipid membrane asymmetry. *Biochemistry* **1991**, *30*, 11819-11827.

(56) Hanamatsu, H.; Fujimura-Kamada, K.; Yamamoto, T.; Furuta, N.; Tanaka, K. Interaction of the phospholipid flippase Drs2p with the F-box protein Rcy1p plays an important role in early endosome to trans-Golgi network vesicle transport in yeast. *Journal of biochemistry* **2014**, *155*, 51-62.

(57) Sturgill, M. G.; Lambert, G. H. Xenobiotic-induced hepatotoxicity: mechanisms of liver injury and methods of monitoring hepatic function. *Clinical chemistry* **1997**, *43*, 1512-1526.

(58) Baldridge, R. D.; Graham, T. R.; Identification of residues defining phospholipid flippase substrate specificity of type IV P-type ATPases. *Proceedings of the National Academy of Sciences.* **2012**, 109, 290-298.

Bibliography

Anderson, N.; Borlak, J. r. Drug-induced phospholipidosis. *FEBS letters* **2006**, *580*, 5533-5540.

Andries, K.; Verhasselt, P.; Guillemont, J.; Gohlmann, H. W.; Neefs, J. M.; Winkler, H.; Van Gestel, J.; Timmerman, P.; Zhu, M.; Lee, E.; Williams, P.; de Chaffoy, D.; Huitric, E.; Hoffner, S.; Cambau, E.; Truffot-Pernot, C.; Lounis, N.; Jarlier, V. A diarylquinoline drug active on the ATP synthase of Mycobacterium tuberculosis. *Science* **2005**, *307*, 223-227.

Axelsen, K. B.; Palmgren, M. G. Evolution of substrate specificities in the P-type ATPase superfamily. *Journal of Molecular Evolution* **1998**, *46*, 84-101.

Baetz, K.; McHardy, L.; Gable, K.; Tarling, T.; Rebérioux, D.; Bryan, J.; Andersen, R. J.; Dunn, T.; Hieter, P.; Roberge, M. Yeast genome-wide drug-induced haploinsufficiency screen to determine drug mode of action. *Proceedings of the National Academy of Sciences of the United States of America* **2004**, *101*, 4525-4530.

Balzi, E.; Goffeau, A. Yeast multidrug resistance: the PDR network. *Journal of Bioenergetics and Biomembranes* **1995**, *27*, 71-76.

Balzi, E.; Wang, M.; Leterme, S.; Van Dyck, L.; Goffeau, A. PDR5, a novel yeast multidrug resistance conferring transporter controlled by the transcription regulator PDR1. *Journal of Biological Chemistry* **1994**, *269*, 2206-2214.

Bauch, C.; Bevan, S.; Woodhouse, H.; Dilworth, C.; Walker, P. Predicting in vivo phospholipidosis-inducing potential of drugs by a combined high content screening and in silico modelling approach. *Toxicology in Vitro* **2015**, *29*, 621-630.

Botstein, D.; Chervitz, S. A.; Cherry, J. M. Yeast as a model organism. *Science (New York, NY)* **1997**, *277*, 1259.

Brachmann, C. B.; Davies, A.; Cost, G. J.; Caputo, E.; Li, J.; Hieter, P.; Boeke, J. D. Designer deletion strains derived from Saccharomyces cerevisiae S288C: a useful set of strains and plasmids for PCR-mediated gene disruption and other applications. *Yeast* **1998**, *14*, 115-132.

Bradford, P.; Marinetti, G. Effects of local anesthetics on phospholipid topology and dopamine uptake and release in rat brain synaptosomes. *The Journal of membrane biology* **1982**, *67*, 211-218.

Braus, G. H. Aromatic amino acid biosynthesis in the yeast Saccharomyces cerevisiae: a model system for the regulation of a eukaryotic biosynthetic pathway. *Microbiological reviews* **1991**, *55*, 349-370.

Breuder, T.; Hemenway, C. S.; Movva, N. R.; Cardenas, M. E.; Heitman, J. Calcineurin is essential in cyclosporin A-and FK506-sensitive yeast strains. *Proceedings of the National Academy of Sciences* **1994**, *91*, 5372-5376.

Brown, E. J.; Albers, M. W.; Shin, T. B.; Ichikawa, K.; Keith, C. T.; Lane, W. S.; Schreiber, S. L. A mammalian protein targeted by G1-arresting rapamycin-receptor complex. *Nature* **1994**, *369*, 756-758.

Brown, E. J.; Albers, M. W.; Shin, T. B.; Ichikawa, K.; Keith, C. T.; Lane, W. S.; Schreiber, S. L. A mammalian protein targeted by G1-arresting rapamycin-receptor complex. *Nature* **1994**, *369*, 756-758.

Butcher, R. A.; Bhullar, B. S.; Perlstein, E. O.; Marsischky, G.; LaBaer, J.; Schreiber, S. L. Microarray-based method for monitoring yeast overexpression strains reveals small-molecule targets in TOR pathway. *Nature chemical biology* **2006**, *2*, 103-109.

Butcher, R. A.; Schreiber, S. L. A small molecule suppressor of FK506 that targets the mitochondria and modulates ionic balance in Saccharomyces cerevisiae. *Chem Biol* **2003**, *10*, 521-531.

Cafferkey, R.; Young, P. R.; McLaughlin, M. M.; Bergsma, D. J.; Koltin, Y.; Sathe, G. M.; Faucette, L.; Eng, W. K.; Johnson, R. K.; Livi, G. P. Dominant missense mutations in a novel yeast protein related to mammalian phosphatidylinositol 3-kinase and VPS34 abrogate rapamycin cytotoxicity. *Mol. Cell. Biol.* **1993**, *13*, 6012-6023.

Cardenas, M. E.; Heitman, J. FKBP12-rapamycin target TOR2 is a vacuolar protein with an associated phosphatidylinositol-4 kinase activity. *The EMBO journal* **1995**, *14*, 5892.

Carvajal, E.; Van Den Hazel, H.; Cybularz-Kolaczkowska, A.; Balzi, E.; Goffeau, A. Molecular and phenotypic characterization of yeast PDR1 mutants that show hyperactive transcription of various ABC multidrug transporter genes. *Molecular and General Genetics MGG* **1997**, *256*, 406-415.

Chen, C.-Y.; Ingram, M. F.; Rosal, P. H.; Graham, T. R. Role for Drs2p, a P-type ATPase and potential aminophospholipid translocase, in yeast late Golgi function. *The Journal of cell biology* **1999**, *147*, 1223-1236.

Chen, J.; Zheng, X.-F.; Brown, E. J.; Schreiber, S. L. Identification of an 11-kDa FKBP12-rapamycin-binding domain within the 289-kDa FKBP12-rapamycin-associated protein and characterization of a critical serine residue. *Proceedings of the National Academy of Sciences* **1995**, *92*, 4947-4951.

Cherry, J. M.; Hong, E. L.; Amundsen, C.; Balakrishnan, R.; Binkley, G.; Chan, E. T.; Christie, K. R.; Costanzo, M. C.; Dwight, S. S.; Engel, S. R. Saccharomyces Genome Database: the genomics resource of budding yeast. *Nucleic acids research* **2011**, gkr1029.

Chiu, M. I.; Katz, H.; Berlin, V. RAPT1, a mammalian homolog of yeast Tor, interacts with the FKBP12/rapamycin complex. *Proceedings of the National Academy of Sciences* **1994**, *91*, 12574-12578.

Dake, M. D.; Madison, J. M.; Montgomery, C. K.; Shellito, J. E.; Hinchcliffe, W. A.; Winkler, M. L.; Bainton, D. F. Electron microscopic demonstration of lysosomal

inclusion bodies in lung, liver, lymph nodes, and blood leukocytes of patients with amiodarone pulmonary toxicity. *The American journal of medicine* **1985**, *78*, 506-512.

DePristo, M. A.; Banks, E.; Poplin, R.; Garimella, K. V.; Maguire, J. R.; Hartl, C.; Philippakis, A. A.; del Angel, G.; Rivas, M. A.; Hanna, M.; McKenna, A.; Fennell, T. J.; Kernytsky, A. M.; Sivachenko, A. Y.; Cibulskis, K.; Gabriel, S. B.; Altshuler, D.; Daly, M. J. A framework for variation discovery and genotyping using next-generation DNA sequencing data. *Nature Genetics* **2011**, *43*, 491-498.

Dorer, R. K.; Zhong, S.; Tallarico, J. A.; Wong, W. H.; Mitchison, T. J.; Murray, A. W. A small-molecule inhibitor of Mps1 blocks the spindle-checkpoint response to a lack of tension on mitotic chromosomes. *Current biology* **2005**, *15*, 1070-1076.

Dujon, B. The yeast genome project: what did we learn? *Trends in Genetics* **1996**, *12*, 263-270.

Evans, M. J.; Saghatelian, A.; Sorensen, E. J.; Cravatt, B. F. Target discovery in small-molecule cell-based screens by in situ proteome reactivity profiling. *Nature biotechnology* **2005**, *23*, 1303-1307.

Furuta, N.; Fujimura-Kamada, K.; Saito, K.; Yamamoto, T.; Tanaka, K. Endocytic recycling in yeast is regulated by putative phospholipid translocases and the Ypt31p/32p,ÄìRcy1p pathway. *Molecular biology of the cell* **2007**, *18*, 295-312.

Galan, J.-M.; Wiederkehr, A.; Seol, J. H.; Haguenauer-Tsapis, R.; Deshaies, R. J.; Riezman, H.; Peter, M. Skp1p and the F-box protein Rcy1p form a non-SCF complex involved in recycling of the SNARE Snc1p in yeast. *Molecular and cellular biology* **2001**, *21*, 3105-3117.

Gassner, N. C.; Tamble, C. M.; Bock, J. E.; Cotton, N.; White, K. N.; Tenney, K.; St Onge, R. P.; Proctor, M. J.; Giaever, G.; Nislow, C.; Davis, R. W.; Crews, P.; Holman, T. R.; Lokey, R. S. Accelerating the discovery of biologically active small molecules using a high-throughput yeast halo assay. *J. Nat. Prod.* **2007**, *70*, 383-390.

Gassner, N. C.; Tamble, C. M.; Bock, J. E.; Cotton, N.; White, K. N.; Tenney, K.; St. Onge, R. P.; Proctor, M. J.; Giaever, G.; Nislow, C. Accelerating the Discovery of Biologically Active Small Molecules Using a High-Throughput Yeast Halo Assay‚ä•. *Journal of natural products* **2007**, *70*, 383-390.

Gerrard, S. R.; Levi, B. P.; Stevens, T. H. Pep12p is a multifunctional yeast syntaxin that controls entry of biosynthetic, endocytic and retrograde traffic into the prevacuolar compartment. *Traffic* **2000**, *1*, 259-269.

Gerstein, A. C.; Chun, H. J.; Grant, A.; Otto, S. P. Genomic convergence toward diploidy in Saccharomyces cerevisiae. *PLoS Genetics* **2006**, *2*, e145.

Giaever, G.; Chu, A. M.; Ni, L.; Connelly, C.; Riles, L.; Veronneau, S.; Dow, S.; Lucau-Danila, A.; Anderson, K.; Andre, B. Functional profiling of the Saccharomyces cerevisiae genome. *nature* **2002**, *418*, 387-391.

Giaever, G.; Chu, A. M.; Ni, L.; Connelly, C.; Riles, L.; Veronneau, S.; Dow, S.; Lucau-Danila, A.; Anderson, K.; Andre, B. Functional profiling of the Saccharomyces cerevisiae genome. *nature* **2002**, *418*, 387-391.

Giaever, G.; Shoemaker, D. D.; Jones, T. W.; Liang, H.; Winzeler, E. A.; Astromoff, A.; Davis, R. W. Genomic profiling of drug sensitivities via induced haploinsufficiency. *Nature genetics* **1999**, *21*, 278-283.

Giaever, G.; Shoemaker, D. D.; Jones, T. W.; Liang, H.; Winzeler, E. A.; Astromoff, A.; Davis, R. W. Genomic profiling of drug sensitivities via induced haploinsufficiency. *Nat Genet* **1999**, *21*, 278-283.

Goffeau, A.; Barrell, B.; Bussey, H.; Davis, R.; Dujon, B.; Feldmann, H.; Galibert, F.; Hoheisel, J.; Jacq, C.; Johnston, M. Life with 6000 genes. *Science* **1996**, *274*, 546-567.

Guldener, U.; Munsterkutter, M.; Kastenmuller, G.; Strack, N.; van Helden, J.; Lemer, C.; Richelles, J.; Wodak, S. J.; Garcia-Martinez, J.; Perez-Ortin, J.; Enrique.

CYGD: the comprehensive yeast genome database. *Nucleic acids research* **2005**, *33*, D364-D368.

Gustafson, G.; Davis, G.; Waldron, C.; Smith, A.; Henry, M. Identification of a new antifungal target site through a dual biochemical and molecular-genetics approach. *Current genetics* **1996**, *30*, 159-165.

Halliwell, W. H. Cationic amphiphilic drug-induced phospholipidosis. *Toxicologic Pathology* **1997**, *25*, 53-60.

Hamaguchi, R.; Tanimoto, T.; Kuroda, Y. Putative biomarker for phospholipid accumulation in cultured cells treated with phospholipidosis-inducing drugs: Alteration of the phosphatidylinositol composition detected using high-performance liquid chromatography-tandem mass spectrometry. *Journal of Chromatography B* **2014**, *967*, 110-117.

Hanamatsu, H.; Fujimura-Kamada, K.; Yamamoto, T.; Furuta, N.; Tanaka, K. Interaction of the phospholipid flippase Drs2p with the F-box protein Rcy1p plays an important role in early endosome to trans-Golgi network vesicle transport in yeast. *Journal of biochemistry* **2014**, *155*, 51-62.

Hanumegowda, U. M.; Regueiro-Ren, A.: Drug-Induced Phospholipidosis: Prediction, Detection, and Mitigation Strategies. In *Tactics in Contemporary Drug Design*; Springer, 2015; pp 261-281.

Heitman, J.; Movva, N. R.; Hall, M. N. Targets for cell cycle arrest by the immunosuppressant rapamycin in yeast. *Science* **1991**, *253*, 905-909.

Heitman, J.; Movva, N. R.; Hall, M. N. Targets for cell cycle arrest by the immunosuppressant rapamycin in yeast. *Science* **1991**, *253*, 905-909.

Hillenmeyer, M. E.; Fung, E.; Wildenhain, J.; Pierce, S. E.; Hoon, S.; Lee, W.; Proctor, M.; Onge, R. P. S.; Tyers, M.; Koller, D. The chemical genomic portrait of yeast: uncovering a phenotype for all genes. *Science* **2008**, *320*, 362-365.

Hirota, T.; Lee, J. W.; John, P. C. S.; Sawa, M.; Iwaisako, K.; Noguchi, T.; Pongsawakul, P. Y.; Sonntag, T.; Welsh, D. K.; Brenner, D. A. Identification of small molecule activators of cryptochrome. *Science* **2012**, *337*, 1094-1097.

Ho, C. H.; Magtanong, L.; Barker, S. L.; Gresham, D.; Nishimura, S.; Natarajan, P.; Koh, J. L.; Porter, J.; Gray, C. A.; Andersen, R. J.; Giaever, G.; Nislow, C.; Andrews, B.; Botstein, D.; Graham, T. R.; Yoshida, M.; Boone, C. A molecular barcoded yeast ORF library enables mode-of-action analysis of bioactive compounds. *Nat Biotechnol* **2009**, *27*, 369-377.

Hoon, S.; Smith, A. M.; Wallace, I. M.; Suresh, S.; Miranda, M.; Fung, E.; Proctor, M.; Shokat, K. M.; Zhang, C.; Davis, R. W.; Giaever, G.; St Onge, R. P.; Nislow, C. An integrated platform of genomic assays reveals small-molecule bioactivities. *Nat Chem Biol* **2008**, *4*, 498-506.

Horak, C. E.; Snyder, M. Global analysis of gene expression in yeast. *Functional & integrative genomics* **2002**, *2*, 171-180.

Hua, Z.; Fatheddin, P.; Graham, T. R. An essential subfamily of Drs2p-related P-type ATPases is required for protein trafficking between Golgi complex and endosomal/vacuolar system. *Molecular biology of the cell* **2002**, *13*, 3162-3177.

Huang, Z.; Chen, K.; Zhang, J.; Li, Y.; Wang, H.; Cui, D.; Tang, J.; Liu, Y.; Shi, X.; Li, W.; Liu, D.; Chen, R.; Sucgang, R. S.; Pan, X. A functional variomics tool for discovering drug-resistance genes and drug targets. *Cell reports* **2013**, *3*, 577-585.

Hughes, T. R. Yeast and drug discovery. *Functional & integrative genomics* **2002**, *2*, 199-211.

Inokoshi, J.; Tomoda, H.; Hashimoto, H.; Watanabe, A.; Takeshima, H.; Omura, S. Cerulenin-resistant mutants of Saccharomyces cerevisiae with an altered fatty acid synthase gene. *Molecular & general genetics : MGG* **1994**, *244*, 90-96.

Ito, T.; Chiba, T.; Ozawa, R.; Yoshida, M.; Hattori, M.; Sakaki, Y. A

comprehensive two-hybrid analysis to explore the yeast protein interactome. *Proceedings of the National Academy of Sciences* **2001**, *98*, 4569-4574.

Kaida, D.; Motoyoshi, H.; Tashiro, E.; Nojima, T.; Hagiwara, M.; Ishigami, K.; Watanabe, H.; Kitahara, T.; Yoshida, T.; Nakajima, H. Spliceostatin A targets SF3b and inhibits both splicing and nuclear retention of pre-mRNA. *Nature chemical biology* **2007**, *3*, 576-583.

Kodavanti, U. P.; Mehendale, H. M. Cationic amphiphilic drugs and phospholipid storage disorder. *Pharmacological Reviews* **1990**, *42*, 327-354.

Kontoyiannis, D. P.; Sagar, N.; Hirschi, K. D. Overexpression of Erg11p by the RegulatableGAL1 Promoter Confers Fluconazole Resistance inSaccharomyces cerevisiae. *Antimicrobial agents and chemotherapy* **1999**, *43*, 2798-2800.

Kunz, J.; Henriquez, R.; Schneider, U.; Deuter-Reinhard, M.; Movva, N. R.; Hall, M. N. Target of rapamycin in yeast, TOR2, is an essential phosphatidylinositol kinase homolog required for G1 progression. *Cell* **1993**, *73*, 585-596.

Lai, M. H.; Bard, M.; Pierson, C. A.; Alexander, J. F.; Goebl, M.; Carter, G. T.; Kirsch, D. R. The identification of a gene family in the Saccharomyces cerevisiae ergosterol biosynthesis pathway. *Gene* **1994**, *140*, 41-49.

Langmead, B.; Salzberg, S. L. Fast gapped-read alignment with Bowtie 2. *Nature Methods* **2012**, *9*, 357-359.

Lee, A. Y.; Onge, R. P. S.; Proctor, M. J.; Wallace, I. M.; Nile, A. H.; Spagnuolo, P. A.; Jitkova, Y.; Gronda, M.; Wu, Y.; Kim, M. K. Mapping the cellular response to small molecules using chemogenomic fitness signatures. *Science* **2014**, *344*, 208-211.

Li, H.; Handsaker, B.; Wysoker, A.; Fennell, T.; Ruan, J.; Homer, N.; Marth, G.; Abecasis, G.; Durbin, R. The sequence alignment/map format and SAMtools. *Bioinformatics* **2009**, *25*, 2078-2079.

Liu, J.; Farmer, J. D.; Lane, W. S.; Friedman, J.; Weissman, I.; Schreiber, S. L. Calcineurin is a common target of cyclophilin-cyclosporin A and FKBP-FK506 complexes. *Cell* **1991**, *66*, 807-815.

Loh, E.; Hong, W. The binary interacting network of the conserved oligomeric Golgi tethering complex. *Journal of Biological Chemistry* **2004**, *279*, 24640-24648.

Lomenick, B.; Hao, R.; Jonai, N.; Chin, R. M.; Aghajan, M.; Warburton, S.; Wang, J.; Wu, R. P.; Gomez, F.; Loo, J. A.; Wohlschlegel, J. A.; Vondriska, T. M.; Pelletier, J.; Herschman, H. R.; Clardy, J.; Clarke, C. F.; Huang, J. Target identification using drug affinity responsive target stability (DARTS). *Proceedings of the National Academy of Sciences of the United States of America* **2009**, *106*, 21984-21989.

Lomenick, B.; Jung, G.; Wohlschlegel, J. A.; Huang, J. Target identification using drug affinity responsive target stability (DARTS). *Current protocols in chemical biology* **2011**, 163-180.

Lopez, A.; Parsons, A. B.; Nislow, C.; Giaever, G.; Boone, C. Chemical-genetic approaches for exploring the mode of action of natural products. *Progress in drug research. Fortschritte der Arzneimittelforschung. Progres des recherches pharmaceutiques* **2008**, *66*, 237, 239-271.

Luesch, H.; Wu, T. Y.; Ren, P.; Gray, N. S.; Schultz, P. G.; Supek, F. A genome-wide overexpression screen in yeast for small-molecule target identification. *Chem. Biol.* **2005**, *12*, 55-63.

Lullmann, H.; Lullmann-Rauch, R.; Wassermann, O. Lipidosis induced by amphiphilic cationic drugs. *Biochemical pharmacology* **1978**, *27*, 1103-1108.

Lum, P. Y.; Armour, C. D.; Stepaniants, S. B.; Cavet, G.; Wolf, M. K.; Butler, J. S.; Hinshaw, J. C.; Garnier, P.; Prestwich, G. D.; Leonardson, A.; Garrett-Engele, P.; Rush, C. M.; Bard, M.; Schimmack, G.; Phillips, J. W.; Roberts, C. J.; Shoemaker, D. D. Discovering modes of action for therapeutic compounds using a genome-wide screen of yeast heterozygotes. *Cell* **2004**, *116*, 121-137.

Lynch, M.; Sung, W.; Morris, K.; Coffey, N.; Landry, C. R.; Dopman, E. B.; Dickinson, W. J.; Okamoto, K.; Kulkarni, S.; Hartl, D. L.; Thomas, W. K. A genome-wide view of the spectrum of spontaneous mutations in yeast. *Proceedings of the National Academy of Sciences of the United States of America* **2008**, *105*, 9272-9277.

Mamnun, Y. M.; Pandjaitan, R.; Mahe, Y.; Delahodde, A.; Kuchler, K. The yeast zinc finger regulators Pdr1p and Pdr3p control pleiotropic drug resistance (PDR) as homo‚Äêand heterodimers in vivo. *Molecular microbiology* **2002**, *46*, 1429-1440.

McIntyre, J. C.; Sleight, R. G. Fluorescence assay for phospholipid membrane asymmetry. *Biochemistry* **1991**, *30*, 11819-11827.

McKenna, A.; Hanna, M.; Banks, E.; Sivachenko, A.; Cibulskis, K.; Kernytsky, A.; Garimella, K.; Altshuler, D.; Gabriel, S.; Daly, M.; DePristo, M. A. The Genome Analysis Toolkit: a MapReduce framework for analyzing next-generation DNA sequencing data. *Genome Research* **2010**, *20*, 1297-1303.

Menacho-Marquez, M.; Murguia, J. R. Yeast on drugs: Saccharomyces cerevisiae as a tool for anticancer drug research. *Clinical & translational oncology : official publication of the Federation of Spanish Oncology Societies and of the National Cancer Institute of Mexico* **2007**, *9*, 221-228.

Mesens, N.; Steemans, M.; Hansen, E.; Verheyen, G. R.; Van Goethem, F.; Van Gompel, J. Screening for phospholipidosis induced by central nervous drugs: comparing the predictivity of an in vitro assay to high throughput in silico assays. *Toxicology in Vitro* **2010**, *24*, 1417-1425.

Monk, B. C.; Goffeau, A. Outwitting multidrug resistance to antifungals. *Science* **2008**, *321*, 367-369.

Morth, J. P.; Pedersen, B. P.; Buch-Pedersen, M. J.; Andersen, J. P.; Vilsen, B.; Palmgren, M. G.; Nissen, P. A structural overview of the plasma membrane Na+, K+-ATPase and H+-ATPase ion pumps. *Nature Reviews Molecular Cell Biology* **2011**, *12*, 60-70.

Nathwani, R. A.; Kaplowitz, N. Drug hepatotoxicity. *Clinics in liver disease* **2006**, *10*, 207-217.

Navarro, V. J.; Senior, J. R. Drug-related hepatotoxicity. *New England Journal of Medicine* **2006**, *354*, 731-739.

Oda, Y.; Owa, T.; Sato, T.; Boucher, B.; Daniels, S.; Yamanaka, H.; Shinohara, Y.; Yokoi, A.; Kuromitsu, J.; Nagasu, T. Quantitative chemical proteomics for identifying candidate drug targets. *Analytical chemistry* **2003**, *75*, 2159-2165.

Ong, S.-E.; Blagoev, B.; Kratchmarova, I.; Kristensen, D. B.; Steen, H.; Pandey, A.; Mann, M. Stable isotope labeling by amino acids in cell culture, SILAC, as a simple and accurate approach to expression proteomics. *Molecular & cellular proteomics* **2002**, *1*, 376-386.

Pappu, A.; Hostetler, K. Y. Effect of cationic amphiphilic drugs on the hydrolysis of acidic and neutral phospholipids by liver lysosomal phospholipase A. *Biochemical pharmacology* **1984**, *33*, 1639-1644.

Park, J.; Oh, S.; Park, S. B. Discovery and Target Identification of an Antiproliferative Agent in Live Cells Using Fluorescence Difference in Two Dimensional Gel Electrophoresis. *Angewandte Chemie International Edition* **2012**, *51*, 5447-5451.

Parsons, A. B.; Lopez, A.; Givoni, I. E.; Williams, D. E.; Gray, C. A.; Porter, J.; Chua, G.; Sopko, R.; Brost, R. L.; Ho, C.-H. Exploring the mode-of-action of bioactive compounds by chemical-genetic profiling in yeast. *Cell* **2006**, *126*, 611-625.

Pawlikowska, L.; Groen, A.; Eppens, E. F.; Kunne, C.; Ottenhoff, R.; Looije, N.; Knisely, A.; Killeen, N. P.; Bull, L. N.; Elferink, R. P. O. A mouse genetic model for familial cholestasis caused by ATP8B1 mutations reveals perturbed bile salt homeostasis but no impairment in bile secretion. *Human molecular genetics* **2004**, *13*, 881-892.

Pomorski, T.; Lombardi, R.; Riezman, H.; Devaux, P. F.; van Meer, G.; Holthuis, J.

C. Drs2p-related P-type ATPases Dnf1p and Dnf2p are required for phospholipid translocation across the yeast plasma membrane and serve a role in endocytosis. *Molecular biology of the cell* **2003**, *14*, 1240-1254.

Poor, F.; Parent, S. A.; Morin, N.; Dahl, A. M.; Ramadan, N.; Chrebet, G.; Bostian, K. A.; Nielsen, J. B. Calcineurin mediates inhibition by FK506 and cyclosporin of recovery from Œ±-factor arrest in yeast. **1992**.

Rask-Andersen, M.; Masuram, S.; Schioth, H. B. Trends in the exploitation of novel drug targets. *Nature reviews Drug discovery* **2011**, *10*, 579-590.

Reasor, M. J. A review of the biology and toxicologic implications of the induction of lysosomal lamellar bodies by drugs. *Toxicology and applied pharmacology* **1989**, *97*, 47-56.

Reiter, L. T.; Potocki, L.; Chien, S.; Gribskov, M.; Bier, E. A systematic analysis of human disease-associated gene sequences in Drosophila melanogaster. *Genome research* **2001**, *11*, 1114-1125.

Ribelin, W. E. The effects of drugs and chemicals upon the structure of the adrenal gland. *Toxicological Sciences* **1984**, *4*, 105-119.

Robinson, J. S.; Klionsky, D. J.; Banta, L. M.; Emr, S. D. Protein sorting in Saccharomyces cerevisiae: isolation of mutants defective in the delivery and processing of multiple vacuolar hydrolases. *Molecular and cellular biology* **1988**, *8*, 4936-4948.

Sabatini, D. M.; Erdjument-Bromage, H.; Lui, M.; Tempst, P.; Snyder, S. H. RAFT1: a mammalian protein that binds to FKBP12 in a rapamycin-dependent fashion and is homologous to yeast TORs. *Cell* **1994**, *78*, 35-43.

Sabers, C. J.; Martin, M. M.; Brunn, G. J.; Williams, J. M.; Dumont, F. J.; Wiederrecht, G.; Abraham, R. T. Isolation of a protein target of the FKBP12-rapamycin complex in mammalian cells. *Journal of Biological Chemistry* **1995**, *270*, 815-822.

Saxena, C.; Bonacci, T. M.; Huss, K. L.; Bloem, L. J.; Higgs, R. E.; Hale, J. E. Capture of drug targets from live cells using a multipurpose immuno-chemo-proteomics tool. *Journal of proteome research* **2009**, *8*, 3951-3957.

Scheurle, C.; Dammrich, M.; Becker, J. U.; Baumgrtel, M. W. Renal phospholipidosis possibly induced by ranolazine. *Clinical kidney journal* **2013**, sft141.

Seydel, J. K.; Wassermann, O. NMR-studies on the molecular basis of drug-induced phospholipidosis,ÄîII. Interaction between several amphiphilic drugs and phospholipids. *Biochemical pharmacology* **1976**, *25*, 2357-2364.

Seydel, J. K.; Wassermann, O. NMR-studies on the molecular basis of drug-induced phospholipidosis—II. Interaction between several amphiphilic drugs and phospholipids. *Biochemical pharmacology* **1976**, *25*, 2357-2364.

Shiwa, Y.; Fukushima-Tanaka, S.; Kasahara, K.; Horiuchi, T.; Yoshikawa, H. Whole-Genome Profiling of a Novel Mutagenesis Technique Using Proofreading-Deficient DNA Polymerase delta. *International journal of evolutionary biology* **2012**, *2012*, 860797.

Singh-Babak, S. D.; Babak, T.; Diezmann, S.; Hill, J. A.; Xie, J. L.; Chen, Y. L.; Poutanen, S. M.; Rennie, R. P.; Heitman, J.; Cowen, L. E. Global analysis of the evolution and mechanism of echinocandin resistance in Candida glabrata. *PLoS pathogens* **2012**, *8*, e1002718.

Stan, R.; McLaughlin, M. M.; Cafferkey, R.; Johnson, R. K.; Rosenberg, M.; Livi, G. P. Interaction between FKBP12-rapamycin and TOR involves a conserved serine residue. *Journal of Biological Chemistry* **1994**, *269*, 32027-32030.

Stieger, B.; Fattinger, K.; Madon, J.; Kullak-Ublick, G. A.; Meier, P. J. Drug-and estrogen-induced cholestasis through inhibition of the hepatocellular bile salt export pump (Bsep) of rat liver. *Gastroenterology* **2000**, *118*, 422-430.

Sturgill, M. G.; Lambert, G. H. Xenobiotic-induced hepatotoxicity: mechanisms of liver injury and methods of monitoring hepatic function. *Clinical chemistry* **1997**, *43*, 1512-1526.

Swinney, D. C.; Anthony, J. How were new medicines discovered? *Nature reviews. Drug discovery* **2011**, *10*, 507-519.

Tang, X.; Halleck, M. S.; Schlegel, R. A.; Williamson, P. A subfamily of P-type ATPases with aminophospholipid transporting activity. *Science* **1996**, *272*, 1495-1497.

Taunton, J.; Hassig, C. A.; Schreiber, S. L. A mammalian histone deacetylase related to the yeast transcriptional regulator Rpd3p. *Science* **1996**, *272*, 408-411.

Thomas, J. H.; Neff, N. F.; Botstein, D. Isolation and characterization of mutations in the beta-tubulin gene of Saccharomyces cerevisiae. *Genetics* **1985**, *111*, 715-734.

Timmermann, B.; Jarolim, S.; Russmayer, H.; Kerick, M.; Michel, S.; Kruger, A.; Bluemlein, K.; Laun, P.; Grillari, J.; Lehrach, H.; Breitenbach, M.; Ralser, M. A new dominant peroxiredoxin allele identified by whole-genome re-sequencing of random mutagenized yeast causes oxidant-resistance and premature aging. *Aging* **2010**, *2*, 475-486.

van der Woerd, W. L.; van Mil, S. W.; Stapelbroek, J. M.; Klomp, L. W.; van de Graaf, S. F.; Houwen, R. H. Familial cholestasis: progressive familial intrahepatic cholestasis, benign recurrent intrahepatic cholestasis and intrahepatic cholestasis of pregnancy. *Best Practice & Research Clinical Gastroenterology* **2010**, *24*, 541-553.

Van Duyne, G. D.; Standaert, R. F.; Schreiber, S. L.; Clardy, J. Atomic Structure of the Rapamycin Human Immunophilin FKBP-12 Complex. *J. Am. Chem. Soc.* **1991**, *113*, 7433-7434.

van Mil, S. W. Klomp, L. W. Bull, L. N. Houwen,H. Roderick. FIC1 disease: a spectrum of intrahepatic cholestatic disorders. *Seminars in Liver Diease.* **2001**, 21, 535-544.

Wacker, S. A.; Houghtaling, B. R.; Elemento, O.; Kapoor, T. M. Using transcriptome sequencing to identify mechanisms of drug action and resistance. *Nature Chemical Biology* **2012**, *8*, 235-237.

Wang, T.; Feng, Y.; Jin, X.; Fan, X.; Crommen, J.; Jiang, Z. Liposome electrokinetic chromatography based in vitro model for early screening of the drug-induced phospholipidosis risk. *Journal of pharmaceutical and biomedical analysis* **2014**, *96*, 263-271.

Weaver, T.; Hieter, P. Genome cross-referencing and XREFdb: implications for the identification and analysis of genes mutated in human disease. *Nat Genet* **1997**, *15*, 339-344.

Wiederkehr, A.; Avaro, S.; Prescianotto-Baschong, C.; Haguenauer-Tsapis, R.; Riezman, H. The F-box protein Rcy1p is involved in endocytic membrane traffic and recycling out of an early endosome in Saccharomyces cerevisiae. *The Journal of cell biology* **2000**, *149*, 397-410.

Williams, D. E.; Craig, K. S.; Patrick, B.; McHardy, L. M.; van Soest, R.; Roberge, M.; Andersen, R. J. Motuporamines, Anti-Invasion and Anti-Angiogenic Alkaloids from the Marine Sponge Xestospongia e xigua (Kirkpatrick): Isolation, Structure Elucidation, Analogue Synthesis, and Conformational Analysis. *The Journal of organic chemistry* **2002**, *67*, 245-258.

Winzeler, E. A.; Shoemaker, D. D.; Astromoff, A.; Liang, H.; Anderson, K.; Andre, B.; Bangham, R.; Benito, R.; Boeke, J. D.; Bussey, H. Functional characterization of the S. cerevisiae genome by gene deletion and parallel analysis. *Science* **1999**, *285*, 901-906.

Woehrmann, M. H.; Gassner, N. C.; Bray, W. M.; Stuart, J. M.; Lokey, S. HALO384 A Halo-Based Potency Prediction Algorithm for High-Throughput Detection of Antimicrobial Agents. *Journal of biomolecular screening* **2010**, *15*, 196-205.

Wride, D. A.; Pourmand, N.; Bray, W. M.; Kosarchuk, J. J.; Nisam, S. C.; Quan, T. K.; Berkeley, R. F.; Katzman, S.; Hartzog, G. A.; Dobkin, C. E. Confirmation of the cellular targets of benomyl and rapamycin using next-generation sequencing of

resistant mutants in S. cerevisiae. *Molecular BioSystems* **2014**, *10*, 3179-3187.

Wu, L.; Pan, J.; Thoroddsen, V.; Wysong, D. R.; Blackman, R. K.; Bulawa, C. E.; Gould, A. E.; Ocain, T. D.; Dick, L. R.; Errada, P.; Dorr, P. K.; Parkinson, T.; Wood, T.; Kornitzer, D.; Weissman, Z.; Willis, I. M.; McGovern, K. Novel small-molecule inhibitors of RNA polymerase III. *Eukaryotic cell* **2003**, *2*, 256-264.

Yamamoto, A.; ADACHI, S.; KITANI, T.; SHINJI, Y.; Seki, K.-i.; NASU, T.; NISHIKAWA, M. Drug-induced lipidosis in human cases and in animal experiments. *The Journal of Biochemistry* **1971**, *69*, 613-615.

Zhou, X.; Graham, T. R. Reconstitution of phospholipid translocase activity with purified Drs2p, a type-IV P-type ATPase from budding yeast. *Proceedings of the National Academy of Sciences* **2009**, *106*, 16586-16591.

Zhu, H.; Klemic, J. F.; Chang, S.; Bertone, P.; Casamayor, A.; Klemic, K. G.; Smith, D.; Gerstein, M.; Reed, M. A.; Snyder, M. Analysis of yeast protein kinases using protein chips. *Nature genetics* **2000**, *26*, 283-289.

田村明; 守脇尚子; 藤井達三. Disturbing effect of cationic amphiphilic drugs on phospholipid asymmetry of the membrane lipid bilayer of human erythrocytes. *Chemical and pharmaceutical bulletin* **1983**, *31*, 1692-1697.